University of Zurich[UZH]

Developing a Spatially Explicit Humanitarian Flood Vulnerability Index for Refugee Camps using Fuzzy Multi-Criteria Decision Analysis

GEO 511 Master's Thesis

Author
Annika Kunz
18-741-538

Supervised by
Bruna Rohling (brohling@ethz.ch)

Faculty representative
Prof. Dr. Ross Purves

30.06.2024
Department of Geography, University of Zurich

Abstract

The increasing number of refugees and the impacts of climate change necessitate improved flood vulnerability assessments for refugee camps. Refugee camps, often located in hazardous areas with inadequate infrastructure, usually face high vulnerability. However, approaches to spatially assess flood vulnerability within these camps are currently lacking. This thesis presents the development of a Humanitarian Flood Vulnerability Index (HFVI) tailored to refugee camps, incorporating expert knowledge through the application of the Fuzzy Analytical Hierarchical Process (FAHP). The methodology takes into account the inclusion of expert judgment in weighting the indicators and integrates uncertainty analysis. A novel approach combines fuzzy logic with the One-at-a-Time (OAT) sensitivity method, providing a spatially explicit representation of weight uncertainties, with the aim of enabling more informed decision-making and better-targeted interventions to ultimately improve the protection of refugees from flooding. The HFVI incorporates multiple vulnerability indicators, including physical and social dimensions, to create a composite raster-based index quantifying flood vulnerability in refugee camps. A case study of the Mahama refugee camp in Rwanda illustrates the application of the HFVI using global and local datasets. The results demonstrate the effectiveness of the HFVI in identifying vulnerability hotspots. However, limitations are discussed concerning the reproducibility and validity of the results, highlighting areas for improvement, ultimately aiming to enhance targeted flood risk mitigation strategies and resilience of refugee camps to increasing flood risks.

Keywords: Flood Vulnerability Assessment, Refugee Camps, Humanitarian Flood Vulnerability Index (HFVI), Fuzzy AHP, Weight Uncertainty

Acknowledgments

I would like to express my deepest gratitude to everyone who has supported me throughout the course of this thesis.

Firstly, I am very grateful to my supervisors Prof. Dr. Ross Purves and Bruna Rohling for their expertise, guidance and time they have taken to support me throughout the process of this thesis. In particular, I would like to thank them for their encouragement and valuable advice that helped me to progress this thesis.

I extend my sincere thanks to the SPUR research team of the Sustainable Humanitarian Settlements project for giving me the opportunity to contribute to this important project. In particular, I would like to thank David Kostwein, Mona Gairing and Laura Schalbetter for providing information, data and support related to the project.

Special thanks goes to all the experts who participated in the questionnaire of this study. Their invaluable knowledge, generous time, and helpful feedback, along with their offers of support, were instrumental in enabling the development of the HFVI. Their contributions have been substantial and greatly appreciated. I would like to specifically acknowledge the following individuals: Dr. Mark Bernhofen, Dr. Daniel Viviroli, Dr. Veruska Muccione, Dr. Kamran Abid, Nadine Antenen, Muhammad Ibrahim, Neel Chaminda Withanage, Chukwunonso Emmanue Ozim, Jonathan Parkinson, Tanja Matijevic, and Kamrul Hasan.

Lastly, I am deeply grateful to my family and friends for their unwavering support and encouragement throughout this journey. Above all, I would like to extend my heartfelt thanks to my mother, Heike Kunz, for carefully proofreading this work.

Contents

1 Introduction **1**

1.1 Research relevance: Interlinking refugee and climate crisis . . . 1
1.2 Key research gaps and problem statement . . . 2
1.3 Research questions and objectives . . . 3
1.3.1 Research questions . . . 3
1.3.2 Research objectives . . . 3
1.4 Structure of the thesis . . . 4

2 Background **5**

2.1 Flood risk and vulnerability assessment . . . 5
2.1.1 Definition of flood vulnerability . . . 5
2.2 Refugee camps vulnerability to flooding . . . 7
2.3 Project on Flood Risk Mitigation for Humanitarian Settlements . . . 8
2.3.1 Risk Mitigation Strategy GIS-tool . . . 8

3 Literature Review **10**

3.1 Methods for assessing flood vulnerability . . . 10
3.1.1 Vulnerability indicators . . . 11
3.2 Using GIS methods for flood vulnerability modelling . . . 12
3.2.1 Spatial quantification of flood vulnerability . . . 13
3.2.2 Uncertainty analysis in flood vulnerability modelling . . . 14
3.3 Flood vulnerability modelling for refugee camps . . . 16
3.3.1 Summarizing outlined research gaps . . . 17

4 Methodology **18**

4.1 Conceptual index development . . . 18
4.1.1 Defining the goals for the HFVI . . . 19
4.1.2 Index scoping . . . 20
4.1.3 Framework for Flood Vulnerability Assessment in Refugee Camps . . . 21
4.1.4 HFVI selection criteria . . . 22
4.1.5 Review of potential indicator sets . . . 23
4.1.6 Selection of final HFVI indicator sets . . . 23
4.1.7 Data collection . . . 26
4.1.8 Weighting and uncertainty incorporation . . . 30
4.1.9 Indicator aggregation . . . 37
4.1.10 Sensitivity analysis and uncertainty incorporation . . . 38
4.2 Mahama Case Study . . . 40

4.2.1 Study area . . . 40
4.2.2 Application of the HFVI on the Mahama refugee camp . . . 41

5 Results **47**
5.1 Conceptual index development . . . 47
5.1.1 Individual experts' AHP weights . . . 47
5.1.2 Consistency analysis . . . 49
5.1.3 Aggregated AHP weights . . . 53
5.1.4 Fuzzy AHP weights . . . 54
5.2 Mahama Case Study . . . 55
5.2.1 Individual flood vulnerability indicator layers . . . 55
5.2.2 Social and physical vulnerability maps . . . 57
5.2.3 HFVI for the Mahama Refugee Camp . . . 58
5.2.4 Spatial analysis . . . 59
5.2.5 Sensitivity analysis . . . 60
5.2.6 Final map layout: Combining HFVI and uncertainty . . . 63

6 Discussion **65**
6.1 HFVI conceptual choices and limitations . . . 65
6.1.1 HFVI conceptual model for refugee camps . . . 65
6.1.2 Spatial modelling of refugee camp vulnerability . . . 67
6.1.3 HFVI indicator weights . . . 68
6.1.4 Addressing uncertainty in vulnerability assessment . . . 71
6.1.5 Incorporating fuzzy logic into the HFVI . . . 71
6.1.6 Sensitivity analysis: The novel FAHP-OAT approach . . . 73
6.2 HFVI case study application and performance . . . 73
6.2.1 Flood vulnerability in the Mahama Refugee Camp . . . 73
6.2.2 Future applicability and validation . . . 78

7 Conclusion **81**

A Appendix **93**
Appendix A: List of vulnerability indicators . . . 93
Appendix B: List of experts . . . 95
Appendix C: AHP expert questionnaire design . . . 96
Appendix D: Mahama Camp Layout Map . . . 103

List of Figures

2.1 Concept of the Risk Mitigation Strategy Tool. 8

4.1 Graphical representation of the methodology. 19
4.2 Phases of vulnerability indicator development. 20
4.3 Framework for Flood Vulnerability Assessment in Refugee Camps. 22
4.4 HFVI Decision Hierarchy. 27
4.5 Triangular fuzzy number membership function. 35
4.6 Triangular fuzzy number membership functions and scale of importance. 36
4.7 Mahama Refugee Camp Overview. 41
4.8 Vector Data for the Mahama Refugee Camp. 42
4.9 Spatial processing steps for the computation of the HFVI. 45

5.1 Distribution of individual priority weights per vulnerability indicator. 48
5.2 Distribution of individual priority weights for vulnerability dimension. 49
5.3 Error frequencies of indicator pairs. 50
5.4 Harker's method and number of iteration runs. 51
5.5 Fuzzy AHP weights and their range of the fuzzy number (wMin, wMax). 55
5.6 Normalized and categorized vulnerability indicator raster layers. 56
5.7 Social and physical flood vulnerability dimension of the HFVI. 57
5.8 Final composite HFVI map for the Mahama Refugee Camp. 59
5.9 Spatial correlation matrix of the individual HFVI indicators. 60
5.10 Mean absolute change rates per CWR. 61
5.11 Spatial weight uncertainty maps for the social and physical HFVI. 62
5.12 Final weight uncertainty for the Mahama Refugee Camp. 63
5.13 Final map layout illustrating the HFVI overlayed with weight uncertainty classes and individual indicator layers for the Mahama Refugee Camp. 64

A.1 Mahama Camp Layout Map. 103

List of Tables

4.1 Selection of criteria for the HFVI indicators and results. 23
4.2 Final flood vulnerability indicator set including social and physical flood vulnerability dimensions. 24
4.3 List of expert groups for the AHP weighting. 28
4.4 Scale of Relative Importance of AHP ranks, their reciprocals and respective Triangular Fuzzy Number (TFN) scale. 28
4.5 Reference table for RI values, adopted from Saaty (1980). 33
4.6 Example of a fuzzified PCM. 36
4.7 Vulnerability ranks of indicators subcategories. 37

5.1 Example of transposed PCM for Expert ID 4. 48
5.2 Corrected individual preference weights and consistency results. 52
5.3 CR values of experts' PCMs. 53
5.4 Transformed CRs of experts' PCMs. 53
5.5 Final AHP weights. 53
5.6 Matrix of Social Vulnerability Indicators with Intervals. 54
5.7 Final FAHP weights. 54
5.8 Moran's I test for spatial autocorrelation of flood vulnerability values. 59
5.9 Range of percentage changes from the fuzzy weights bounds to the original value. . . . 61

A.1 Potential Indicators found in the existing literature. 94

List of Abbreviations

Abbreviation	Definition
AHP	Analytic Hierarchy Process
BBC	Bogardi-Birkmann-Cardona conceptual framework
CI	Consistency Index
CR	Consistency Ratio
CRs	Consistency Ratios
DIM	Vulnerability Dimension
ECD	Early Child Development
FAHP	Fuzzy Analytic Hierarchy Process
FPCM	Fuzzy Pairwise Comparison Matrix
GIS	Geographic Information Systems
GTH	Geneva Technical Hub
HFVI	Humanitarian Flood Vulnerability Index
IPC	Increments of Percentage Change
JRC	Joint Research Centre
MCDA	Multi-Criteria Decision Analysis
MOVE	Methods for the Improvement of Vulnerability Assessment in Europe
OAT	One-At-a-Time
OECD	Organization for Economic Cooperation and Development
OSM	OpenStreetMap
PCA	Principal Component Analysis
PCM	Pairwise Comparison Matrix
PHY	Physical Vulnerability Indicator
PHY1	Shelter Type
PHY2	Critical Infrastructure
PHY3	Facilities Physical Vulnerability
PHY4	Roads
PULS	Planning Landscape and Urban Systems
RI	Random Consistency Index
RPC	Range of Percent Change
SDC	Swiss Development Cooperation
SDG	Sustainable Development Goals
SOC	Social Vulnerability Indicator
SOC1	Population Density
SOC2	Vulnerable Groups
SOC3	Facilities of Social Importance
SOC4	Land Use
TFN	Triangular Fuzzy Number
UNHCR	United Nations High Commissioner for Refugees

1 Introduction

This introduction highlights the relevance of assessing flood vulnerability within refugee camps and summarises the key research gaps related to the issue. Building on this foundation, the research questions and objectives are presented, providing a clear road map for the investigation. An overview of the thesis structure is provided at the end of this introduction to guide readers through the subsequent chapters and sections.

1.1 Research relevance: Interlinking refugee and climate crisis

Over the past decade, the number of refugees has increased alarmingly. As of the end of 2023, the number of forcibly displaced people worldwide reached an estimated 117.3 million, marking a significant increase from previous years. This includes refugees, asylum-seekers, internally displaced people, and others forced to flee due to persecution, conflict, violence, and human rights violations, many of whom are living in refugee camps. This upward trend has continued into 2024, with estimates indicating that the number of forcibly displaced people exceeded 120 million by summer 2024 (UNHCR, 2024). As a result of climate change, the number of displaced people will continue to rise, which will further increase the need for refugee camps that provide temporary shelter. At the same time, climate change is projected to lead to more frequent and severe floods with greater impacts on affected regions (Seneviratne et al., 2021). Understanding flood vulnerability as an integral part of flood risk assessment is a primary objective for mitigating rising flood risk (Chan et al., 2022) and enables decision-makers to reduce potential damage and fatalities (Fernandez et al., 2016). The interlinked perspective of refugee and climate crises emphasises the relevance of this study.

The importance of reducing social and material losses caused by water-related disasters is underscored by the United Nations, emphasizing the protection of the most vulnerable groups to achieve the Sustainable Development Goals (SDGs). Goals 1, 11, and 13 focus on reducing disaster vulnerability and enhancing resilience to extreme events. Flooding poses an increasing challenge for cities, disproportionately affecting marginalized communities (UNISDR, 2015). Residents of refugee camps and informal settlements are particularly susceptible to the impacts of climate change, as highlighted by numerous researchers. Factors contributing to this increased risk include their location on hazardous land, including flood-prone areas, inadequate urban planning, insufficient infrastructure and services, and elevated levels of socioeconomic vulnerability (Akola et al., 2019; Anwana & Owojori, 2023; Hassan et al., 2018; Owen et al., 2023). Socioeconomic vulnerability is thereby increased due to a higher proportion of young, elderly, malnourished, and individuals with health or disability issues. Legal and bureaucratic constraints limit their mobility. Being new to the location, camp residents often lack normal coping mechanisms and resources (ARSET, 2024).

Quantifying vulnerability proves challenging. Definitions of vulnerability found in the literature range widely, including aspects from physical exposure to socioeconomic and sociological factors (Yi & Xie, 2010). Given the multi-dimensionality of vulnerability as a concept, assessing vulnerability necessitates considering various relevant factors. With the increasing availability of high spatial and temporal resolution in-situ data and the emergence of precise flood hazard models, flood vulnerability assessment on a regional or sub-regional scale has advanced in recent years. However, socio-economically or geographically marginalized population groups are generally not taken into account in such regional assessments, as is the case with refugees housed in refugee camps (Owen et al., 2023). Due to the temporary nature of the camps and their particular built environment, their remote location, and high population density, those camps are by nature highly vulnerable to increasing flood risk (Bernhofen et al., 2023), considering physical as well as socioeconomic vulnerabilities (Kaufmann et al., 2022; Yi & Xie, 2010). The absence of adequate support and guidance for camp managers in assessing potential flood vulnerability, compounded by insufficient knowledge and, above all, the lack of local data and the understanding of associated uncertainties, contributes significantly to this ignorance of potential flood risk in refugee camps (Bernhofen et al., 2023). Consequently, the existing strategies to mitigate flood risks within most refugee camps fall short of adequacy (Sphere Association, 2018). As flood events intensify and impact vulnerable communities, particularly due to their limited coping and adaptive capacities (Malgwi et al., 2021), an urgent requirement emerges for tailored flood vulnerability modelling within refugee camps. Such models are essential to facilitate effective flood risk mitigation strategies (Owen et al., 2023).

In response to the pressing need to accurately assess flood risk in refugee camps, the United Nations High Commissioner for Refugees (UNHCR) has launched a project in close collaboration with the ETH Zurich. The "Sustainable Humanitarian Settlements" project aims to develop a GIS tool that supports the UNHCR staff in decision-making for flood risk mitigation in refugee camps. The project is described in more detail in Section 2.3. This thesis is part of the ongoing project, explicitly aiming to propose a refined vulnerability index which can be incorporated into the flood risk mapping GIS tool to improve the understanding of spatial vulnerability in refugee camps.

1.2 Key research gaps and problem statement

To date, only a few studies have concentrated on assessing the vulnerability of refugee camps to natural hazards, particularly floods (Bernhofen et al., 2023; Owen et al., 2023; Tschirpig, 2022). This gap emphasizes the need to develop flood vulnerability models specifically designed for the context of refugee camps. There is little scientific literature on methods that support spatial modelling of flood vulnerability in areas with limited data, which are based on GIS or remote sensing techniques (An et al., 2022; Ganji et al., 2022; Malgwi et al., 2020; Ramkar & Yadav, 2021). Malgwi et al. (2021), for example, demonstrate the potential of indicator-based flood vulnerability methods incorporating expert-based data collection to counteract the lack of empirical data. Such approaches hold promise for adaptation within the specific context of refugee camps. However, to date, no standardized model or index quantifies flood vulnerability in refugee camps. Also, general urban vulnerability models tailored to the local scale are still missing accuracy assessment, as there has been no standardized workflow for model validation and quantification of uncertainty (An et al., 2022). Given the limited data availability and the multifaceted nature of vulnerability within refugee camp settings, quantifying flood vulnerability becomes a complex task. Hence, sensitivity analyses and uncertainty assessments are

necessary to address this complexity in quantifying vulnerability to floods in refugee camps. However, as emphasized by An et al. (2022), the existing literature lacks applications of uncertainty analyses specifically in the context of refugee settlements, which is why this thesis aims to address this gap.

1.3 Research questions and objectives

1.3.1 Research questions

The problem statement and the associated research gaps in the current literature give rise to the following key research question (RQ) and its subordinated questions (RQ1.1. and RQ1.2).

RQ1: How can flood vulnerability as a multi-dimensional concept be modelled to fit the context of refugee camps?

RQ1.1: Which key factors contribute to the flood vulnerability within refugee camps?

RQ1.2: What are the main challenges in spatially modelling flood vulnerability in refugee camps, and how can those challenges be overcome?

1.3.2 Research objectives

Given the defined research questions and the need for methodologies to quantify flood vulnerability in refugee camps, this thesis aims to develop a conceptual model and construct a standardized flood vulnerability index specifically tailored to the unique circumstances of refugee camp environments, hereafter referred to as the Humanitarian Flood Vulnerability Index (HFVI). This index accommodates the inherent structural limitations and data scarcity prevalent in such settings. A key focus lies in evaluating multi-criteria vulnerability components and their relative influences by incorporating expert knowledge. Physical and social dimensions of the vulnerability within refugee camps are examined individually and in combination using a composite index approach. Further, the index addresses the sensitivity and uncertainties of these vulnerability components stemming from subjective conceptual decisions. Rather than disregarding these uncertainties, the developed index aims to uncover and quantify them, thereby facilitating a more transparent communication of the index outcomes. This work's objectives align with the "Flood Risk Mitigation for Humanitarian Settlements" project and aim to improve the flood vulnerability assessment as an essential part of the developed "Risk Mitigation Strategy GIS Tool". Ultimately, the expanded view of flood vulnerability using the developed Humanitarian Flood Vulnerability Index (HFVI) should help local UNHCR camp managers make more informed decisions, considering potential areas of uncertainty, to mitigate future flood risks in refugee camps.

To address the research goal, this thesis applies the following methodological measures, all aiming to answer the key research question (RQ1) and the subordinated questions (RQ1.1 and RQ1.2):
a) A literature review to select relevant factors influencing flood vulnerability in refugee camps, b) expert surveys to explore the relative importance of influential factors, c) the conceptual development of an index called HFVI and d) a case study approach applying and testing the HFVI.

1.4 Structure of the thesis

The thesis is organized as follows: Chapter 2 briefly describes the thematic background, providing definitions of flood risk and vulnerability and introducing the project on "Flood Risk Mitigation for Humanitarian Settlement". Chapter 3 reviews the related work in the context of spatial flood vulnerability assessment and implementation in refugee camps. The methodology in Chapter 4 summarizes the steps followed to construct the conceptual model of the HFVI, including the experts' weighting methodology and the incorporation of uncertainty using fuzzy logic. In addition, the methodological steps of applying the developed HFVI and the subsequent sensitivity analysis are described using a case study in Rwanda, Mahama. Chapter 5 describes the results of developing, applying and spatially mapping the HFVI for the Mahama refugee camp. These results are critically discussed in Chapter 6. Finally, the conclusion in Chapter 7 summarises the key findings for answering the research questions, highlighting potential future work.

2 Background

This chapter outlines the essential components of flood risk assessment, the complexities of defining and quantifying flood vulnerability, and the unique challenges refugee camps face in managing flood risks. Additionally, it introduces the "Sustainable Humanitarian Settlements" project and its efforts to develop a GIS tool for enhancing flood risk mitigation in these vulnerable settings.

2.1 Flood risk and vulnerability assessment

Flood risk assessment is a crucial process in natural hazard research. Generally, risk is defined as the anticipated likelihood of harmful consequences or losses arising from the interplay between natural or human-induced hazards and vulnerability conditions, along with human exposure (Kienberger, 2013). Flood risk assessment involves three main components: flood hazard, exposure and vulnerability assessments. However, in flood risk management, the exposure term is often regarded as part of the hazard component, leading to a risk concept based on the interplay of flood hazard and vulnerability (Nasiri et al., 2016). Flood hazard assessment focuses on determining the probability of the occurrence of a flood event, described by the time frame and location, while flood exposure refers to the measure of susceptible elements within a region threatened by a hazard, indicating the likelihood of impact by flooding on humans and physical items (Kienberger, 2013; Nasiri et al., 2016). Vulnerability assessment evaluates the susceptibility of specific targets to damage in the event of a flood (Apel et al., 2008). Vulnerability can be considered the most important element of risk assessment as it determines whether the exposure of a system or community will actually lead to a disaster (Ouma & Tateishi, 2014).

It is crucial to recognize that while flood hazard may be consistent for a particular area in terms of intensity, the actual risk can vary based on specific conditions described through the flood vulnerability (Baky et al., 2019). Consequently, flood vulnerability can vary significantly in space and time, greatly influencing the overall flood risk. Hence, vulnerability and its spatial behaviour are key factors in flood risk management, playing a central role in assessing and mitigating the impacts of floods to guarantee the safety and well-being of people in flood-prone areas. To mitigate flood risk, vulnerability reduction is crucial, increasing the resilience of communities (Nasiri et al., 2016).

2.1.1 Definition of flood vulnerability

Given the lack of a universal definition of vulnerability, researchers from diverse backgrounds have presented various interpretations, underscoring the absence of a common language on this topic (Birkmann et al., 2013). Consequently, the definition of vulnerability is not straightforward due to its multidimensional and contextual aspects. In the scientific literature, vulnerability often refers to the

likelihood of harm and the potential for damage or loss in elements that are exposed, including physical or economic assets, as well as individuals and their livelihoods, when affected by either single or combined hazard events (Birkmann et al., 2013; Cutter et al., 2003). Vulnerability research, therefore, typically integrates societal resilience and physical susceptibility for a specific place and context (Cutter et al., 2003; Ouma & Tateishi, 2014), combining natural and social science perspectives (IPCC, 2012). Natural science researchers often concentrate on quantifying vulnerability factors, aiming to define damage ranges through vulnerability curves to establish acceptable levels of potential losses (Kienberger et al., 2009; Papathoma-Köhle et al., 2019). On the other hand, social science approaches have a broader focus, examining the likelihood of harm or losses to individual households or communities from environmental hazards, along with the economic contextual factors influencing social vulnerability (Birkmann et al., 2013). However, while substantial research has focused on exploring the physical vulnerability and the vulnerability of engineered structures (Ford et al., 2015), the understanding of socio-economic vulnerability remains limited. The aspects of vulnerability arising from social factors are often disregarded, primarily due to the quantification challenges. Consequently, social losses are frequently omitted in post-disaster evaluations, contributing to a lack of attention towards socially created vulnerabilities (Cutter et al., 2003). Especially in the context of humanitarian settlements, special attention should be paid to including socio-economic factors for flood vulnerability assessment (Ouma & Tateishi, 2014).

The framework employed in flood vulnerability assessments can greatly affect the results of vulnerability methodologies, underscoring the importance of carefully considering conceptual decisions in the assessment process (J. S. Lee & Choi, 2018). Given the absence of a universally accepted definition of vulnerability, it becomes essential to adopt a framework suitable for the specific context in which the assessment is conducted. Within the scope of this thesis, the conceptualization of vulnerability will follow a modified version of the widely accepted MOVE framework (Methods for the Improvement of Vulnerability Assessment in Europe), also adapting elements from the holistic BBC (Bogardi-Birkmann-Cardona) conceptual framework (Bogardi & Birkmann, 2004; Cardona, 2004). Constructing a simplified vulnerability framework tailored to refugee camp conditions is further described in the Methods Chapter 4.1.3 building on the Flood Risk in Humanitarian Settlements project. In the here developed "Framework for Flood Vulnerability Assessment in Refugee Camps", risk is defined as the product of hazard and vulnerability, where the flood exposure term is regarded as an integral part of the flood hazard. Therefore, vulnerability can be quantified independently of the exposure (Cutter et al., 2003). Vulnerability is a dynamic concept and can be affected by various factors such as livelihoods, access to resources, resilience or assets (Barclay et al., 2022; Ullah, 2016). Accordingly, vulnerability assessment should incorporate both social and physical dimensions to comprehensively analyze and address natural hazard risks (Guillard-Gonçalves & Zêzere, 2018). Therefore, the framework developed for this study takes up this two-dimensionality in defining vulnerability as the proneness of social and physical elements at risk of experiencing harm due to flooding events.

- *Social dimension:* The likelihood of harm to human well-being caused by disturbances to the individual (mental and physical health) and collective (health, education services, etc.) social systems, including their characteristics like gender and marginalization of social groups.
- *Physical dimension:* The likelihood of harm to physical assets, e.g., infrastructure, buildings or open spaces.

Birkmann et al. (2013) further describe vulnerability's economic, cultural, ecological, and institutional dimensions. Nevertheless, these dimensions are of negligible significance within the particular context of vulnerability assessment in refugee camps or are not considered due to a lack of sufficient data and, thus, are not further elaborated upon here.

2.2 Refugee camps vulnerability to flooding

Recently, thousands of refugees have been suffering due to El Niño-triggered heavy rains and severe flooding across East Africa in late 2023 and early 2024. In Kenya, nearly 20,000 people in the Dadaab refugee camps have been displaced, facing collapsed latrines and the associated risk of water-borne diseases. In Burundi, around 32,000 refugees are in flood-affected areas, causing an increase in food and service prices. In Tanzania, over 200,000 refugees have been impacted, with damaged shelters and a flooded UNHCR office in Kigoma (United Nations, 2024). These events highlight the urgent need for immediate assistance and reduced vulnerabilities within refugee camps to support the affected populations.

Refugee camps are temporary facilities established to offer immediate aid and protection to individuals forced to flee their homes due to violence, conflict, or persecution. Although these camps are initially designed as short-term solutions for specific emergencies, the duration of ongoing crises can extend, leading to people living in camps for years or even decades (UNHCR, 2023b). While not intended to be permanent solutions, these camps function as safe havens for refugees by providing essential necessities such as food, water, shelter, medical care, and other basic services during emergencies. When displacement becomes prolonged, the range of services is expanded to include educational and livelihood opportunities and materials for constructing more permanent homes, thereby helping individuals rebuild their lives (UNHCR, 2021). As highlighted by Anwana and Owojori (2023), refugee camps are particularly vulnerable to natural hazard risks, such as flood events, due to the locations on hazardous land, poor planning and lack of infrastructure and increased socioeconomic vulnerability of the marginalized community. Political considerations and available land often influence refugee camp placement rather than optimal, low-risk locations. Camps are commonly situated near international borders, away from main populated areas, leading to their establishment in remote regions with minimal infrastructure and limited location data. These decisions may not fully account for the risks associated with the sites (ARSET, 2024). Moreover, Bernhofen et al. (2023) points out that inadequate shelter structures in camps may not offer sufficient protection from extreme weather events like floods. The temporary structures in camps are particularly susceptible to floods, and high population density increases the criticality of support infrastructure. Additionally, many camps lack adequate drainage systems, exacerbating flood risks (ARSET, 2024).

Given the importance of assessing flood vulnerability to mitigate flood risk and the emerging scientific interest in developing methods to quantify flood vulnerability in urban areas, there still is a lack of risk assessments for rural or remote locations and specifically for informal settlements and refugee camps (Anwana & Owojori, 2023; Bernhofen et al., 2023; Mwalwimba et al., 2024). This research gap could be explained by the fact that top-down national assessments often overlook remote regions. In addition, data for flood risk assessment is strongly limited as the areas made available for refugee camps are generally far from urban centres. The lack of sufficient local flood risk data and the inaccuracy of available global datasets for such remote areas hampers effective adaptation and mitigation measures for refugee camps (Bernhofen et al., 2022, 2023).

2.3 Project on Flood Risk Mitigation for Humanitarian Settlements

The work of this thesis is part of the Humanitarian Planning Hub project on "Sustainable Humanitarian Settlements" (Kaufmann et al., 2022). The project is led by the Planning Landscape and Urban Systems (PLUS) research group from the ETH Zurich in a collaborative effort with the United Nations High Commissioner for Refugees (UNHCR) and the Swiss Development Cooperation (SDC) through the Geneva Technical Hub (GTH) and focuses on developing innovative technologies to address challenges faced by displaced people. The ongoing aim of the project is to create a GIS tool for flood risk mitigation in refugee camps, ultimately proposing a catalogue of flood risk measures to assist UNHCR staff in mitigation efforts and decision-making. The project aims to enhance natural hazard risk management and environmental sustainability in humanitarian settlements, supporting long-term resilience and sustainability (Kaufmann et al., 2022; Rohling et al., 2023). The current GIS tool, along with its guidelines and information, is made available online as part of a comprehensive compendium and can be accessed via the following link: https://www.humanitarian-risk.org/index.php.

2.3.1 Risk Mitigation Strategy GIS-tool

The Risk Mitigation Strategy GIS Tool is designed as a QGIS and ArcGIS plugin and aims to help UNHCR field staff to assess and manage flood risks in refugee settlements. Using global data and local knowledge, the tool integrates hazard and vulnerability into a final risk map. The tool enables users to create detailed risk maps by defining settlement extents and uploading relevant data, allowing for manual adjustments of flood zones and elements at risk. The tool then calculates and visualizes flood risks for a given refugee camp under examination. The flood risk calculation in the Risk Mitigation Strategy Tool involves a multi-step process as illustrated in Figure 2.1.

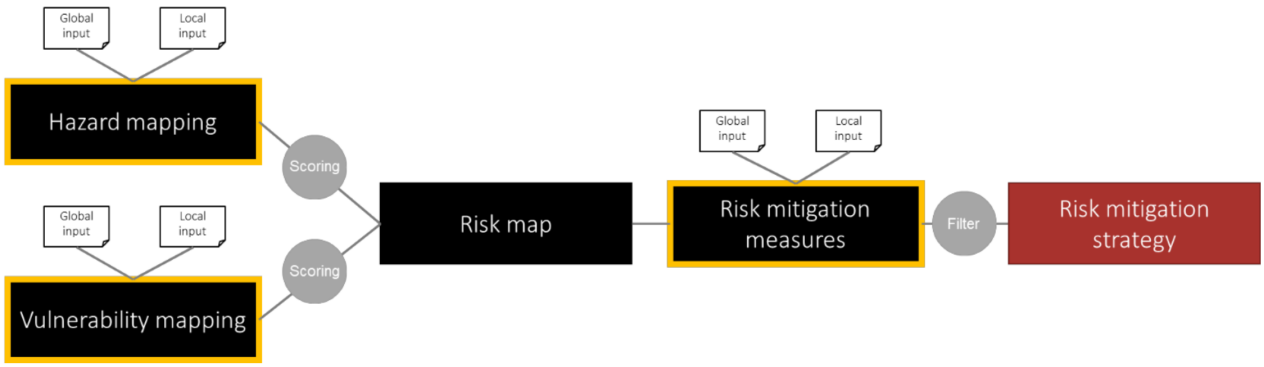

Figure 2.1: Concept of the Risk Mitigation Strategy Tool from Kaufmann et al. (2022).

First, hazard mapping is conducted to identify flood hazards using global or, if available, local pluvial data (Kaufmann et al., 2022). The global data used for the hazard assessment is the riverine flood dataset provided by the Joint Research of the European Commission, containing information about the frequency and magnitudes of flood events worldwide. With a resolution of 30 arcseconds, each cell indicates water depth in meters calculated for different return periods, enabling flood hazard assessment in any global location (Dottori et al., 2016). Next, vulnerability mapping assesses the susceptibility of assets, namely buildings, transport infrastructure, and technical infrastructure, to flood damage. Vulnerable assets in refugee settlements are defined as elements likely to suffer in the event of a flood. These assets face damage that impacts humans, infrastructure, and ecosystems while constraining social, economic, and operational processes (Kaufmann et al., 2022). The vulnerability

assessment combines automated global data with manual inputs and local data collected through participatory workshops. The tool then integrates these hazard and vulnerability maps to create a final risk map. A risk matrix is used to determine the overall risk levels, combining the physical and social vulnerabilities with the hazard levels to assign a risk score, showing the levels of flood risk for different assets (Gairing et al., 2024). The resulting assessment helps prioritize mitigation measures and aims to improve the resilience of refugee settlements by providing tailored risk mitigation strategies, including structural and non-structural measures (Rohling et al., 2023).

The existing procedure for vulnerability mapping uses a simple risk matrix to assess vulnerability. Primarily, it employs vector-based data of camp assets, assigning vulnerability ranks to the physical assets for risk calculation (Gairing et al., 2024). This method may not fully capture the complexity and nuances of the multi-dimensional vulnerability present in refugee camps, as some components contributing to the vulnerability may have varying influences on the overall flood risk. Furthermore, the method lacks techniques like sensitivity analyses and uncertainty quantification, which are essential for robust vulnerability modelling. To expand the GIS tool developed by ETH Zurich, this work on creating an index specifically designed for refugee camps can be integrated by incorporating expert-derived multi-criteria indicator weights. Therefore, a refined and raster-based index is developed tailored to refugee camps' conditions, illustrating physical and socioeconomic vulnerability dimensions as standalone and composite indices. The final index leverages expert knowledge to address the complexity of different flood vulnerability components and their influence on the overall vulnerability. Embedding this raster-based index into the GIS tool aims to allow for a better understanding of the spatial behaviour of vulnerability within refugee camps and its associated uncertainties.

3 Literature Review

This literature review synthesizes existing research on general flood vulnerability assessment, culminating in a focused examination of flood vulnerability assessment specific to refugee camps. It provides a comprehensive overview of current methodologies, particularly focusing on index-based methods, which are typically developed for application in urban areas. This chapter also highlights the unique challenges associated with these approaches. Additionally, it identifies key areas for future research, emphasizing the need for tailored models to accurately assess flood vulnerability in refugee camps located in remote and data-scarce regions. The review underscores the critical gap in appropriate flood risk assessment tools for these vulnerable populations and calls for innovative solutions incorporating local knowledge and context-specific factors.

3.1 Methods for assessing flood vulnerability

More comprehensive assessment methods and a better understanding of flood vulnerability can help decision-makers to reduce damage and fatalities. However, measuring vulnerability is a complex process, especially when limited by data availability and is influenced by various environmental, economic, social, and even political factors at the local scale, including, for example, settlement conditions, infrastructure, social inequities and coping capacities or economic factors (Gao et al., 2007).

Numerous methods for assessing flood vulnerability have been developed over the past few decades (Nasiri et al., 2016), which can be quantified into distinct groups: vulnerability curves, disaster loss data methods or computational modelling methods and vulnerability indicators (Malgwi et al., 2020). Papathoma-Köhle et al. (2019) discusses the use of vulnerability curves, also named damage-grade models, as an approach for assessing the physical vulnerability of the built environment to floods. The method depicts the relationship between flood hazards, particularly predicted flood depth and degree of damage, quantified by damage grades or values for monetary loss. It is commonly used to predict flood damage. Zhang et al. (2021), for example, uses disaster loss data obtained from high-quality field survey data to establish spatial flood loss models, assessing direct economic losses from flood disasters. However, applying such a method requires empirical data on flood depth and related building damage patterns gained from damage surveys or statistical data about monetary losses after historical flood events (Totschnig & Fuchs, 2013). Further studies, such as Baky et al. (2019), have also indicated the importance of identifying elements at risk through land use mapping approaches to enhance flood vulnerability assessments using flow models. Moreover, J.-Y. Lee and Kim (2021) utilize logistic regression and machine learning models like Naive Bayes and random forests to estimate flood vulnerability and detect areas prone to flooding effectively. Given the scarcity of data in regions of refugee camps, significant challenges in developing accurate damage-grade models are posed (Niang et al., 2014). Since the damage data are also very location- and event-specific, the transferability to

other regions or camps is limited (Nasiri et al., 2016), this method is not suitable for application to refugee camps.

3.1.1 Vulnerability indicators

Another method which is commonly used to assess vulnerability to floods is based on the application of vulnerability indicators. Such indicators are used, for example, in the studies of Birkmann (2013), Chan et al. (2022), H. Chen et al. (2011), and J. S. Lee and Choi (2018). Indicator-based methods are the most common approach used in the literature to assess flood vulnerability (Malgwi et al., 2020; Nasiri et al., 2016), and aim to measure the level to which a given flood event will impact a system. Vulnerability indicators are based on aggregated vulnerability factors, depicting the condition of a system (Birkmann, 2007). Birkmann et al. (2013) propose a manual for constructing composite vulnerability indices for natural hazards assessment on a local scale, proposing theoretical requirements for indicator weighting and aggregation. Composite indices are essential tools for integrating multiple indicators into a single metric, effectively capturing the multi-dimensional nature of vulnerability. They simplify complex and multi-faceted phenomena through a mathematical process known as aggregation (Fozaie & Wahid, 2022).

3.1.1.1 Multi-dimensionality of flood vulnerability indicators

Vulnerability indicators are commonly applied to model the physical vulnerability of systems and elements at risk, ignoring other factors contributing to vulnerability (Malgwi et al., 2020). While some studies concentrate on a specific vulnerability dimension, for example, Dall'osso et al. (2009)), others explore multiple dimensions, such as Kienberger et al. (2009)). Birkmann (2013) highlighted that opting for a multidimensional study design is worthwhile only if data of a certain quality and quantity are available, meeting the scale requirements of the study. Especially, the inclusion of social vulnerability is still largely lacking in current practices, despite its critical importance for risk analysis and disaster response reduction (Tate et al., 2021). Tascón-González et al. (2020) highlights the need for further advances in measuring and incorporating social vulnerability into flood risk assessment. Cutter et al. (2003) and Houston et al. (2020), for example, developed social flood vulnerability indices, presenting a measure to capture the vulnerability to floods better, hence underlining the importance of tailored social indicators in vulnerability assessments. To address this research gap, vulnerability indicators are particularly useful as they allow for the incorporation of multidimensional components influencing flood vulnerability.

3.1.1.2 Spatial scale of flood vulnerability indicators

The spatial scale at which a vulnerability indicator approach is applied varies depending on data availability and the assessment's objectives (Ruiter et al., 2017). Vulnerability assessments can be conducted at micro, meso or macro spatial scales. Microscale assessments, as required for the refugee camp scale, often pose challenges in data collection, especially in developing countries where metadata on land use, exposure, and population may be lacking. Despite these challenges, microscale assessments (the smallest spatial scale, focusing on very detailed, localized areas) can provide an overview of vulnerability hotspots across larger areas, enabling decision-makers to allocate resources effectively for emergency responses or risk mitigation (Malgwi et al., 2020). Other indicators operate on larger scales, such as mesoscale (regional to national) and macroscale (international) (Malgwi et al., 2020). However, it must be considered that since vulnerability indicators are adaptable to a regional context,

a set of indicators chosen for a specific region may not necessarily apply to another region (Papathoma-Köhle et al., 2019).

Of the methods analysed, the indicator approach appears to be the most suitable for use in data-scarce regions and, thus, for assessing micro-scale vulnerability in refugee camps, as its need for empirical data is comparatively low. Further, by integrating multiple drivers contributing to flood vulnerability, the indicator approach can be easily tailored to specific conditions, providing a clearer picture of the overall vulnerability and a holistic view of the individual vulnerability contributing factors (Malgwi et al., 2020). Further, the vulnerability can be represented in a spatial context, allowing decision-makers to take more informed mitigation measures in specific regions (Nasiri et al., 2016). This claim has been justified by H. Chen et al. (2011), who found that the indicator-based approach gives a better understanding of vulnerability assessment compared to other methods used and additionally enables the integration of uncertainty communication, operationalizing uncertainty analysis in the decision-making process.

3.2 Using GIS methods for flood vulnerability modelling

Natural disasters inherently possess a spatial dimension, necessitating access to comprehensive geographic information concerning hazards and vulnerable areas to prepare for such events (Ouma & Tateishi, 2014) adequately. Geographic Information Systems (GIS) offer enhanced decision-making capabilities by enabling the identification and assessment of predetermined criteria through overlay processes. GIS allows comparisons across spatial units and integrates qualitative and quantitative assessments, enabling dynamic logical and numerical operations. GIS has, therefore, long been an indispensable tool for analysing natural hazards, which are multidimensional and inherently spatial (Coppock, 1995). Cutter et al. (2003) highlights the importance of integrating spatial relations into the vulnerability assessment concept, stressing the vulnerability concept's strong relationship to the particularities of a specific place. However, spatial approaches to evaluate vulnerability at a local level in rural or developing countries are still lacking (Kienberger, 2013), even though it is evident from a conceptual standpoint that vulnerability possesses distinct spatial and temporal dimensions (Kienberger, 2012). Integrating the concept of vulnerability into a GIScience context further helps to understand better the characteristics of vulnerability, where Kienberger (2013) defines those characteristics using the following principles:

- WHERE: Vulnerability differs spatially
- WHEN: Vulnerability changes over time
- WHAT: Vulnerability encompasses different dimensions
- WHY: Vulnerability assessments primarily address policies aimed at minimizing or preventing the adverse consequences of disasters.
- HOW: Vulnerability is indirectly assessed and characterized by specific indicators that enable the representation and monitoring of various vulnerability dimensions.

Kienberger (2013) emphasises the strong dependency of vulnerability on the principles of scale where "vulnerability can exist everywhere at any place, but it depends on its degree, whereby in certain areas it may be close to zero, while in others it may have a higher degree". Providing essential responses to

the questions of "where", "what", and "how" are crucial for overcoming challenges in a cooperative planning context, particularly in the case of disaster risk reduction (Kienberger, 2013), which is why this thesis attaches the greatest importance to these three questions.

3.2.1 Spatial quantification of flood vulnerability

To answer "how" vulnerability can be assessed, the abstract flood vulnerability concept and its contributing variables need to be quantified using spatial operations. Due to the multidimensional nature of vulnerability as a concept, there is a need to condense the potentially available spatial data into a set of key indicators influencing the vulnerability. This simplification aids in estimating vulnerability more effectively (Birkmann, 2013). As described by Fozaie and Wahid (2022), aggregation of indicators into a composite index is commonly performed using spatial approaches such as multi-criteria decision analysis (MCDA).

3.2.1.1 Multi-Criteria-Decision-Analysis for flood vulnerability assessment

Multi-Criteria Decision Analysis (MCDA) is an umbrella term encompassing a collection of methods used to evaluate multiple conflicting criteria in decision-making processes (Hussain et al., 2021). MCDA allows for a comparative evaluation of alternatives based on multiple criteria, providing a structured method to organize information and facilitate confident decision-making (Sadr et al., 2018). The process typically involves several steps, including formulating the decision problem, developing a model with hierarchical criteria, selecting a suitable MCDA method, and aggregating information to make informed decisions (Greene et al., 2011).

Integrating Multi-Criteria Decision Analysis (MCDA) techniques into disaster risk management has gained prominence in today's research (Y. Chen et al., 2013). Numerous studies have utilized MCDA in spatial flood vulnerability assessments, allowing the integration of multiple factors that influence flood vulnerability from various geographical layers into a single index using GIS (Y. Chen et al., 2010). As the MCDA can evaluate interactions between numerous components in multi-layered problems (Nachappa et al., 2020), it is well suited for assessing flood vulnerability. A recent study by Osman and Das (2023) employed GIS-based MCDA to evaluate flood hazard, vulnerability, and risk in the Shebelle River Basin in southern Somalia. Their research underscored the effectiveness of MCDA in examining flood-related factors. Similarly, Gupta and Dixit (2022) utilized MCDA-AHP in flood risk mapping in Assam, India, highlighting the value of MCDA in identifying and integrating flood risk assessment factors at regional and administrative levels. The literature also emphasizes the importance of integrating MCDA in flood vulnerability assessments across diverse geographical contexts. For example, Hussain et al. (2021) utilized GIS-based MCDA for flood vulnerability assessment in District Shangla, Pakistan, highlighting the applicability of MCDA in evaluating coping capacities in spatial vulnerability analyses.

Fozaie and Wahid (2022) stress that the weighting system is the most critical aspect of aggregating data for a composite index. While some studies employ equal weights, this approach is unsuited for complex phenomena like flood vulnerability. Further Fozaie and Wahid (2022) conclude that the most reliable weighting system is the expert weighting method, where a panel of experts in the relevant field is tasked with selecting the weights for the individual indicators contributing to the flood vulnerability. Therefore, MCDA often uses the Analytical Hierarchy Process (AHP) to derive expert-based indicator weights (Y. Chen et al., 2010).

3.2.1.2 Indicator weighting through the Analytical Hierarchy Process (AHP)

Within the GIS-based MCDA, the Analytical Hierarchical Process (AHP) is the most frequently used method in today's literature to determine criteria weights (Y. Chen et al., 2010; Nachappa et al., 2020; Torfi et al., 2010). As introduced by Saaty (1977), AHP is a methodology based on pairwise comparisons, intending to derive weights (also called priorities) for a set of criteria of a given multiple-criterion decision problem. The approach uses expert judgments to establish priority measures to obtain criteria weights by generating a pairwise comparison matrix (Saaty, 1977, 1987, 2008). A detailed description of the mathematical procedure of the AHP-criteria weights calculation is given in Chapter 4.1.8.1. Within the particular case of flood risk modelling, AHP is a widely implemented geospatial method due to its ability to combine heterogeneous data extensively and the ease of acquiring weights for numerous criteria (Y. Chen et al., 2010). AHP is, for example, used in recent studies from Ganji et al. (2022), Lyu et al. (2018), Ramkar and Yadav (2021), and Xie et al. (2011). Further, Ramkar and Yadav (2021) highlight that AHP is a highly suitable tool for examining flood vulnerability in data-scarce regions, as it enables the understanding of individual factors that influence vulnerability by using experts' knowledge to bridge the lack of data. However, this method has limitations due to subjectivity, uncertainty, and inconsistency (Fozaie & Wahid, 2022), which are often ignored in studies using MCDA methods (Y. Chen et al., 2013).

Multiple recent studies have stressed the urgency of addressing this issue by integrating sensitivity and uncertainty analysis into MCDA and AHP, such as H. Chen et al. (2011), Y. Chen et al. (2010), Y. Chen et al. (2013), Refsgaard et al. (2007), and Walker et al. (2003). Future studies should acknowledge the uncertainties arising from AHP for flood vulnerability modelling to enhance the reliability of the results (An et al., 2022; Ramkar & Yadav, 2021), hence facilitating informed and tailored mitigation actions.

3.2.2 Uncertainty analysis in flood vulnerability modelling

Generally, two sources of uncertainty in risk assessment are distinguished in academic sources, including aleatory uncertainty, which refers to inherent variability or randomness in quantities across time, space, or among populations, and epistemic uncertainty arising due to human limitations in understanding, measuring, and describing the system under study, resulting from lack of knowledge, ignorance, or specification errors (Apel et al., 2008; Xie et al., 2011). For the particular case of this thesis, modelling flood vulnerability in data-scare regions, the assessment of epistemic uncertainty is of significant interest. Delavar and Sadrykia (2020) further categorises different sources of epistemic uncertainty, namely vagueness and non-specificity, the latter including inconsistency and ignorance of information.

Epistemic uncertainty within the AHP methodology arises from various sources, including raw data, data processing, criteria selection, and weighting, whereof the determination of criteria weights tends to be a primary source of controversy and uncertainty (Y. Chen et al., 2013). This can stem from decision makers' incomplete awareness of their criterion preferences or ambiguity surrounding the nature and scale of the criteria. In cases involving multiple decision makers, deriving a single set of weights may not be feasible; instead, ranges of weights are obtained, resulting in multiple sets of outcomes (Y. Chen et al., 2010). Although recognizing uncertainty has increased in the current literature, effective incorporation of uncertainty analysis in MCDA is rarely performed (H. Chen et al., 2011).

Since uncertainty is ignored in the AHP, the Triangular Fuzzy Number (TFN) - AHP, here denoted as FAHP, is preferred when dealing with complex decision problems with multiple attributes. Instead of using crisp numbers to assign the degree of importance of an indicator criterion, (Ganji et al., 2022) suggests using FAHP fuzzy numbers based on triangular fuzzy membership functions. By replacing crisp numeric weights with fuzzy numbers that encode the most likely value and its spread, the FAHP can consider subjectivity and vagueness in assigning weights to criteria (Dutta, 2015). Implementing fuzzy sets into the flood vulnerability quantification using the FAHP approach is a particularly suitable tool to address epistemic weight uncertainties.

Ouma and Tateishi (2014) highlighted the potential of combining AHP with fuzzy logic techniques in urban flood vulnerability and risk mapping. By integrating FAHP with GIS techniques, the researchers have developed a comprehensive flood vulnerability index that considers multiple parameters and uncertainties in flood risk assessments, using a case study in the Eldoret Municipality in Kenya. Ganji et al. (2022) conducted a recent study employing the FAHP methodology to the vulnerability of Aq'Gala, Iran, to riverine floods. The authors quantified flood vulnerability rates using geospatial data and MCDA, where the weights of the vulnerability criteria were obtained through an AHP-based questionnaire fuzzification using triangular fuzzy numbers. Additionally, the study compared flood vulnerability mapping outcomes derived solely from AHP weights with those derived from FAHP, which incorporates considerations for uncertainty. This comparative analysis revealed a notable alignment between FAHP-derived results and a specific historical flood event, evidenced by satellite time series data (Ganji et al., 2022).

3.2.2.1 Sensitivity analysis in spatial flood vulnerability models

Numerous studies have highlighted the impact of weighting on composite indices, raising concerns about the robustness and validity of the results of flood vulnerability models due to associated uncertainties and doubts (An et al., 2022; Fozaie & Wahid, 2022; Hussain et al., 2021). An approach to acknowledge the effect of weight uncertainties on flood vulnerability is to include weight sensitivity analysis to the flood vulnerability assessment process (Mekonnen et al., 2023). Sensitivity analysis is crucial in improving the robustness and reliability of flood vulnerability modelling methodologies that incorporate MCDA techniques. Despite its importance, sensitivity analysis is not commonly practised in the literature, leading to a lack of understanding of the spatial aspects of weight sensitivity (Y. Chen et al., 2010). For instance, Mekonnen et al. (2023) compared flood hazard zoning in the Upper Awash River Basin in Ethiopia using AHP and sensitivity analysis. By validating flood hazard maps through sensitivity analysis, the study showcased the effectiveness of AHP in evaluating flood vulnerability and emphasized the role of sensitivity analysis in refining flood risk assessments. Furthermore, Radmehr and Araghinejad (2015) utilized fuzzy spatial MDCA for flood vulnerability analysis in the Tehran urban basin and conducted sensitivity analysis by adjusting the weights of decision-making criteria. This methodology enabled the assessment of various scenarios and the identification of the most influential criteria in flood vulnerability modelling, thereby enhancing the overall reliability of the assessment. Addressing the gap of including sensitivity analysis to MCDA flood vulnerability modelling hampers the ability to visualize spatial change dynamics in relation to decision-making problems, which is crucial for more accurate and effective assessments (Y. Chen et al., 2010).

3.3 Flood vulnerability modelling for refugee camps

While considerable research has been conducted on flood vulnerability modelling in urban regions, there remains a significant gap in literature specifically addressing the unique challenges in modelling flood risk and vulnerability in refugee camps. A smaller number of studies, such as An et al. (2022), Anwana and Owojori (2023), Malgwi et al. (2020), and Mwalwimba et al. (2024) focus on the assessment in remote locations, such as humanitarian settlements or refugee camps, where limited data and minimal infrastructure pose significant challenges.

Given that refugee camps exhibit different flood vulnerability issues compared to those of a settled population, it is crucial to assess the flood vulnerability using an approach specifically tailored to the refugee camp context (ARSET, 2024). Few recent studies have begun to focus on this critical area, highlighting the importance of tailored flood risk and vulnerability assessments that account for these temporary settlements' distinctive socio-economic and physical conditions (Bernhofen et al., 2023; Owen et al., 2023). Even though several studies have recently stressed the importance of flood risk assessments for refugee camps (Anwana & Owojori, 2023; Cutter et al., 2003), practical spatial approaches to quantify the specific in-camp vulnerability are non-existent to date.

Bernhofen et al. (2023) highlight the importance of assessing flood risk in refugee camps, emphasizing using global flood risk data to understand and manage potential flood hazards. The study quantifies vulnerability as a part of the flood risk model utilizing building footprint data and local camp population data to estimate flood exposure in Ethiopian refugee camps. Further, Bernhofen et al. (2023) introduce simple hazard vulnerability thresholds to quantify flood exposure, tailored explicitly to refugee camps. The hazard vulnerability thresholds are thereby dependent on the flood hazard intensities (given by flood depth and velocity) corresponding to varying levels of impact. Recognizing the absence of specific thresholds for refugee camps, the authors developed four flood depth thresholds based adapted to the refugee camp context. These thresholds categorize risk into four levels: low, medium, high, and very high, focusing on immediate risks to life. Incorporating these thresholds into the overall flood risk analysis, the study calculated the flood risk faced by camp inhabitants. To illustrate that, the results showed that most flood-exposed refugees (80 - 85% of inhabitants of the analyzed refugee camps in Ethiopia) were exposed to flooding with low risk to life, corresponding to flood depth of below 0.15 m. However, significant health risks due to flooded latrines, increasing disease risk, and structural damage to tents and temporary structures are well expected (Bernhofen et al., 2023). The approach utilized global flood models, enabling cost-effective solutions to mitigate flood risks in refugee camps. However, the approach primarily addresses the exposure component of flood risk rather than modelling vulnerability as a standalone concept. Hence, it does not account for the inherent vulnerability of the elements or systems themselves, which would include multiple factors such as the physical robustness, socio-economic status, and adaptive capacities of the affected population and infrastructure. Further, they ignore the social vulnerabilities of camp inhabitants. Factors like economic status, age, gender, marital status, flooding experience, and household size can impact disaster resilience, yet they are not accounted for in this approach. (Bernhofen et al., 2023) conclude by addressing the urgency of integrating knowledge of camp planners and managers into refugee flood risk analysis, highlighting the importance of their understanding of the internal organization and vulnerability of the camps. Additionally, they emphasize the necessity for a globally applicable methodology to evaluate flood risks in refugee camps, encompassing all sites housing forcibly displaced individuals. Such an approach would enable international agencies to comprehend their global risk

exposure more effectively and provide a standardized initial risk assessment for managers and planners at each camp (Bernhofen et al., 2023).

A recent NASA project from 2024 uses earth observation data to assess flood risks, heat stress, and drought impacts in refugee camps, highlighting the topicality of the here-discussed issue. One of the three-part training lectures on the NASA ARSET training program on "Earth Observations for Humanitarian Applications" addresses flood risk mapping for refugee camps, integrating geospatial and demographic data to quantify climate risks and support decision-making in humanitarian contexts (ARSET, 2024). Within the frame of the program, an online workshop was conducted in June 2024, presenting the work done by Bernhofen et al. (2022, 2023) with the aim to government ministries, international agencies, NGOs, academics, and researchers involved in humanitarian response (ARSET, 2024).

Further, Owen et al. (2023) present a novel methodology to measure climatic and environmental exposure in refugee camps systematically. Using remote sensing and geospatial data, the authors present an index quantifying the camp's exposure relative to a simulated population of potential camp locations within the hosting country. Applying the index to five countries in East Africa, the findings indicate that seven out of the seventeen camps fall within the upper two quartiles of exposure, implying that over six hundred thousand refugees live in camps facing higher exposure than other potential locations. The study highlights the importance of reliable, low-cost, and standardized methods for collecting and analyzing climatic and environmental data in geographically remote humanitarian settings (Owen et al., 2023). While the approach provides valuable insights into the exposure levels faced by refugee camps, it does not delve into the detailed spatial assessment of vulnerabilities within the camps themselves.

3.3.1 Summarizing outlined research gaps

Ultimately, this literature review has pointed out significant research gaps, which this thesis aims to address. Summarizing these gaps, flood vulnerability modelling in refugee camps faces significant challenges due to data scarcity and the unique socio-economic conditions of these areas. Existing vulnerability models often rely on empirical data that is not readily available in these settings, limiting their accuracy and transferability. Furthermore, many methodologies overlook critical social vulnerability factors essential for a comprehensive flood vulnerability and risk assessment. The need for tailored vulnerability indices that incorporate local knowledge and context-specific factors is evident, as current models primarily designed for urban areas fail to address the specific needs of refugee populations. Additionally, integrating uncertainty and sensitivity analysis into GIS technologies in these assessments remains underutilized despite their potential to enhance decision-making. Addressing these gaps through innovative and inclusive approaches is crucial for developing a robust flood vulnerability model that can effectively support disaster risk reduction in refugee camps.

4 Methodology

This chapter covers the methodology for developing a flood vulnerability index tailored to the context of refugee camps in data-scarce regions - the Humanitarian Flood Vulnerability Index (HFVI). The methodology of this thesis can be divided into two major subsections. The overall methodical procedure is illustrated graphically in Figure 4.1.

1. Conceptual index development: This section describes the steps to develop and construct a composite HFVI. The structure of the conceptual index development follows the steps proposed by the JRC and OECD (2008) to procedure composite indicators. Data and concepts are also described within this chapter, as their usage is part of the indicator development.
2. Case Study in Mahama: The case study covers steps related to working with spatial data and their analysis in more detail by implementing the constructed HFVI into a real-world application for the Mahama refugee camp in Rwanda. The case study helps to evaluate the index performance and results.

R Studio and ArcGIS Pro are used to calculate the index weights, perform the spatial mapping and analysis, and perform the uncertainty analysis using the spatial data from the case study. The markdown files containing the code used to derive the AHP and FAHP weights and the geospatial steps for applying the index to the Mahama Case Study are published on the following GitHub repository: https://github.com/akinnaznuk/HFVI).

4.1 Conceptual index development

Given that vulnerability is a multifaceted concept (Chan et al., 2022), it relies on various parameters, referred to here as "vulnerability indicators". These indicators play a role in influencing and conveying the extent of harm or damage to a system. Combining different indicators that significantly indicate the vulnerability of such systems into a single so-called composite index helps to simplify and quantify the multidimensional concept of vulnerability (Malgwi et al., 2020).

To establish a composite index, it is essential to develop a conceptual model that addresses the interconnection of key components of the indicator. For this purpose, the index development process will follow the guidelines and methodology proposed in the "Handbook on Constructing Composite Indicators" prepared by the OECD (Organization for Economic Cooperation and Development) in collaboration with the Applied Statistics and Econometrics Unit of the Joint Research Centre (JRC) of the European Commission (JRC and OECD, 2008). As proposed by JRC and OECD (2008), the conceptual model for a composite index should be adaptable to potential future system changes, enabling its use in analyzing potential flood risk. This adaptability may involve modifications to

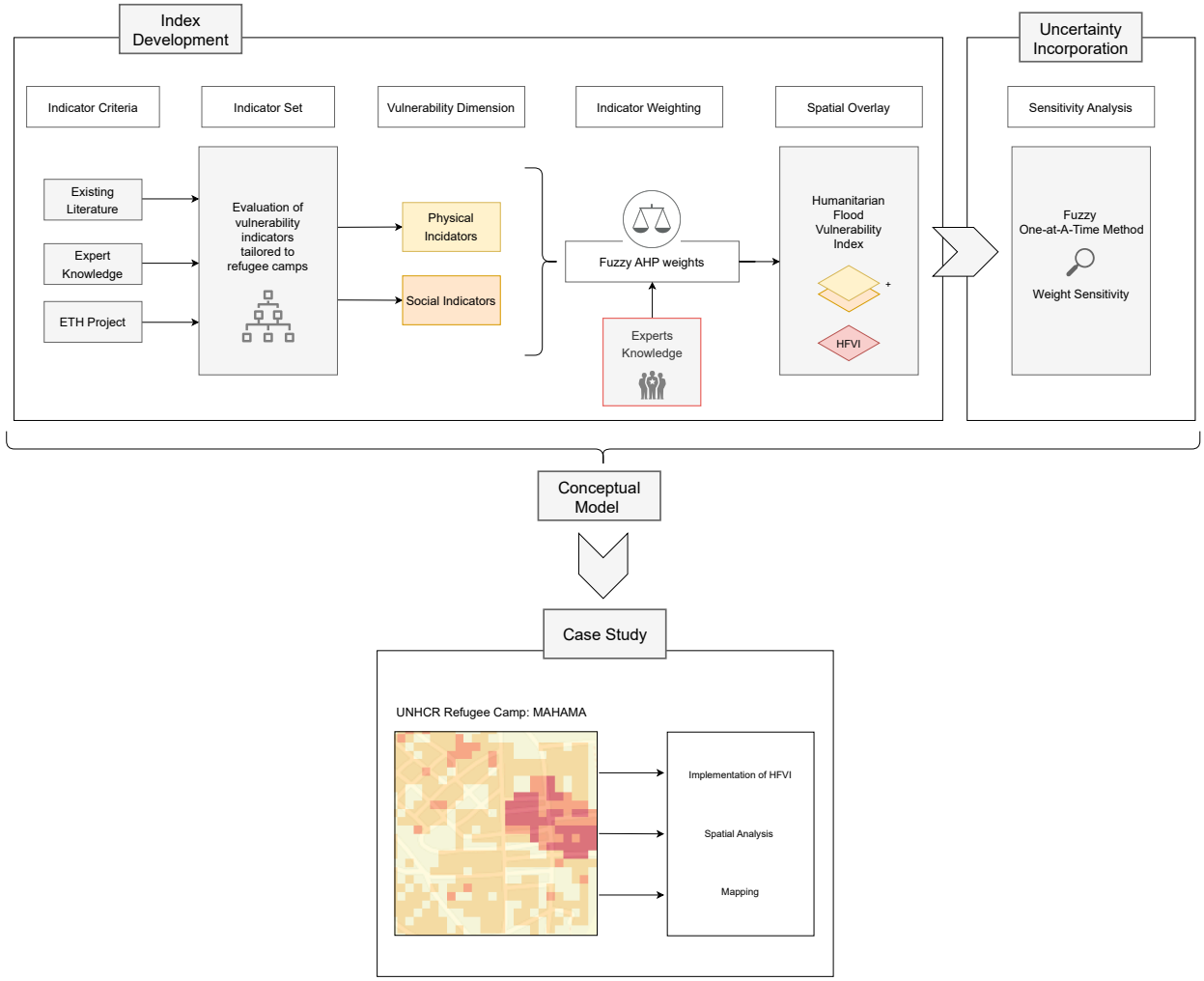

Figure 4.1: Graphical representation of the methodology.

selected indicators or their weights. The conceptual model encompasses various elements, called indicator elements, which clearly define the scope of applicability and validity of the derived index. Fundamental elements that define the conceptual model of a vulnerability index include its objective, the vulnerability dimension, spatial scale, and the application region (JRC and OECD, 2008; Malgwi et al., 2020). Birkmann (2013) comprehensively outlines nine pivotal phases for developing indicators. In developing an index called the Humanitarian Flood Vulnerability Index (HFVI), which is specifically tailored for the refugee camp setting, these phases are adopted and subtly modified to align with the research objective of integrating uncertainty arising from the experts' weighting process (Figure 4.2). The following sections highlight each of the individual phases, framing the conceptual model of the HFVI.

4.1.1 Defining the goals for the HFVI

Generally, the initial step in constructing a conceptual model for indices involves defining the purpose, encompassing various vulnerability dimensions to be evaluated (Birkmann, 2013). This ensures that the individual vulnerability indicators and the resulting index align with the overarching flood risk assessment framework (JRC and OECD, 2008; Malgwi et al., 2020), which in this case is dependent on the Flood Risk Mitigation for Humanitarian Settlements project and its implementation into the

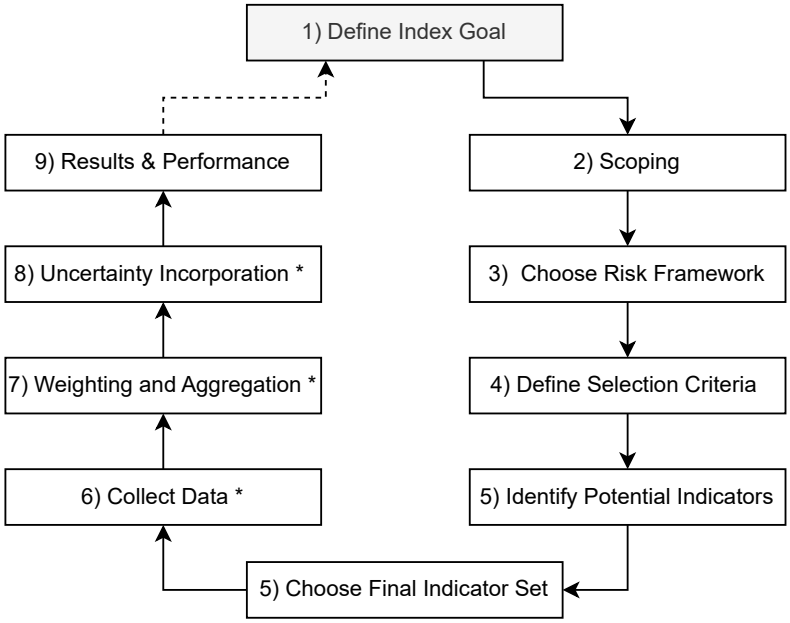

Figure 4.2: Phases of vulnerability indicator development adopted and adjusted from Birkmann (2013). Steps marked with (*) are added to fit the research objective.

developed Risk Mitigation Strategy GIS-tool.

The goal of the developed HFVI is to quantify vulnerability in refugee camps to floods in order to help improve vulnerability assessment and flood risk mitigation in refugee camps. By composing a refined composite index, which incorporates social and physical flood vulnerability dimensions, the effect of those dimensions and their associated indicators can be analyzed independently and in conjunction, forming an overall flood vulnerability index. With that, the effect of various factors influencing the vulnerability within a given refugee camp could be analyzed to help tailor flood risk mitigation actions. Further, the HFVI incorporates expert knowledge on flood vulnerability indicator weights. The importance of individual social and physical indicators to the overall flood vulnerability can be refined by interrogating a broad field of experts in an interdisciplinary field that combines natural hazard processes, flood vulnerability modelling, and humanitarian work. The elaborated experts' weights and the proposed combination thereof with the selected vulnerability indicators show a new approach to quantifying flood vulnerability, specially tailored to refugee camps, which could be integrated into the Risk Mitigation Strategy GIS tool. Additionally, the index also adds a secondary information source by providing a quantification of weight uncertainty associated with the developed HFVI. With this add-on, UNHCR staff and decision-makers using the Risk Mitigation Strategy GIS tool could be enabled to interpret flood vulnerability in a more informed way by providing information on uncertainty, which in turn should lead to better decision-making (Delavar & Sadrykia, 2020; Ganji et al., 2022).

4.1.2 Index scoping

In the second step of the index development phase, the scope of the HFVI is defined by identifying the target group and the purpose for which the HFVI will be used. Further, the spatial and temporal scope of the index is defined (Birkmann, 2013). For the development of the HFVI, the following scope

is set:

- **Target group:** The HFVI is developed for UNHCR staff and camp officers operating in refugee camps. It is designed to be integrated into the Risk Mitigation Strategy GIS-Tool created by the Flood Risk Mitigation for Humanitarian Settlements project, which aims to enable local staff to monitor flood risk within their camps and implement associated mitigation measures.
- **Purpose:** By offering stakeholders a refined and understandable flood vulnerability index, the HFVI aims to enhance the understanding of the spatial behaviour of flood vulnerability and, consequently, flood risk (as a combination of vulnerability and hazard) within the local refugee camp. This involves identifying areas with high vulnerability to flooding events. Additionally, the index should provide insights into the impact of individual factors and their contributions to overall vulnerability, allowing for the development of targeted mitigation actions.
- **Spatial bound:** The HFVI is designed for local-scale implementation, covering the typical extent of UNHCR refugee camps. Its resolution is detailed enough to identify small-scale spatial differences within a camp, pinpointing vulnerable areas. Additionally, the HFVI ensures reproducibility, allowing it to be applied to any refugee camp globally.
- **Temporal bound:** The HFVI reflects the current state of flood vulnerability but is designed to be easily adjustable to accommodate the dynamic nature of camp settings and evolving definitions of vulnerability.

4.1.3 Framework for Flood Vulnerability Assessment in Refugee Camps

The third phase involves selecting an appropriate conceptual flood risk framework, which structures the indicators and integrates the vulnerability part into the broader flood risk assessment framework. The choice of framework depends on the indicators' purpose, the definition of the vulnerability concept, the target audience, and data availability (Birkmann, 2013). A new framework has been elaborated since no existing framework in the literature is ideally suited for the HFVI's defined scope and its incorporation into the Risk Mitigation Strategy GIS-Tool specification. Even though this thesis only focuses on the flood vulnerability assessment, a broader flood risk framework has been proposed to guarantee the designed vulnerability index is in line with the work done in the Flood Risk in Humanitarian Settlements project. The "Framework for Flood Vulnerability Assessment in Refugee Camps" is specifically tailored to evaluate the effect of flood vulnerability in refugee camps independently and facilitates the integration of the HFVI into the GIS Tool for a general flood risk assessment. The framework adapts elements from the holistic BBC (Bogardi & Birkmann, 2004; Cardona, 2004) and MOVE Birkmann et al. (2013) conceptual framework, defining risk as the product of hazard and vulnerability and combines it with the conceptual framework of the Flood Risk in Humanitarian Settlements project.

$$Risk = Hazard \times Vulnerability$$

Key components of the risk concept are, on the one hand, the hazard assessment, which is based on determining the exposure to flooding (use of climate models and geographical information systems to identify areas at risk of flooding within the camp) and the possible intensity and frequency of flooding events (Maskrey, 1989). The flood risk exposure term, as defined by Kienberger (2013), is here regarded as part of the hazard component. On the other hand, vulnerability can be evaluated as

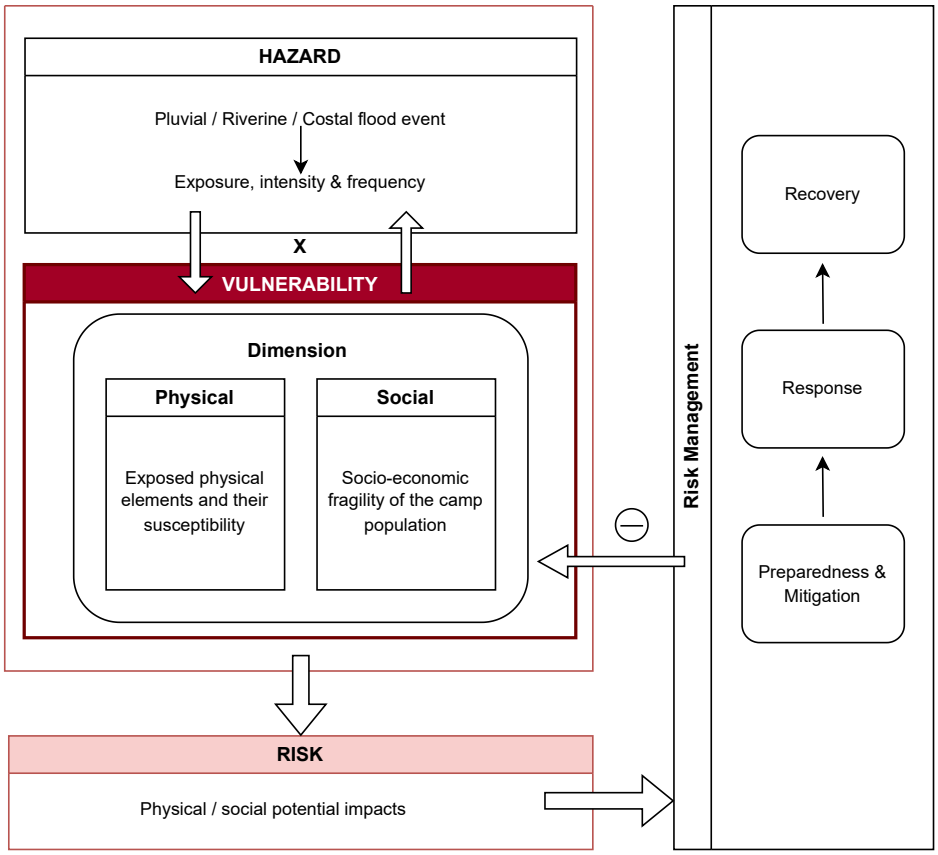

Figure 4.3: The Framework for Flood Vulnerability Assessment in Refugee Camps. The thesis and the developed HFVI focus on the vulnerability part of the framework. The framework's Hazard and Risk Management parts align with Rohling et al. (2023).

a multidimensional construct, incorporating both social and physical dimensions. The physical vulnerability dimension can be described by the exposure and susceptibility, including physical elements within the camp that are exposed to flooding (e.g., shelters, infrastructure) and the likelihood of damage to these elements based on their location or construction quality. Hence, physical vulnerability constraints the operational processes in the camps (Birkmann, 2013; Gairing et al., 2024). On the other hand, the social vulnerability dimension can be described as the social fragility of the camp population or the negative socioeconomic consequences when an asset or system is damaged due to a flood event (Gairing et al., 2024). Social vulnerability includes factors such as vulnerable population groups and access to resources and facilities contributing to the community's vulnerability (Birkmann, 2013). The adopted framework, adjusted to the scope of the HFVI index, is shown in Figure 4.3. The physical and social dimensions are described by a series of indicators that quantify the respective vulnerability of the dimension.

4.1.4 HFVI selection criteria

The fourth phase involves defining selection criteria for potential indicators. While there's a broad agreement on what makes a "good-quality" indicator-like being "scientifically valid," "responsive to change," and "based on accurate and accessible data" - there is a need to tailor these criteria to fit the specific context and goals (Birkmann, 2013). This is especially important when used for refugee

camps where data is often scarce. Hence, data accuracy and, more importantly, data availability is essential. Building on the standard criteria for index development evaluated by Birkmann (2013), criteria for selecting indicator sets are adapted to focus on the defined scope of the HFVI and are summarized in Table 4.1. Policy relevance and cost-effectiveness as standard criteria, as defined by Birkmann (2013), are ignored here, as it is difficult to interpret the fulfilment of these criteria under the given conditions of the refugee camps.

Table 4.1: Selection of criteria for the HFVI indicators and results, adopted from Birkmann (2013).

Indicator Criteria	
– Measurable / Quantifiable	– Easy to interpret
– Relevant (represents an issue that is important to the relevant topic)	– Validity / Accuracy
– Analytically and statistically sound	– Reproducible
– Understandable	– Based on available data
– Sensitivity (sensitive and specific to the underlying phenomenon)	– Data comparability
	– Appropriate scope

4.1.5 Review of potential indicator sets

The selection of potential indicators for flood vulnerability in refugee camps is based on an extensive and broad literature review (see Section 3 in the field of flood-related natural disaster management and assessment. The elaborate work from the Flood Risk in Humanitarian Settlements project (Kaufmann et al., 2022; Rohling et al., 2023) and the exchange with the team members further provided refugee camp-specific information and an understanding of the existing conditions. The resulting set of potentially suitable indicators is categorized according to their vulnerability dimension. The collection of the potential flood vulnerability indicators is summarized in Appendix A.

4.1.6 Selection of final HFVI indicator sets

Based on the preliminary collection of potentially suitable vulnerability indicators, a final set of indicators is selected based on fulfilling the predefined indicator criteria (Table 4.1). According to the indicator criteria, the selection process specifically focused on the availability of data and the indicator's relevance for the specific context of the refugee camp but also considered the remaining criteria. Firstly, indicators must be measurable and quantifiable. For categorical indicators, it should be possible to derive sub-indicators with different weightings and to calculate counts per area or density. Secondly, the relevance of each indicator is assessed in exchange with the Flood Risk Mitigation for Humanitarian Settlements project team, ensuring alignment with the specific conditions and settings of refugee camps. Lastly, reproducibility and data availability are prioritized. This criterion encompasses the use of both global data and local data, utilizing standard UNHCR camp maps and incorporating local knowledge. The final selection process resulted in a set of eight flood vulnerability indicators tailored to the given humanitarian context, summarized in Table 4.2.

4.1.6.1 Definition of the selected HFVI indicators

Based on the proposed framework, the vulnerability indicators are divided into a social and a physical vulnerability dimension, containing four indicators each. The social indicators are abbreviated

Table 4.2: Final flood vulnerability indicator set including social and physical flood vulnerability dimensions.

Dimension	Abbr.	Indicator name	Data Source	Description	Data Type	Ordinal Encoding	Scope
Social	SOC1	Population	Google Open Buildings Dataset (Sirko et al., 2021)	Population density (derived from camp population and shelter count per area)	quantitative	continuous	global
	SOC2	Vulnerable groups	PGIS mapping workshop with camp officers (Gairing et al., 2024)	Presence of vulnerable groups	qualitative	categorical > boolean	local
	SOC3	Facilities of social importance	UNHCR camp site layout	Frequency of facility type per area	qualitative	categorical > integer	local
	SOC4	Land use	Global Land Cover and Land Use (Potapov et al., 2022) or UNHCR camp site layout	Land Cover class of social importance	qualitative	categorical > boolean	global / local
Physical	PHY1	Shelter type	Google Open Buildings (Sirko et al., 2021) and PGIS mapping workshop with camp officers	Residential shelter types	qualitative	categorical > integer	global / local
	PHY2	Critical Infrastructure	PGIS mapping workshop with camp officers	Presence and type of critical infrastructure	qualitative	categorical > integer	local
	PHY3	Facilities physical vulnerability	UNHCR camp site layout	Counts of facility type per area	qualitative	categorical > integer	local
	PHY4	Roads	Open Street Map Highways Dataset (OpenStreetMap contributors, 2017)	Frequency of road types per area	categorical	categorical > integer	global

SOC1-4 and include population, vulnerable groups, facilities of social importance, and land use. The physical dimension includes the indicators PHY1-4, namely shelter type, critical infrastructure, facilities' physical vulnerability, and roads. The individual vulnerability indicators are described below. Detailed spatial data processing steps for the individual indicators on a grid layer basis are explained in more detail using the case study application and its results in Section 4.2.

Population (SOC1): Population density is selected as the first indicator influencing social vulnerability towards floods. Population density directly influences the level of exposure and potential impact of floods on individuals residing in refugee camps. A higher population density in an area increases the number of people at risk during a flood event, intensifying the population's vulnerability to flood-related hazards (P. Wang et al., 2022). The population indicator is quantified as the average number of people per shelter within a camp. Shelters are counted for each raster cell to determine the population density for each cell within the area of interest.

Vulnerable Groups (SOC2): Vulnerable groups, such as children, women, elderly individuals, and individuals with disabilities, may be disproportionately affected by floods in densely populated settings, highlighting the importance of considering demographic characteristics in vulnerability assessments (Saeedullah et al., 2021). The location of vulnerable groups within a refugee camp is obtained by information through participatory mapping workshops with the local UNHCR camp officers, as proposed by Rohling et al. (2023). The presence of vulnerable groups can then be mapped and quantified using Boolean coding, whereby grid cells that spatially correspond to the location of vulnerable groups are assigned the value 1, and grid cells in which no vulnerable groups are present or where no information is known are assigned the value 0.

Facilities of social importance (SOC3): The social importance of facilities, such as healthcare centres, schools, and community spaces, plays a critical role in enhancing the adaptive capacity of refugee populations in the face of floods. Access to essential services and infrastructure can mitigate the

impacts of floods on vulnerable communities and contribute to their overall resilience (Alduraidi et al., 2021). The social importance of camp facilities is quantified by encoding the categorical data of facility types using predefined vulnerability ranks and integrating them with spatial data on facility locations. The ranks used to assess the social vulnerability of these facility types were evaluated as part of the Risk Mitigation for Humanitarian Settlements project, in collaboration with UNHCR employees (Rohling et al., 2023). The following facility types are taken into account: Schools (Lower Primary Schools, Early Child Development facilities), Health Centers (Health Centers, Temporary Health posts, Isolation center), Cultural facilities (Community centres, Religious centres, Markets), Youth/women centres (Youth centers, Women/Girls opportunity centre, Child-friendly spaces), Administrative Facilities (Agencies compound, UNHCR offices), Security (Police station), Nutrition Centers, and Distribution centre.

Land use (SOC4): Incorporating the social importance of specific land uses, such as agricultural land, tree cover and protected forests, and sensitive ecological areas, into a flood vulnerability index for refugee camps is essential for understanding the unique vulnerabilities and resilience factors associated with different types of land use within the camp setting (Rohling et al., 2023). The socioeconomic importance of agricultural land in the context of flood vulnerability assessment for refugee camps could provide valuable insights into food security, livelihoods, and community resilience in the face of flood events. Especially agricultural land is crucial in enhancing the livelihoods and food security of refugees living in camps. Studies have shown that refugees often use crop production as a primary agricultural activity to improve their food security and household incomes (Muhangi et al., 2022). The classification of land use types includes categories such as built-up areas, agricultural land, vegetation, water, and open spaces. Among these, only agricultural land is considered highly vulnerable in terms of its ecosystem services. Since built-up areas are already accounted for in other indicators, they are not considered vulnerable in this context.

Shelter Type (PHY1): Incorporating shelter type as part of the physical vulnerability towards floods in a flood vulnerability index for refugee camps is crucial as the type of shelter can significantly impact its resilience to flood events. Emergency or transitional shelter structures like tents may not have a foundation slab, making them vulnerable to flooding, especially if refugees sleep on the floor with no higher ground to move their possessions to during a flood (Bernhofen et al., 2023). Typical shelter types can be classified into emergency, transitional, durable and abandoned (Rohling et al., 2023):

- Emergency Shelters are habitable covered living spaces designed to provide a secure and healthy environment with privacy and dignity. Typically, simple one-room structures are implemented to offer critical life-saving emergency assistance.
- Transitional Shelters encompass a range of shelter options that assist populations affected by humanitarian crises in progressing from initial emergency arrangements to more suitable shelter solutions better adapted to their needs in terms of habitability.
- Durable Shelters describe shelters beyond the emergency and transitional phases. These shelters are adapted and contextualized based on elements such as climate, cultural practices and habits, local availability of skills, access to adequate construction materials, and geographical context.
- Abandoned: Shelters, which are not inhabited but often show fragile structure

Critical Infrastructure (PHY2): The critical infrastructure (CI) indicator includes spatial information about water and sanitation facilities, drainage systems, communication networks, power stations, and

water storage within refugee camps (Rohling et al., 2023). Further, buildings in critical condition are considered within the CI indicator as to illustrate their enlarged potential for higher physical vulnerability due to reduced resilience (Nkwunonwo, 2021). It is essential to consider critical infrastructure in the physical vulnerability dimension of the HFVI, as these infrastructures are vital for maintaining health, managing floodwater, coordinating responses, and ensuring essential services. Evaluating their vulnerability helps prioritize maintenance, upgrades, and resilience-building measures to safeguard refugees during flood events (Bruijn et al., 2015; Len et al., 2018; Pant et al., 2017).

Facilities physical vulnerability (PHY3): The physical vulnerability of facilities is highlighted as a critical element at risk during floods (Kaoje et al., 2021). Assessing and mapping the physical vulnerability of individual facilities alongside socioeconomic vulnerabilities, a more holistic approach to flood vulnerability assessment can be achieved (An et al., 2022). Analog to the social vulnerability ranks of the camp facilities, ranks quantifying the physical vulnerability are adopted from Rohling et al. (2023).

Roads (PHY4): The roads indicator describes the vulnerability of transport infrastructure for internal and external mobility, including internal roads and walkways, access roads, bridges, and gas stations (Kaufmann et al., 2022). Roads and transport elements are often affected by flooding, as they play a critical role in facilitating access to and from refugee camps, and their vulnerability to floods can significantly impact the camp's overall resilience and response capabilities (Balijepalli & Oppong, 2014). Road networks determine access to various areas, including emergency services, hospitals, and evacuation routes. By incorporating road data into flood vulnerability assessments, planners can identify areas that may become inaccessible during floods, helping to prioritize response efforts in planning evacuation routes, accessing essential services, and the overall camp infrastructure integrity (Aahlaad et al., 2021). The roads and respective vulnerabilities are categorized according to the official OSM tags: residential, service, unclassified, path, footway and ridge (OpenStreetMap contributors, 2017).

4.1.6.2 HFVI decision hierarchy

Based on the selected and defined final HFVI indicators, a decision hierarchy is conceptualized (Figure 4.4, where the index goal represents the highest level of the hierarchy, and subsequent levels contain the vulnerability dimensions and their associated vulnerability indicators upon which the goal depends (Saaty, 2008). In a later step, the hierarchy will be used as a basis to develop an appropriate weighting scheme using the Analytical Hierarchy Process (AHP) through expert consultation.

4.1.7 Data collection

4.1.7.1 AHP survey data

In order to explore the relative importance and the degree of contribution of each individual vulnerability indicator to the overall flood vulnerability in a specific area of the refugee camp, the selected vulnerability indicators were ranked by a selected group of experts. This participatory procedure is intended to evaluate suitable weights for the individual vulnerability indicators based on the experts' knowledge using AHP to increase the robustness and reliability of the approach. The ranking is performed by designing and conducting a survey questionnaire, where the participants were asked to compare the individual indicators pairwisely and assign associated ranks of the relative importance of one indicator over another. The questionnaires are designed to be easily understandable, and their

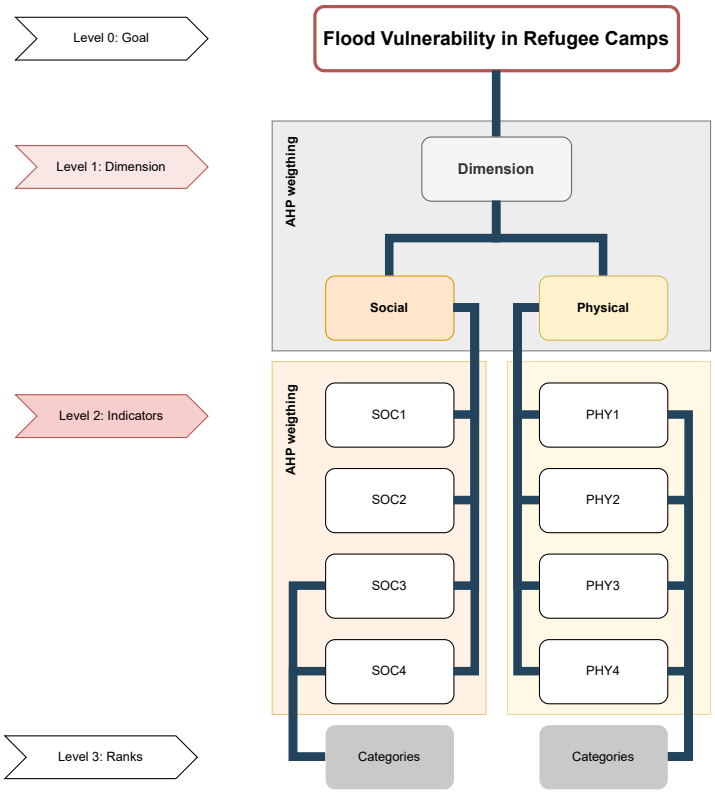

Figure 4.4: HFVI Decision Hierarchy and respective hierarchy levels, including social and physical vulnerability indicators.

structure is based on the previously developed AHP hierarchy, containing the comparison of the different vulnerability indicators within their respective dimensions: social & physical vulnerability (Level 2: indicators). Detailed instructions were given to introduce the participants to the topic, define relevant terms, and explain the individual indicators, which are compared repetitively. The questionnaire template is attached in Appendix A.

Next to comparing the relative importance of the individual vulnerability indicators (Level 2), the influence of the vulnerability dimensions (Level 1) is also assessed within the experts' questionnaires. Initially, the definition of flood vulnerability and its framework encompassed exposure as an integral part of the vulnerability concept, serving as a secondary domain next to the vulnerability dimensions. Consequently, exposure and its sub-components, such as proximity to water bodies, slope, and elevation, were included in the questionnaire and regarded as additional vulnerability indicators. However, subsequent deliberations led to the decision to exclude exposure from the definition and framework of vulnerability based on expert feedback, asserting that exposure should be assessed separately from vulnerability. Hence, exposure is distinctly separated from the vulnerability definition and framework, aligning with the perspective of disaster and climate risk experts. Therefore, only the pairwise comparison of the importance of the social and physical vulnerability dimensions is assessed, neglecting the exposure component. Hence, the weights of the social and physical vulnerability dimensions are later re-scaled to show their relative importance.

A total sample size of fifty-five questionnaires was distributed among experts specializing in flood risk management and modelling, refugee climate risk research, and humanitarian aid. Of these, twenty-five

questionnaires were sent to UNHCR officials in refugee camps around the world, while the remaining questionnaires were sent individually to researchers and experts in the fields mentioned. The distribution of these questionnaires to UNHCR officers was added to a larger survey conducted by the ETH research team, focusing on flood risk in refugee camps. The questionnaire was designed as an online survey for UNHCR officers and as an interactive PDF file for the remaining experts; however, it showed the same structure. Its design aimed for simplicity and clarity, ensuring that participants did not need prior knowledge of the AHP methodology. Every participant was then requested to assess the indicator pairs using a numerical scale from 1 to 9. A priority rank of 1 means that two indicators are indifferent regarding their influence on the flood vulnerability in an area within any given refugee camp, while a score of 9 illustrates extreme priority to one indicator over another (Saaty, 1977). Eleven responses were received out of the total sample size, yielding a response rate of 20%. Unfortunately, no responses were yielded from the UNHCR camp officers' expert group. The experts who participated in the questionnaire can be categorized into two groups, as summarized in Table 4.3 based on the field of expertise: the "Hazard Modelling Group" (Expert IDs: 01-06) and the "Humanitarian Group" (Expert IDs: 07 - 11). A list of the experts and their areas of expertise can be found in Appendix A.

Table 4.3: List of expert groups for the AHP weighting.

Categorization of expert groups and their respective fields of expertise	
Hazard Modelling Group: Expert IDs: 01-06	**Humanitarian Group:** Expert IDs: 07-11
– Natural Hazards Modeling and GIS – Climate Change research – Disaster Management	– Refugee Climate Risk – Humanitarian Aid – Interdisciplinary fields

For the subsequent analysis, each participant received a unique ID, and their questionnaire results were transformed into three separate pairwise comparison matrices (PCM). These matrices illustrate the hierarchical structure of the AHP, depicting indicator components and their levels, whereby two matrices are created for level 2 comparisons and one for level 1 comparisons, respectively. Each cell in a PCM thereby indicated the degree to which one indicator outweighs another concerning their importance towards the defined target (Saaty, 1977), here the overall flood vulnerability. Within this AHP matrix, the factor on the vertical axis is considered more important than the one on the horizontal axis, leading to scores ranging from 1 to 9. Conversely, the reciprocal values, ranging from 1/2 to 1/9, are assigned to the horizontal axis factors. The relative scale of importance is summarized in Table 4.4, showing the Linguistic scale of importance as well as the assigned priority ranks.

Table 4.4: Scale of Relative Importance of AHP ranks, their reciprocals and respective Triangular Fuzzy Number (TFN) scale (for further explanation see Chapter 4.1.8.7).

Linguistic Scale of Importance	AHP Priority Rank	Reciprocal	TFN scale
Equal importance	1	1	(1, 1, 1)
Moderate importance	3	1/3	(2, 3, 4)
Strong importance	5	1/5	(4, 5, 6)
Very strong importance	7	1/7	(6, 7, 8)
Extreme importance	9	1/9	(9, 9, 9)
Intermediate values	2,4,6,8	1/2, 1/4, ...	(1, 2, 3), (3, 4, 5), ...

4.1.7.2 Geospatial datasets

Based on the index development phases and, in particular, the selection of the eight final flood vulnerability indicators based on the predefined selection criteria, data is collected to quantify the indicator values. These geospatial datasets can be categorised into global and local data. As summarized in Table 4.2, global data is used to derive values for indicators SOC1, SOC4 and PHY1, whereas local data is used for SOC2, SOC3, PHY1, PHY2 and PHY3.

4.1.7.3 Global data

The initial data search prioritized open-source global datasets that align with the defined indicator criteria (Table 4.1). These datasets are chosen because they support the reproducibility of the index at a global scale, facilitating the comparison of data across different regions. Additionally, the use of freely available and global datasets aligns with the goals of the Flood Risk Mitigation for Humanitarian Settlements project (Rohling et al., 2023), which aims to map flood risk in refugee camps worldwide. By employing these datasets, the index ensures both the accessibility and comparability of the data.

Buildings: The Open Buildings dataset (v3 polygons) from 2023 is used, which is created from satellite imagery of 50 cm resolution, where deep learning algorithms are used to detect building footprints. The outputs were trained and tested for different housing categories, including rural, urban, and towns, as well as settlements for refugees or internally displaced people. The resulting dataset contains building polygon geometries and information about the confidence score assigned to each detected building. The accuracy of the dataset is thereby influenced by the completeness and actuality of the data as well as the detection errors of the model (Sirko et al., 2021).

From the Open Buildings dataset, the following indicators are derived as described:

- SOC1: Population density
- SOC3 and PHY3: Geometries of facility buildings
- PHY1: Geometries of shelters

Population density: Rasterized global population maps are commonly used to quantify the effects of population density on flood vulnerability in national or regional flood risk assessments (Bernhofen et al., 2022). However, Bernhofen et al. (2023) demonstrate in a recent paper that such global population datasets do not accurately capture the camp populations. In fact, they claim that even the most accurate global population datasets available, on average, overlook three-fifths of the actual camp population exposed to flooding. To counteract this mismatch, Bernhofen et al. (2023) propose an alternative method for representing the exposed camp population by integrating reported camp population estimates with building footprints, which is used here to map the dynamic camp population most accurately. Therefore, the Open Buildings global dataset is used as the camp building footprint, filtered to contain only residential shelters, and augmented with the latest UNHCR camp reports information on the actual camp population. The camp population is thereby distributed evenly across the shelters within the camp boundary.

Roads / Transport: To quantify the roads and transport vulnerability indicator, the OpenStreetMap (OSM) Highways dataset is used. OSM provides open-access road data, which is frequently updated by a global community of contributors (OpenStreetMap contributors, 2017). This makes it a valuable resource for conducting flood vulnerability assessments, especially in areas where official data may be

limited or outdated. OSM refers to any road, route, or path on land that connects different locations as "Highways". It includes any route that has been paved or improved, even if just by frequent use, allowing travel by motorized vehicles, cyclists, pedestrians, horse riders, and more (excluding trains, which are covered under Railways). The highway dataset is further classified into different highway categories. Within the refugee camp environment, the classes "Roads" and "Paths" are of main interest, including road tags such as:

- Roads: motorway, trunk, primary, secondary, tertiary, unclassified, residential, service
- Paths footway, cycleway, bridleway, path, steps, escalator

The OSM Highways dataset is used to derive indicator layer PHY4.

Land Use: The land use indicator can be derived from the Global Land Cover and Land Use (GLCLUC) dataset (Potapov et al., 2022). This dataset, sourced from the Landsat archive, provides comprehensive global coverage of land cover and land use changes from 2000 to 2020. The open-source dataset contains gridded data with a resolution of 30 meters. It includes detailed classifications of various land use types such as agricultural land, tree cover, protection forests, and sensitive ecological areas. Integrating this dataset helps to accurately quantify and analyze the socioeconomic significance of different land uses within the study area. Alternatively, official UNHCR camp layout maps can be used for additional spatial land use information or the validation of the GLUCLUC data in the given study area.

4.1.7.4 Local data

Integrating local data alongside global datasets is crucial for enhancing the accuracy and relevance of flood vulnerability assessments. Bernhofen et al. (2023) emphasize the importance of augmenting global data with local information to comprehensively evaluate flood risks and flood vulnerability in refugee camps. To construct the HFVI, local data is used to derive categorical indicators, such as the existence of Vulnerable Groups (SOC2) or Facilities of physical vulnerability (PHY3). However, as local datasets are in general not (freely) available for refugee camp areas due to their remote locations and rapid changes in camp conditions and environment (Bernhofen et al., 2023; Owen et al., 2023), local information is gained from official UNHCR camp site maps or from local knowledge through interviews or participatory mapping with experts, staff or residents of refugee settlements.

Local data and participatory knowledge are used for the following vulnerability indicators:

- SOC2: Presence of especially vulnerable groups
- SOC3: Classification of facilities of social importance
- PHY1: Classification and location of shelter types
- PHY2: Presence of critical infrastructure
- PHY3: Classification of facilities of physical importance

4.1.8 Weighting and uncertainty incorporation

The weights obtained through the AHP questionnaires serve as critical inputs for weighting and aggregating the individual indicators to form the HFVI. This process ensures a robust and balanced portrayal of vulnerability factors based on expert opinions. Subsequent sections elaborate on detailed

insights into the AHP methodology, the weight calculation and the fuzzification procedure.

4.1.8.1 The Analytical Hierarchy Process (AHP)

The Analytical Hierarchy Process (AHP) stands out as an ideal methodology for prioritising multi-attribute decision problems due to its ability to handle both qualitative and quantitative data, accommodating various criteria, here also called indicators. Its popularity stems from its simplicity in obtaining criterion weights and its capability to integrate heterogeneous data, particularly in situations where specifying exact relationships among numerous evaluation criteria is challenging (Y. Chen et al., 2013; Yang et al., 2013), as is the case for flood vulnerability in refugee camp settings. AHP's reliance on pairwise comparisons enhances the reliability of criterion weight determination compared to direct weight assignments, as it simplifies the process by facilitating attribute comparisons (Torfi et al., 2010).

The AHP commonly involves four operational steps to systematically make decisions and establish priorities (Ganji et al., 2022; Ouma & Tateishi, 2014; Saaty, 1977, 2008; Zahedi, 1986). In the first step, a decision hierarchy is conceptualized based on the defined goal of the underlying problem at the highest level, with further criteria and sub-criteria defined on lower levels upon which the goal depends (Saaty, 2008). This hierarchical structure has already been established for the HFVI during the conceptual index development phases as a subsequent step of the final indicator selection. The second step of the AHP involves pairwise comparisons of these criteria to assign relative importance values, as previously discussed in the AHP survey section. Following this, the "eigenvalue" method is used in the third step to calculate the relative weights of all indicators. Finally, these values are aggregated in a fourth step to derive a final set of indicator weights (Zahedi, 1986).

4.1.8.2 Mathematical derivation of AHP weights

This section focuses on the mathematical steps to calculate the indicator weights based on the constructed AHP hierarchy. The following derivation is guided by the research from (Ouma & Tateishi, 2014; Saaty, 1987, 2008). All processing steps to assess the final indicator weights based on the AHP survey data are performed in R using the "ahpsurvey" package (Cho, 2019), developed for AHP survey data analysis. The code can be found in the HFVI repository in the "AHP.Rmd" file.

As a first data processing step, each participant's collected individual priority scores from the completed AHP questionnaires are analyzed, where C is the evaluated set of indicator components per AHP hierarchy level, here denoted as criteria.

$$C = \{C_j \mid j = 1, 2, ..., n\} \tag{4.1}$$

Each criterion j in the set of C is compared to every other criterion i. Consequently, three independent positive reciprocal pairwise comparison matrices (PCMs) are constructed for each participant, depicting the respective AHP hierarchy levels (SOC, PHY and DOM), where n is the number of criteria. The resulting PCM can be presented as an n x n matrix A.

$$A = \begin{array}{c} \\ C_1 \\ C_2 \\ \vdots \\ C_n \end{array} \begin{array}{c} \begin{array}{cccc} C_1 & C_2 & \cdots & C_n \end{array} \\ \begin{bmatrix} a_{11} & a_{12} & \cdots & a_{1n} \\ a_{21} & a_{22} & \cdots & a_{2n} \\ \vdots & \vdots & \ddots & \vdots \\ a_{n1} & a_{n2} & \cdots & a_{nn} \end{bmatrix} \end{array} \quad with \;\; a_{ii}, = 1, a_{ji} = 1/a_{ij}, a_{ij} \neq 0 \tag{4.2}$$

Each element a_{ij} (where i,j = 1,2, ..., n) in the matrix represents the importance or priority assigned to criterion C_i compared to criterion C_j. These matrix elements, denoted as a_{ij}, represent the quotients of relative importance and inherently possess positive values (Ouma & Tateishi, 2014). In case criterion i, which is stored in the row, is believed to have higher priority compared to the criterion j in the column, the quotient is noted as an integer value $a_{ij} \in$ [1,9]. In contrast, a lower priority of the row criterion compared to the column will be noted as reciprocal value $a_{ji} = 1/a_{ij} \in [\frac{1}{2}, \frac{1}{9}]$. In case of equal importance (main diagonal elements), the quotient will be given the value 1 (Saaty, 1977). As a further step, the column values are normalized using the following formula (Ouma & Tateishi, 2014) so that all columns add up to 1:

$$r_{ij} = \frac{a_{ij}}{\sum_{i=1}^{n} a_{ij}} \tag{4.3}$$

4.1.8.3 Individual and aggregated criteria weights

Next, the relative criteria weights are analyzed for each participant and PCM. The individual criteria weights are derived by computing the *right eigenvector* (v), which corresponds to the *largest eigenvalue* (λ_{max}) as given in Equation 4.4, where A_w depicts the weighted matrix.

$$A_w = \lambda_{max} v \tag{4.4}$$

To calculate the right eigenvector v, the normalized matrix elements r_{ij} are averaged across each row (Torfi et al., 2010) using the *ahp.indpref* function. The result is a set of 11 individual criteria weights for each vulnerability indicator of each comparison level. The individual criteria weights can be compared in a later step to assess differences in participants' priorities and inconsistencies. Additionally, the aggregated criteria weights are computed by aggregating the individual priorities of all participants. The aggregation is done by calculating the arithmetic mean of the individual responses using the *ahp.aggpref* function from the ahpsurvey package.

4.1.8.4 Consistency analysis

Saaty (1980) has demonstrated that the eigenvalue λ_{max} is always higher or equal to n, which is the number of indicators components (at one level of the hierarchy). Smaller deviation of λ_{max} and n indicate a higher consistency of the weighting results. In the case of total consistency of the pairwise comparison results, λ_{max} equals n (Ouma & Tateishi, 2014; Zahedi, 1986). With this assumption, the consistency of the pairwise comparison judgement can be estimated to analyse the quality of the results. The consistency is determined by the relationship among the entries of a matrix A (Ouma & Tateishi, 2014), and hence by the answers of the pairwise comparison questionnaire. To evaluate the consistency of a PCM, the Consistency Index (CI) as given in Equation 4.5 (Saaty, 1980) has been

computed as a first step, depicting the coherence of the experts' judgment during the questionnaire evaluation (Aguarón et al., 2003).

$$CI = \frac{\lambda_{max} - n}{n - 1} \tag{4.5}$$

Having determined the CI, the final Consistency Ratio (CR) is computed using the *ahp.cr* function to conclude the overall consistency of the individual evaluation results. The CR is the ratio of the CI and the Random Consistency Index (RI). The RI is an average index for randomly generated weights developed by Saaty (1980). The reference values for the RI with n $\leq$ 10 can be extracted from Table 4.5. The CR value for each individual evaluation result is calculated using Formula 4.6:

$$CR = CI/RI \tag{4.6}$$

The value of CR is then compared to a predefined threshold, which depicts the interval in which the experts' judgment is accepted to fluctuate in consistency (Torfi et al., 2010). In the literature, a threshold of CR = 0.1 is widely accepted, where smaller values close to zero illustrate higher consistency. Therefore, here the consistency threshold is also set to $CR_T = 0.1$. In case of a threshold exceedance, the results should be ignored or reevaluated to resolve inconsistencies in the pairwise comparison (Aguarón et al., 2003; Zahedi, 1986).

Table 4.5: Reference table for RI values, adopted from Saaty (1980).

n	1	2	3	4	5	6	7	8	9	10
RI	0	0	0.58	0.90	1.12	1.24	1.32	1.41	1.45	1.49

4.1.8.5 Dealing with inconsistency

After evaluating the consistency of the rank values, inconsistencies are identified in the individual PCMs to analyse the source of these inconsistencies and improve the overall weighting results. To identify such inconsistent responses, the sample matrices are compared with a perfectly consistent Saaty matrix generated from preference weights calculated using the dominant eigenvalue method to identify those inconsistencies in pairwise comparisons. This comparison is facilitated by the *ahp.error* function, which iterates through all individual PCMs, providing a list of error consistency matrices and the mean consistency error for each matrix. The function *ahp.pwerror* automates the process further by extracting the pairwise comparison with the maximum inconsistency error, thereby returning a list of each participant's most inconsistent pairwise comparisons. Additionally, it generates a data frame highlighting the top three most inconsistent pairwise comparisons for each participant, which helps to find criteria pairs with the most frequent judgment errors (Cho, 2019).

4.1.8.6 Transforming inconsistent PCMs

Having identified the data inconsistencies, the next step involves transforming inconsistent PCMs to derive more reliable criteria weights. While some studies suggest reevaluating survey results based on inconsistent participant feedback (Brito et al., 2018), such reassessment was deemed too time-consuming for the experts within the context of this thesis. Alternatively, other studies have developed methods to autonomously adjust inconsistent PCMs for rectifying inconsistencies in AHP studies when

direct interactions aren't feasible (Pascoe, 2022). Through stochastic simulation, (Finan & Hurley, 1997) discovered that adjusting the pairwise comparison matrix post hoc to enhance consistency also enhanced the reliability of preference weights. Subsequently, several algorithms have been devised to adjust the preference matrix to minimize inconsistency.

Saaty (2003), for example, proposes the so-called Harker's algorithm. Harker's algorithm aims to improve the consistency of pairwise comparison matrices in the Analytic Hierarchy Process (AHP). It starts by identifying the entry in the matrix that is farthest from ideal consistency (pairwise comparison with max. error). To identify such entries, Harker suggests calculating a new matrix where each element is the result of dividing the original matrix element by the product of the corresponding row and column weights. Once the entry with the largest value in this new matrix is found, the algorithm focuses on improving the judgment associated with this entry by replacing the max. error by 0, eliminating the influence of the inconsistent judgment on the overall comparison. The corresponding diagonal entries are replaced with 2. In a pairwise comparison matrix, the diagonal entries should indicate perfect consistency as those entries represent the comparison of each criterion with itself. Assigning a value of 2 to the diagonal entries ensures that each criterion remains consistent with itself, maintaining the relative importance of criteria in the overall comparison process Harker (1987).

To compute the Harker's adjustment, the *ahp.harker* function from the ahp.survey package (Cho, 2019) is used to transform inconsistent PCMs by iterating through the individual PCMs. The ahp.harker function thereby replaces inconsistent PCMs by iterating through the most inconsistent comparison pairs. The iteration parameter determines the number of pairwise comparisons to be modified. For instance, when iterations = 3, ahp.harker adjusts the top three most inconsistent pairwise comparisons. The number of maximum iterations is thereby based on the number of matrix elements n and can be determined by calculating

$$n_{max,iter} = \frac{n * (n-1)}{2} \tag{4.7}$$

However, it should be considered that each adjustment leads to some loss of information. Therefore, after a comparative analysis of the iteration results, the number of iterations is set to the minimum value, at which the number of inconsistent values did not change. Also, the algorithm is set to stop the iteration when a consistency ratio of CR = 0.1 is reached (Cho, 2019). Essentially, Harker's method involves pinpointing the most problematic comparison, adjusting it to match the overall comparison pattern better, and recalculating weights to ensure consistency.

After optimizing the individual PCMs using Harker's adjustment, new CR values are calculated and compared to the consistency threshold of $CR_T = 0.1$. Answers that are still inconsistent are filtered out and not considered when calculating the aggregated criteria weights.

4.1.8.7 The Fuzzy Analytical Hierarchy Process

Despite the effectiveness and popularity of the AHP to handle multi-criteria problems, the method has been criticised in the current literature for its inability to deal with uncertainty and imprecision. Using the traditional AHP approach for pairwise comparison and criteria weighting evaluation assumes that the experts can make a numerically unambiguous judgement, whereas in reality, their preferences are uncertain or imprecise. Given the already vague definition of flood vulnerability, the underlying decision problem is difficult to evaluate using crisp numbers of priority ranks. In fuzzy logic, crisp

numbers refer to values that are not fuzzy or uncertain but rather deterministic. Fuzzy logic allows for representing degrees of truth, enabling statements to be partially true or partially false rather than strictly true or false. This multi-valued approach in fuzzy logic contrasts with the traditional binary logic, providing a more nuanced and flexible framework for reasoning and decision-making (Metzger et al., 2018). The concept of crisp values is fundamental in understanding the transition from classical logic to fuzzy logic, where the boundaries between truth values become blurred, allowing for a more realistic representation of uncertainty and vagueness in various applications (Pinheiro et al., 2018). Therefore, an extended method of the traditional AHP is used to represent the fuzzy multi-attribute environment of the flood vulnerability concept through fuzzy logic, called the Fuzzy Analytic Hierarchy Process (FAHP) (Torfi et al., 2010). The R code containing the FAHP weight calculations can be found in the "FAHP.Rmd" file on the HFVI repository.

In contrast to the traditional AHP method, the FAHP is able to tolerate inherent uncertainty and vagueness stemming from human decision-making, potentially enhancing the accuracy and reliability of the results (Roy et al., 2023). The FAHP methodology was introduced by Chang (1996) and is based on the Fuzzy set theory developed by Zadeh (1965). A fuzzy set is thereby defined as a group of objects with an associated degree of membership between 0 and 1. The degree is described by a membership function, which expresses how strongly an object belongs to the set (Yang et al., 2013). On the contrary, crisp set objects have a membership degree of either 0 or 1 (Delavar & Sadrykia, 2020). Within the Fuzzy set theory, a Triangular Fuzzy Number (TFN) is expressed by a lower bound (l), a modal value (m), and an upper bound (u) and denoted as *A = (l, m, u)*. The upper and lower bounds thereby specify the interval fuzzy degree, while m depicts the most probable risk value. The associated membership function is defined as in Equation 4.8 and can be plotted as illustrated in Figure 4.5.

$$\mu_A(x) = \begin{cases} \frac{(x-l)}{m-l} & l \leqq x \leqq m \\ \frac{x-u}{m-u} & m \leqq x \leqq u \\ 0 & \text{otherwise} \end{cases} \qquad (4.8)$$

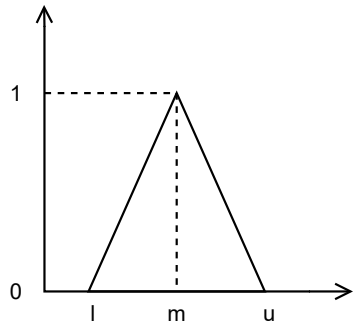

Figure 4.5: Triangular fuzzy number membership function.

Implementing the membership function from Equation 4.8, the individual TFNs can be derived directly from the assigned crisp AHP ranks (1-9) as illustrated in Table 4.4 (in Section 4.1.7.1), where the initially assigned AHP priority rank (1-9) will become the modal TFN value m, with l and u depicting the neighbouring priority ranks. Accordingly, the individual PCMs of the traditional AHP are fuzzified with respect to the TFN scale (see Figure 4.6, resulting in PCMs constructed from fuzzy numbers (Ganji et al., 2022; Mosadeghi et al., 2015; Roy et al., 2023), here denoted as fuzzy PCMs or FPCMs. An example of a transformed FCPM can be seen in Table 4.6.

The FAHP methodology proposed by Fozaie and Wahid (2022) is adopted to obtain the fuzzy weights, which offers guidance to researchers aiming to enhance expert weights. To determine the fuzzy weights

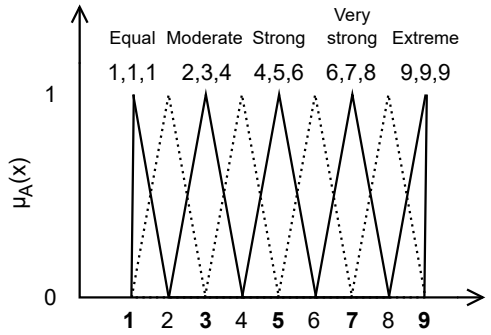

Figure 4.6: Triangular fuzzy number membership functions and scale of importance.

Table 4.6: Example of a fuzzified AHP PCM (FPCM) for the social vulnerability indicators containing assigned ranks as fuzzy numbers

Indicator	SOC1	SOC2	SOC3	SOC4
SOC1	(1, 1, 1)	(1/7, 1/6, 1/5)	(1/8, 1/7, 1/6)	(1/2, 1, 2)
SOC2	(5, 6, 7)	(1, 1, 1)	(1/2, 1, 2)	(6, 7, 8)
SOC3	(6, 7, 8)	(1/2, 1, 2)	(1, 1, 1)	(6, 7, 8)
SOC4	(1/2, 1, 2)	(1/8, 1/7, 1/6)	(1/8, 1/7, 1/6)	(1, 1, 1)

based on the newly generated individual FPCMs, Buckley's geomean method is implemented (Buckley, 1985). This process involves multiplying the lower bound of the TFN for each column together, raised to the power of 1/n, where n represents the number of variables. Here, 'l' denotes the first integer corresponding to the triangular fuzzy value set l, m, u of indicator i. Mathematically, this is expressed as the geometric mean and can be derived using Equation 4.9:

$$r_l = [l_{i1} \times l_{i2} \times ... \times l_{i1n}]^{1/n}, \qquad analog : r_m, r_u \tag{4.9}$$

As an illustration, applying this calculation to column 1 from the example FPCM yields $r_l = [(1 \times 1/7 \times 1/8 \times 1/2)]^{1/4} = 0.3074$. The rowsum of each indicator is calculated. This step is then repeated for the m and u values to obtain r_l, r_m, and r_u, where the geometric mean is calculated for each individual indicator i. As a next step, the fuzzy weights are obtained for each indicator, reflecting their relative importance. By multiplying the inverse of the sum of each column r_i with the corresponding values in column r_i, this step effectively normalizes the weights and ensures that they sum up to 1, making them suitable for use in the subsequent analysis. After completing this step for each individual indicator, the resulting output comprises three columns representing the fuzzy weights (w_l, w_m, w_u) of the triangular fuzzy sets. The further step in the FAHP method involves the defuzzification and normalization of the fuzzy indicator weights. Therefore, the arithmetic mean is calculated by averaging the fuzzy weights for each indicator i. (Fozaie & Wahid, 2022). The described FAHP procedure is then applied to all individual PCMs stemming from the individual AHP survey responses.

As a last step, the fuzzy as well as the defuzzified indicator weights of the individual expert responses are aggregated into a mean fuzzy weight and a mean defuzzified weight per indicator. These aggregated fuzzy indicator weights serve as the final weights to be applied to the composite index following the application of the FAHP method.

4.1.9 Indicator aggregation

After determining the individual indicator weights, the next crucial step is integrating the spatial data to apply the Humanitarian Facility Vulnerability Index (HFVI) to any camp using an MCDA approach. This involves creating individual raster layers for each vulnerability indicator as proposed by (Y. Chen et al., 2010; Radmehr & Araghinejad, 2015). The chosen raster resolution is 30 meters per grid cell, which allows the HFVI to capture local differences and spatial patterns within a camp. The final HFVI is computed using a weighted linear combination, incorporating the determined FAHP weights.

4.1.9.1 Raster calculations

Table 4.7: Vulnerability ranks of indicators subcategories: 0 = no vulnerability, 1 = low vulnerability, 2 = moderate vulnerability, 3 = high vulnerability.

Indicator	Name	Subcategory	Rank
SOC1	Population Density	-	-
SOC2	Vulnerable Groups	Presence of vulnerable groups	3
		No presence of vulnerable groups	0
SOC3	Facilities of social importance	Schools and ECD	2
		Health Center	3
		Cultural Facilities	2
		Youth/women Center	2
		Administrative Facilities	2
		Security	3
		Nutrition Center	3
		Distribution Center	2
SOC4	Land Use	Built-Up	0
		Vegetation and Water	0
		Open Space	2
		Agricultural land	3
PHY1	Shelter Type	Emergency Shelters	3
		Transitional Shelters	2
		Durable Shelters	1
		Abandoned	0
PHY2	Critical Infrastructure	Fragile Building Infrastructure	3
		Sanitary Infrastructure	3
		Water Tanks	3
		Drainage System	2
		Communication Infrastructure	3
		Power Station Infrastructure	3
PHY3	Facilities physical vulnerability	Schools and ECD	2
		Health Center	2
		Cultural Facilities	3
		Youth/women Center	2
		Administrative Facilities	2
		Security	2
		Nutrition Center	2
		Distribution Center	2
PHY4	Roads	Residential Road	2
		Service Road	3
		Path	1
		Footway	1
		Bridge	3
		unclassified	1

The process begins by quantifying and normalizing the individual indicator layers to obtain raster values ranging from 0 to 1. Quantification of the indicator values is conducted on a raster cell basis, where each cell represents counts of elements, densities, or the presence of elements, depending on the indicator. For indicators that can be directly quantified by numerical values (such as population density), values are normalized and classified into vulnerability classes based on equal intervals, with higher densities indicating higher vulnerability. For indicators of a categorical nature, sub-categories (e.g., different facility or road types) are first assigned predefined vulnerability ranks partly based on the evaluated ranks outlined by Rohling et al. (2023). Table 4.7 summarises selected indicator subcategories and their assigned ranks. The occurrence of each category per grid cell is then counted, and a weighted sum of the relative categories is calculated using these vulnerability ranks. The resulting raster values are subsequently normalized to a scale of 0 to 1. As an additional step, these normalized indicator values are categorized into four vulnerability classes: "NONE" (0 or no vulnerability), "LOW" (1 or low vulnerability), "MODERATE" (2 or moderate vulnerability), and "HIGH" (3 or high vulnerability).

4.1.9.2 Weighted Rraster overlay

Spatial raster overlay using the weighted linear combination is a widely used method in Multi-Criteria Decision Analysis (MCDA) for spatial modelling and analysis. This technique involves integrating the individual raster layers of social and physical vulnerability indicators, assigning weights to each layer based on the evaluated FAHP results, and overlaying them to construct the composite HFVI (Hussain et al., 2021; Ndabula & Oyatayo, 2021). The spatial overlay process consolidates all spatial data into a single map layer. First, all physical indicators are overlaid to produce a composite physical vulnerability layer, while all social indicators are combined to create a social vulnerability layer. These two layers are then overlaid to construct the final HFVI, resulting in a comprehensive flood vulnerability map incorporating physical and social factors. Social and physical vulnerability dimensions weights are also defined based on the experts' judgment on their relative importance to the overall flood vulnerability. Therefore, the HFVI is computed using the following formula:

$$HFVI = \text{wSOC}_{dim} \times \left[\sum_{i=1}^{n} \left(\text{soc}_i \ \times f\_\text{w\_soc}_i\right)\right] + \text{wPHY}_{dim} \times \left[\sum_{j=1}^{m} \left(\text{phy}_j \ \times f\_\text{w\_phy}_j\right)\right] \tag{4.10}$$

where;

- wSOC_{dim} and wPHY_{dim} are the FAHP weights for the vulnerability dimension SOC and PHY
- soc_i represents the raster for the i-th social indicator.
- $f\_\text{w\_soc}_i$ is the FAHP weight for the i-th social indicator.
- phy_j represents the raster for the j-th physical indicator.
- $f\_\text{w\_phy}_j$ is the FAHP weight for the j-th physical indicator.
- n is the total number of social indicators.
- m is the total number of physical indicators.

The HFVI values range from 0 to 1, where values close to 1 depict high relative flood vulnerability, and low values near 0 represent no flood vulnerability. Based on the given HFVI equation, the vulnerability of the social and physical dimension can also be calculated and mapped separately, only taking into account the individual addends without their dimensions weight, resulting in a HFVI_{SOC} and a HFVI_{PHY}.

$$HFVI_{SOC} = \sum_{i=1}^{n} \left(\text{soc}_i \ \times f\_\text{w\_soc}_i\right) \tag{4.11}$$

$$HFVI_{PHY} = \sum_{j=1}^{m} \left(\text{phy}_j \ \times f\_\text{w\_phy}_j\right) \tag{4.12}$$

4.1.10 Sensitivity analysis and uncertainty incorporation

To analyze the HFVI weights' sensitivity and identify areas of potential uncertainty, sensitivity analysis using the One-At-a-Time (OAT) method developed by Daniel (1973) is employed. This method aims

to ensure the robustness of the flood vulnerability assessment by testing the stability of the weights assigned to different indicators (Y. Chen et al., 2010). This is done by varying one indicator's weight at a time while keeping the others constant and observing the impact on the overall vulnerability map (Archer et al., 1997; Crosetto & Tarantola, 2001). The first step in carrying out OAT is to define a feasible range within which the weight changes can deviate. The range can be defined as a bounded set of discrete percentage changes, known as the Range of Percent Change (RPC), from the original criterion weight value used in the base run. A single range can be applied to all criteria, or different ranges can be specified for each criterion as needed (Y. Chen et al., 2010). To take into account the uncertainty in the indicator weights, which were evaluated through the experts' consultation, the RPC values are adopted to represent the spread in the bounds of the calculated fuzzy weights (w_l, w_m, w_u) of the triangular fuzzy sets before defuzzification. Therefore, the lower and upper bounds of the fuzzy weight are used as bounds for each indicator's RPC spread: $RPC_{min} = w_l$ and $RPC_{max} = w_u$. Integrating fuzzy numbers into the OAT methodology within MCDA is a novel approach not previously found in the literature. Consequently, the results of applying this FAHP-OAT method are thoroughly reviewed and discussed in the subsequent chapters of this thesis.

For the further realisation of the OAT method, the theoretical procedure described by Y. Chen et al. (2010) is followed. A series of evaluation runs is conducted where each criterion weight is altered in increments of percentage change (IPC), defined here as plus or minus 1%, across its feasible range. During this process, the weights of the other indicators are adjusted proportionally to satisfy the additivity constraint, ensuring that all indicator weights at any percentage change (PC) sum to one. The total number of simulation runs is then calculated as in Equation 4.13:

$$Runs = \sum_{i=1}^{n} \mathrm{r}_i \quad \text{and} \quad w_l \leq PC \leq w_u \tag{4.13}$$

where n is the number of indicators, and r_i is the number of IPCs within the RPC of each indicator i. When adjusting the weight of a specific indicator as the main changing criterion c_m under consideration, its weight $W(c_m, \mathrm{pc})$ at a particular PC level can be calculated using the formula:

$$W(c_m, \mathrm{pc}) = W(c_m, 0) + W(c_m, 0) \times \mathrm{PC}, \quad 1 \leq m \leq n \tag{4.14}$$

Here, $W(c_m, 0)$ represents the weight of the main changing criterion c_m in the base run.

To ensure the additivity constraint is satisfied, the weights of the other criteria $W(c_i, \mathrm{pc})$ are adjusted proportionally based on the weight $W(c_m, \mathrm{pc})$ calculated above:

$$W(c_i, \mathrm{pc}) = \frac{(1 - W(c_m, \mathrm{pc})) \cdot W(c_i, 0)}{(1 - W(c_m, 0))}, \quad i \neq m, \quad 1 \leq i \leq n \tag{4.15}$$

where $W(c_i, 0)$ is the weight of the i-th criterion c_i in the base run.

By varying the weight of the main changing criterion across different IPCs within the fuzzy RPCs, a series of evaluation maps are produced for each simulation run. These maps, along with a summary table for each criterion, quantify the changes in both input weights and evaluation outcomes in the geographical space (Y. Chen et al., 2010).

The outlined methodology for implementing the OAT method can be realized in R utilizing spatial

indicator raster data. A novel R package termed SpatMCDA developed by H. Wang et al. (2024) is employed to facilitate this process. SpatMCDA represents an innovative toolset initially crafted for evaluating areas at risk of infectious diseases through spatial multi-criteria decision analysis (MCDA). This package proves particularly advantageous in scenarios characterized by limited data availability. Notably, SpatMCDA incorporates an intrinsic function named "oat," which facilitates the execution of the aforementioned methodology. Consequently, it empowers users to generate a comprehensive uncertainty map, illustrating spatial weight uncertainty within the decision-making framework (H. Wang et al., 2024).

4.2 Mahama Case Study

The case study serves as a real test environment that allows the developed HFVI to be implemented in the specific context of a selected refugee camp and its functionality to be evaluated. The aim of the case study is to test and analyze the index results and its performance. In addition, the case study helps to illustrate the spatial data processing steps required when implementing the HFVI in any camp worldwide. The HFVI is applied using the global and local geospatial datasets described in the conceptual part of the index development (Section 4.1.7) and is implemented for the Mahama refugee camp in south-eastern Rwanda near the border with Tanzania (UNHCR, 2023a). Within the Flood Risk Mitigation for Humanitarian Settlements project, a case study was already conducted in the Mahama Refugee camp during the summer of 2022 to test the developed GIS tool. Through participatory workshops involving the Mahama camp officers, local data has been collected by Kaufmann et al. (2022), which are used within this case study.

4.2.1 Study area

Mahama Refugee Camp is located in Kirehe District, within Rwanda's Eastern Province. Established in 2015, the camp today spans 160 hectares and is, therefore, the largest refugee camp in the country. Mahama refugee camp hosts approximately 62'500 refugees, predominantly from Burundi. The camp's population is notably young, with around 51% under the age of 18. Managed by Rwanda's Ministry of Emergency Management (MINEMA) in collaboration with the United Nations High Commissioner for Refugees (UNHCR), the camp is divided into two sites, Mahama I and II, and further subdivided into 18 villages. Mahama camp offers comprehensive services, including health care, education, and various livelihood programs, facilitated by multiple humanitarian partners. More relevantly, the region is susceptible to seasonal flooding, impacting both the refugee and local communities, necessitating ongoing disaster risk management initiatives (UNHCR & MINEMA, 2023).

According to the Global Facility for Disaster Reduction and Recovery (GFDRR), river flood hazards in Kirehe are classified as high based on modelled flood information. This indicates that potentially damaging and life-threatening river floods are expected to occur at least once in the next ten years (GFDRR, n.d.). Project planning, design, and construction methods must account for this high level of river flood hazard. Additionally, surface flood hazards in both urban and rural areas may also be possible in this region and should be considered alongside river flooding when planning urban projects (GFDRR, n.d.). Kirehe District has faced significant challenges in recent years due to various climate hazards, including prolonged droughts and recent heavy rainfall. These conditions have heightened the risk of unprecedented run-offs, leading to potential flooding and landslides. The consequences have been devastating, destroying homes, eroding topsoil, and submerging crops. Among the severely

affected areas is also the Mahama sector. The latest flooding event occurred in 2019, where severe flooding affected local communities and agricultural lands (FAO, 2023). The refugee camp, housing tens of thousands of refugees, is located near the Kagera River, making it susceptible to flooding, especially during periods of heavy rainfall and because of inadequate drainage systems (Nsengiyumva, 2012). According to the researchers of the project for Flood Risk Mitigation in Humanitarian Settlements, UNHCR officers have stated in joint discussions that the camp is affected by regular flooding. Such disaster situations can exacerbate the already challenging living conditions for the refugees, many of whom are vulnerable populations, including women, children, and the elderly.

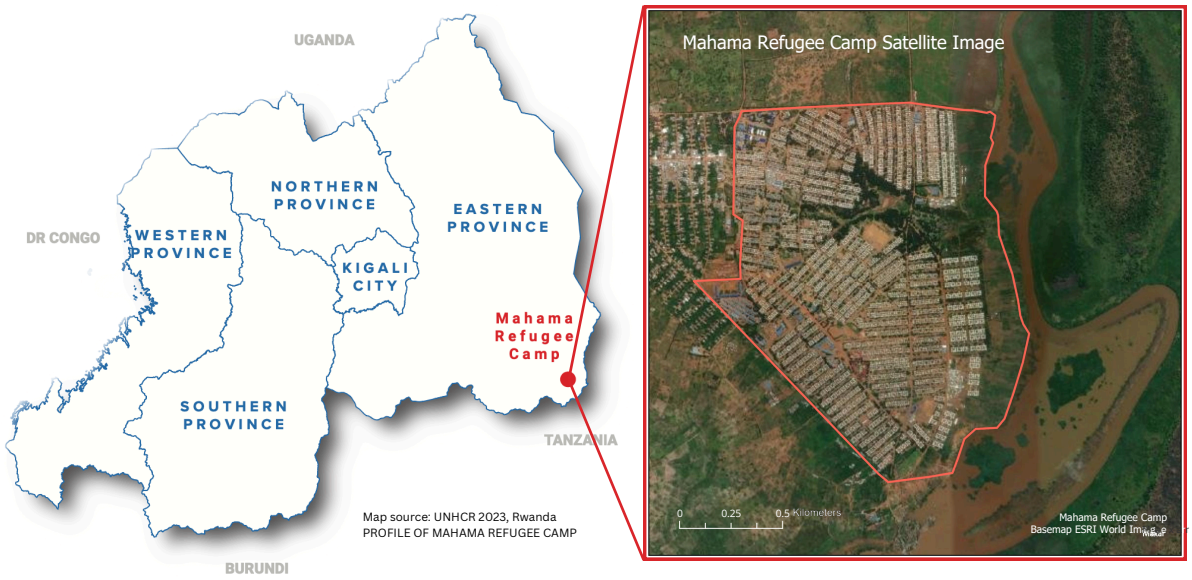

Figure 4.7: Left: Rwanda Map (UNHCR, 2023a). Right: Mahama Refugee Camp and camp boundary (ESRI World Image).

4.2.2 Application of the HFVI on the Mahama refugee camp

The code for the HFVI application to the Mahama case study, which includes quantifying the vulnerability indicators using rasterized data and spatially overlaying them to create the HFVI, can be found on the GitHub repository in the R markdown "HVFI.Rmd."

4.2.2.1 Data preprocessing

Before implementing the developed procedure of the HFVI, the geospatial data is preprocessed in ArcGIS Pro. ArcGIS Pro is utilized for data preprocessing due to the program's simplicity in digitizing, correcting and visualizing spatial data. As some local vulnerability indicator elements are derived from the latest UNHCR camp layout map or from the spatial information based on the maps from participatory workshops, these maps must be georeferenced to the Mahama camp extent. For this purpose, the latest Mahama camp layout map (UNHCR, 2020) (attached in the Appendix A) is used. The georeferenced camp layout facilitates digitising elements such as the camp boundary, facility areas, and the classification of sanitary units and land use information. Spatial information from the participatory mapping workshops conducted in 2022 is digitized into polygons, highlighting locations

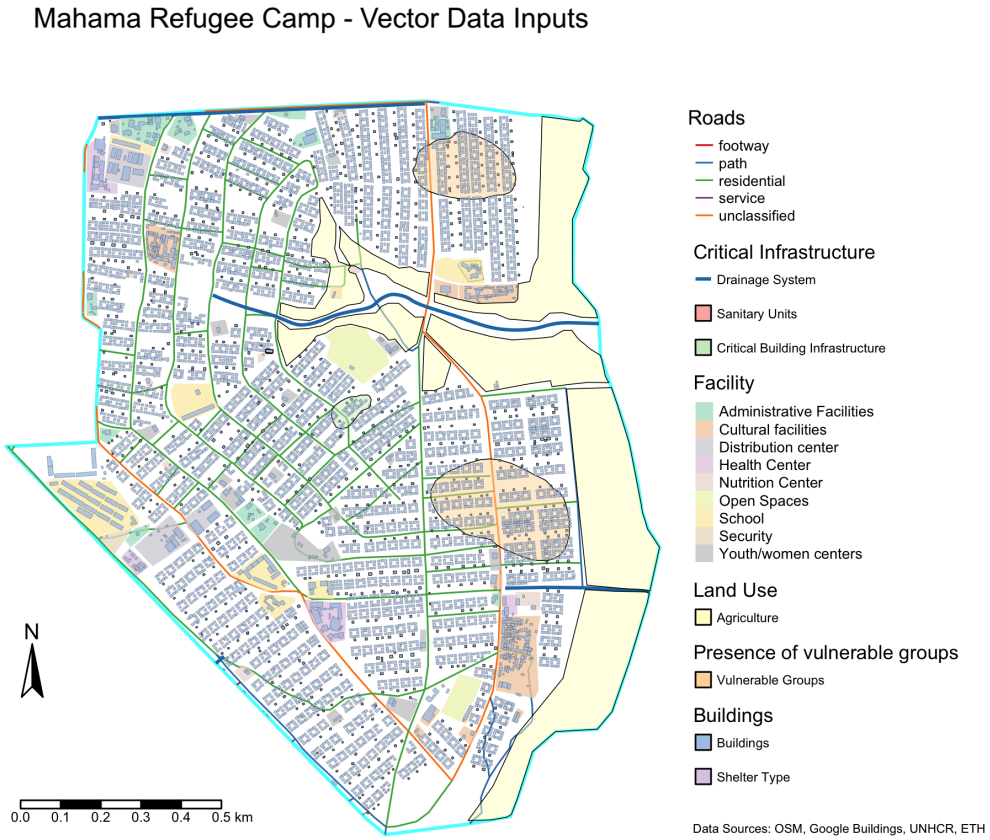

Figure 4.8: Processed vector data inputs for the HFVI mapping in the Mahama Refugee Camp.

where especially vulnerable individuals are housed and where shelters or facilities are abandoned or in poor condition. Facility areas are digitized as polygons and classified into different facility types based on the campsite map legend (UNHCR, 2020). These attributes are categorized into the defined facility type categories, as summarized in Table 4.7 (see Section 4.1.9.1. Subsequently, the global buildings dataset (Sirko et al., 2021) is clipped to the camp boundary extent and then divided into facility buildings and shelters by removing the facility areas from the building polygons using the *Erase* geoprocessing tool in ArcGIS Pro. Sanitary units are filtered out using an area threshold to differentiate between residential shelter buildings and sanitary units. This procedure results in three distinct building feature classes: residential shelters, facility buildings and sanitary units. Additionally, apparent errors in the building's dataset are corrected by comparing the polygons with the ESRI World Image Satellite Basemap from December 2022 and the camp map layout, removing inaccuracies. The attribute tables of each feature class are populated with the relevant information and their associated sub-categorization. After completing these steps, the processed data is saved and exported as shapefiles for further spatial operations in R. The resulting vector data used as inputs for the HFVI calculation are visualized in Figure 4.8.

4.2.2.2 Calculation of gridded indicator layers

As the HFVI index is conceptualized as a raster-based index depicting spatial patterns in raster cell information, the vector-based shapefiles containing the spatial information of the indicator elements and their subcategories are quantified into gridded data layers. Therefore, a 30x30-meter resolution

grid is created using the bounding box of the Mahama camp. This grid layer is utilized in the following steps to calculate grid-based metrics quantifying the spatial behaviour of the individual vulnerability indicators within the Mahama refugee camp. Finally, all layer values are normalized to a scale between 0 and 1 to enable spatial overlay, ensuring the results are standardized and comparable across different grid cells.

Population Density (SOC1): As previously mentioned in Section 4.1.7, global population datasets show insufficient accuracy to depict the small-scale spatial pattern within the refugee camp extent. Therefore, the methodology by Bernhofen et al., 2023 is adopted to derive the population density for the Mahama refugee camp by combining building footprint (from the Open Buildings dataset, version 2023 (Sirko et al., 2021)) and population statistics (from official UNHCR reports). According to the latest figures from September 2023, there are a total of 6,928 shelters in the camp. All residential shelters in the Mahama camp are uniform and have the same structural design, described as semi-permanent shelters (UNHCR, 2023a). An average occupancy per shelter is calculated by dividing the camp population by the number of available shelters. In September 2023, the camp population was at 6'2486 residents (UNHCR, 2023a). This results in an average occupancy of approximately 8 people per shelter. This number aligns with the UNHCR Mahama camp statistic, which states that one shelter is designed to accommodate two families. In other camps, where the residential shelters vary significantly in size, the number of camp residents could be distributed among the shelters by normalizing them to the area of the shelter. In the next step, the centroids of the shelters are calculated and joined with the overlaying grid to count the number of shelters per grid cell. By combining the average occupancy per shelter with the shelter count per grid cell, the population in each grid cell can be estimated, resulting in a gridded layer of population density (number of inhabitants per $900m^2$) within the camp extent.

Vulnerable Groups (SOC2): The layer for SOC2 has been obtained as previously described in Section 4.1.7, indicating the presence of especially vulnerable groups within the Mahama refugee camp. The information about the location of potentially vulnerable groups stems from the before-mentioned mapping workshop with the Mahama camp officers, where the approximate locations were mapped onto the Camp Layout Map. The mapped locations of the vulnerable groups are, in particular, mentioned to be areas where older people live (Gairing et al., 2024). Those areas are digitized as polygons in a later step and joined with the grid. Grid cells intersecting the vulnerable groups' locations are assigned a value of 1 and the remaining a value of 0. Here, the existence of vulnerable groups corresponds to a vulnerability rank of 3 / "HIGH" vulnerability and 0 to rank 0 or vulnerability class "NONE".

Land Use (SOC4): The land use data is obtained from the GLCLUC dataset Potapov et al. (2022), where the latest raster layer from 2020 is analyzed. The raster layer is, therefore, intersected with the camp boundaries. When comparing the mapped land use classes with satellite images from 2020 (CNES airbus in Google Earth Engine), it becomes apparent that the GLCLUC dataset can map the approximate extent of the built-up and cropland area. The dataset matches the spatial resolution of the index well since it is presented as a 30m resolution grid. In the data set, areas classified as cropland are categorised as agricultural land and assigned a vulnerability rank of 3 (see Table 4.7). The built-up areas are assigned a rank of 0, as the vulnerability of these areas is already taken into account in indicators SOC1 and PHY1. Further, locations of open spaces within the camp (e.g. playgrounds) are extracted from the Mahama camp site layout (UNHCR, 2020) and assigned a vulnerability rank of 2. The land use data is then merged with the grid. The available land use class is multiplied by

the assigned vulnerability rank for each grid cell and then normalised.

Facilities: Social and Physical Vulnerability (SOC3 & PHY3): To quantify the facilities' social and physical vulnerability into a raster layer, the same procedure has been followed for both indicators. Based on the facility vector data, which can be classified into the subcategories based on the Mahama Campsite layout information (UNHCR, 2020), the facilities are first assigned their associated vulnerability rank as provided in Table 4.7. Next, a spatial intersection is performed to determine which parts of the facility buildings overlap with the grid cells. Given the significant variation in facility sizes, the areas of each intersection are calculated and grouped by facility category. For each grid cell and facility category, the total intersection area is calculated and normalized by the total grid cell area to obtain a relative area per category and grid cell. Subsequently, the relative facility areas per category are multiplied by the corresponding vulnerability rank to account for the differences in the facility types' importance on the physical and social vulnerability. The weighted category values are summarized per grid cell.

Shelter Type (PHY1): The shelter type layer is calculated using shelter counts per grid cell, which were already calculated to derive the population indicator. Next, information about the shelter type is integrated. This information is derived from the participatory mapping workshop with the Mahama Camp officers (Gairing et al., 2024). However, only one area within the camp thereby was mentioned to have characteristic differences in shelter type. Here, the camp officers mentioned the presence of abandoned shelters, which are structurally sensitive but with uncertain locations. The mapped area is digitized as a polygon and joined with the shelter density grid. Grid cells containing abandoned shelters are assigned a rank of 0 to avoid duplicating the impact of fragile infrastructure, as the sensitivity of these structures is already addressed in PHY2. Due to missing information on the remaining shelters and their structural types, as well as the uniformity of the shelters within the Mahama camp, shelter density grid values are not further weighted (rank = 1 for the semi-permanent / durable shelters) in the case of no additional information of shelter type for a given grid cell.

Critical Infrastructure (PHY2): The critical infrastructure indicator quantifies the presence of fragile building infrastructure, sanitation network, drainage system, water tanks, communication infrastructure, and power stations. However, data is only available for the Mahama refugee camp for the first three sub-categories mentioned. Spatial information on the location of fragile building infrastructure and drainage channels is extracted from the participatory mapping workshop data. During the workshop, camp officers at the Mahama camp cited that the drainage channels are particularly vulnerable points where flooding occurs more frequently (Gairing et al., 2024). The location of the sanitary units is derived from the UNHCR Mahama camp site layout. Further, the sanitary building network is quantified as sanitary unit density analogue to the shelter density, calculating counts per grid cell per area. The final layer for the combined critical infrastructure is then calculated using a weighted raster overlay that multiplies the quantified grid cells by the assigned vulnerability ranks. The vulnerability ranks are again assigned to the individual subcategories based on the values from Table 4.7, where fragile building infrastructure presence is weighted with a vulnerability rank of 3, grid cells spatially intersecting drainage channels are weighted with a rank of 2 and sanitary units count with a rank of 3.

Roads (PHY4): The "OSM Highways" dataset is clipped to the Mahama camp boundary to assess the flood vulnerability of camp roads. The road types are assigned their given vulnerability rank as defined in 4.7 and are subsequently intersected with the grid. The ranks of existing road segments are

then summed and normalised for each grid cell. Grid cells with no road intersections are assigned a vulnerability rank of 0.

The results of the quantification steps of the individual vulnerability indicators are gridded spatial layers, which are then normalised and transformed into raster layers using the *st_rasterize* function from the stars package (Pebesma & Bivand, 2023) in R to enable spatial raster overlay. The individual raster layers cropped to the extent of the Mahama refugee camp boundaries, showing each indicator's quantified and normalized vulnerability values. The spatial calculation steps performed are graphically shown in Figure 4.9.

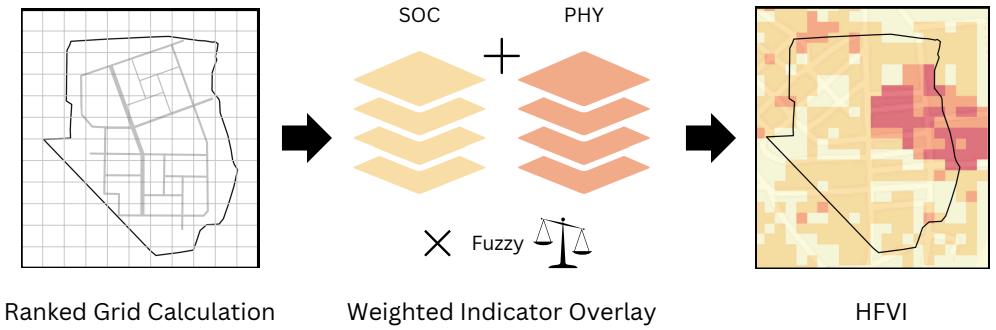

Figure 4.9: Spatial processing steps for the computation of the HFVI performed for the Mahama Case Study.

4.2.2.3 HFVI calculation, mapping and sensitivity analysis

Once the indicator layers are prepared as quantitative normalised vulnerability values on a raster basis, the HFVI for the Mahama refugee camp can be calculated using the formula described in Equations 4.11 and 4.12 , where the individual social and physical vulnerability indicators are multiplied by their associated fuzzy AHP weight and then summed to produce a final HFVI raster layer using the HFVI equation (Equation 4.10). In the final step, the HFVI values are again normalised to a scale of 0 to 1 and displayed visually on a raster map. In addition, individual maps are created separately for social and physical vulnerability in order to assess the relative influence of the social and physical vulnerability dimensions on the overall flood risk and, thus, on the HFVI results.

Furthermore, the results are mapped to assess the spatial patterns visually. Two methods are tested for the mapping of the final HFVI: Jenks classification and focal smoothing. The Jenks natural breaks classification is designed to optimize the placement of class breaks by minimizing variance within classes and maximizing variance between them. This method effectively highlights natural groupings in the HFVI values, providing a clear and intuitive visualization of areas with distinct levels of flood vulnerability (J. Chen et al., 2013) In fact, according to (Moreira et al., 2021), Jenks classification has proven to be the most suitable classification method for classifying flood vulnerability index values. Here, the HFVI values are categorized into the four vulnerability classes: "NONE", "LOW", "MODERATE", and "HIGH". The classification serves two primary purposes. First, it makes the index values more understandable for decision-makers and UNHCR camp officers. Second, categorizing vulnerability into classes 0 to 3 allows the HFVI to be seamlessly integrated into the Risk Mitigation Strategy GIS tool developed by (Kaufmann et al., 2022) for further risk calculations, which use the same classification system. This enables the index to be directly utilized within the tool, enhancing its practical applicability. Additionally, a focal smoothing filter is used to map a smoothed representation

of the HFVI. This approach applies a low-pass filter using a 3x3 kernel matrix, where the mean HFVI value within the 3x3 neighbourhood around each pixel is calculated. This focal filter effectively reduces noise by averaging out extreme values (Xu & Xie, 2019). The resulting map provides a more continuous and less fragmented depiction of flood vulnerability and hence accounts for the spatial uncertainty of the vulnerability values. Ultimately, a final map overlaps the HFVI and uncertainty values.

Based on the resulting spatial HFVI outputs, spatial analysis is performed by calculating spatial autocorrelation and creating a correlation matrix. Moran's I is used to measure the degree of spatial autocorrelation, indicating whether the global spatial pattern of the HFVI is clustered, dispersed, or random across the Mahama Camp (Anselin et al., 2005). Additionally, a correlation matrix using Pearson's correlation coefficient is created to assess the linear relationships between the different vulnerability indicators and their influence on the HFVI (Jackson et al., 2010).

Lastly, the already introduced OAT method (see Chapter 4.1.10 is implemented as a final step to perform weight sensitivity analysis, assessing and quantifying the weight uncertainty within the HFVI results.

5 Results

This chapter provides an overview of the key results and findings of this work. These results form the foundation for the subsequent discussion aimed at answering the research questions defined in Chapter 1. Specifically, the results aim to support a discussion on how flood vulnerability, as a multidimensional concept, can be effectively modelled for refugee camps and, with that, to identify the most significant factors contributing to flood vulnerability within these settings. Further, the spatial results help to discuss the primary challenges in spatial modelling of flood vulnerability in refugee camp contexts, proposing potential solutions to overcome these challenges.

The primary focus lies on the outcomes derived from weighting vulnerability indicators through the experts' consultation as part of the conceptual Humanitarian Flood Vulnerability Index (HFVI). This includes a summary of the individual vulnerability preference weights assigned by experts through the AHP procedure. Following this, the results from the AHP consistency analysis are presented, culminating in the aggregated AHP weights. Through the implementation of fuzzy logic, resulting fuzzy AHP weights are presented in a subsequent step, serving as the final input weights for the HFVI calculation. In the Mahama Case Study context, spatially explicit results are presented, applying the HFVI with the determined vulnerability indicator weights. Here, individual indicator raster layers are graphically illustrated. The final HFVI resulting from the spatial overlay of the indicator rasters are showcased (also presenting individual $HFVI_{SOC}$ and $HFVI_{PHY}$ maps) for further visual assessment. Subsequently, the chapter presents weight sensitivity and uncertainty analysis results, utilizing the outputs from the Mahama Case Study. These analyses provide the basis for further discussion on the performance of the HFVI.

5.1 Conceptual index development

5.1.1 Individual experts' AHP weights

The assessment of AHP questionnaires regarding the relative significance of individual vulnerability indicators in refugee camps' flood vulnerability yields a series of weights for each indicator within the social and physical vulnerability dimensions.

The experts' questionnaire responses are transformed into corresponding pairwise comparison matrices (PCMs). This process generates eleven 4x4 PCMs, each representing a comparison of social indicators' relative importance concerning flood vulnerability. Likewise, eleven 4x4 PCMs are created to assess the significance of physical vulnerability indicators. Additionally, the evaluation of vulnerability dimensions yields eleven 3x3 PCMs. An example of an individual PCM is illustrated in Table 5.1, summarizing the answers of Expert 4 into the AHP matrix structure. The decimal numbers thereby represent the reciprocals, illustrating the preference for the column indicator over the row indicator.

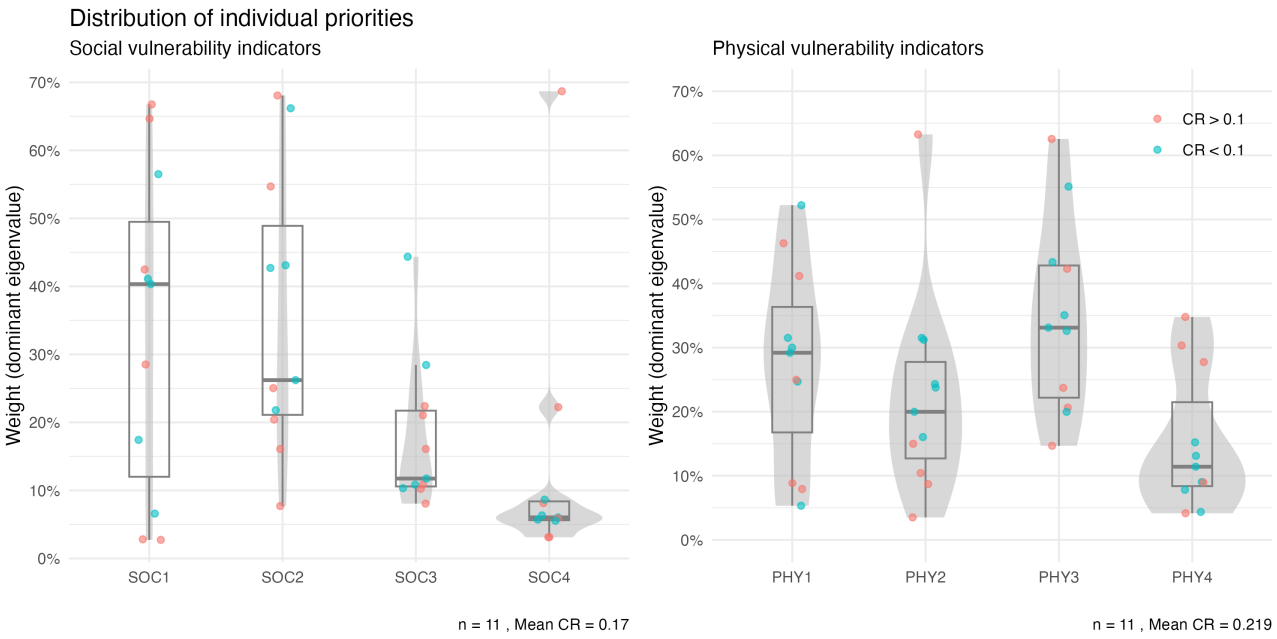

Figure 5.1: Distribution of individual priority weights per vulnerability indicator based on the AHP-questionnaire results using Saatys eigenvalue method (Saaty, 2003). The jitter points represent the experts' priority weights and the Consistency Ratio (CR) value illustrates the consistency of the experts' answers. CR values are based on the PCMs of the individual experts (see Table 5.3).

For example, the entry 0.143 in the third row and the second column indicates that SOC3 (Facilities of Social Importance) is considered 1/7 as important as SOC2 (Vulnerable Groups), indicating "very strong importance" of Vulnerable Groups over Facilities of Social Importance.

Table 5.1: Example of transposed PCM for Expert ID 4.

	SOC1	**SOC2**	**SOC3**	**SOC4**
SOC1	1.000	0.200	3.000	2.000
SOC2	5.000	1.000	7.000	9.000
SOC3	0.333	0.143	1.000	3.000
SOC4	0.500	0.111	0.333	1.000

Subsequently, the AHP methodology is employed as outlined in the Methods Section 4.1.8.1. The weights for individual indicators, including the social and physical vulnerability indicators, are computed for all eleven PCMs using the dominant eigenvalue method (Saaty, 2003), resulting in individual priority weights. The distribution of the individual indicator weights derived from the experts' priorities is shown in Figure 5.1 for each vulnerability indicator. The plots demonstrate the distribution of the weights assigned to the different vulnerability indicators. The width of the violin plot shows the density of the individual weights. The jitter points are superimposed on the violin plot, illustrating the weights of each expert's priority on the importance of an individual indicator on the overall vulnerability. Analyzing the median values of the individual priority weights of the social indicator, it becomes apparent that the experts rank Population Density (SOC1) to have the highest relative importance towards the overall flood vulnerability within a given refugee camp compared to the remaining social indicators. The median priority weight of the population density indicator is 40.33%, followed by Vulnerable Groups (SOC2) with 26.22% and Facilities of Social Importance (SOC3) with 11.75%. Population Density (SOC1) and Vulnerable Groups (SOC2) show a large range in experts' priority

weights, which illustrates disagreement between experts' judgments. The lowest median weight of the social dimension is given to Land Use (SOC4) with only 6.04%. The data points range from around 0% to approximately 10%, with one outlier around 70%. Ignoring this inconsistent outlier, the Land Use indicator (SOC4) demonstrates the smallest range of individual priority weights, indicating higher unanimity between experts' judgments. Comparing the relative importance of the physical indicators to flood vulnerability in refugee camps, the indicators for Facilities Physical Vulnerability (PHY3) and Shelter Type (PHY1) score the highest priority, with 33.12% and 29.20%, respectively. Critical Infrastructure (PHY2) results in a median priority weight of 19.98%, and Roads (PHY4) shows the lowest priority weight with a median value of 11.42%. Overall, it can be observed that the physical indicators show smaller disagreement in priority weights, with tighter clustering and fewer extreme outliers, suggesting slightly higher agreement among individuals on these indicators as compared to the social vulnerability indicators, exhibiting a larger variability of individual priorities.

For the pairwise comparison of the overall importance of the social versus the physical vulnerability dimension (DIM), the individual weights are calculated in the same way as the indicator weights. As the results are re-scaled after aggregation and fuzzification, the individual priority weights here exhibit low values (not summing up to 1) due to excluding the exposure domain[1] while keeping the given PCM structure. Figure 5.2 shows the distribution of the relative priority weights of the social versus the physical vulnerability domain. The plot illustrates similar importance based on the experts' judgment for the two vulnerability dimensions, where both dimensions exhibit a median weight of approximately 20%. However, the physical vulnerability dimension shows a much higher range in the individual weights.

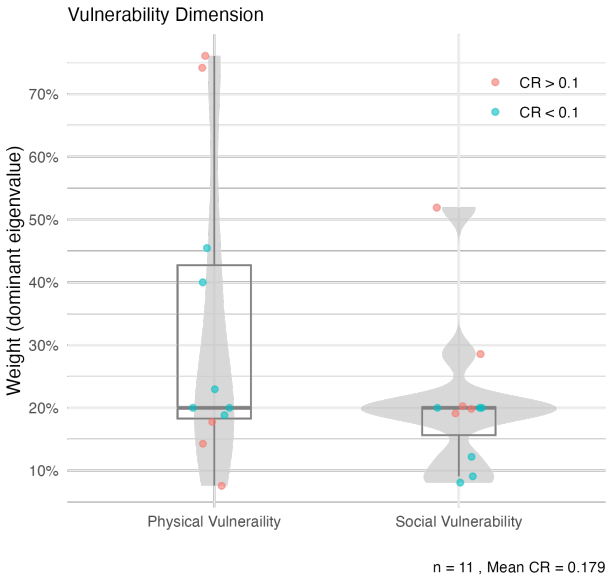

Figure 5.2: Weights distribution for the vulnerability dimensions based on the experts' judgment.

5.1.2 Consistency analysis

5.1.2.1 Inconsistent responses

As depicted in Figures 5.1 and 5.2, many experts' responses result in inconsistent outcomes, indicated by a consistency ratio (CR) greater than 0.1 (red weight points). Specifically, for the pairwise comparison of social vulnerability indicators, 6 out of 11 responses are inconsistent. Similarly, for the physical indicators and the comparison between social and physical dimensions, 5 out of 11 responses show inconsistency. Table 5.3 summarizes the CR values for each comparison structure (SOC and PHY indicators and vulnerability dimensions). CR values highlighted in red exceed the defined threshold value of CR_T = 0.1, indicating inconsistency.

Having identified which experts' answers lead to inconsistencies by calculating the CR for the indi-

[1]The exposure factor, which was still part of the questionnaire, leading to a 3 x 3 comparison structure between the social and physical vulnerability dimension and the exposure component, is neglected in the further analysis.

vidual PCMs, the potential source of such inconsistencies is subsequently analyzed. By implementing the app.error function in R, as introduced in Section 4.1.8, pairwise comparisons with the maximum inconsistency error are extracted for each PCM. This process identifies indicator pairs with the most frequent judgment errors compared to a perfectly consistent AHP matrix. The results show each expert's top three most inconsistent pairwise indicator comparisons. Figure 5.3 summarizes these results by illustrating each indicator pair and its associated inconsistency rank, depicted by the frequency of judgment errors made by the experts in their pairwise comparisons of the vulnerability indicators within the questionnaire. It categorizes these errors by their rank of inconsistency into top1, top2, and top3. Top1 represents the pairwise comparisons with the highest inconsistency error for each expert, indicating the most problematic comparisons. Top2 and top3 follow as the second and third most inconsistent comparisons, respectively. Each bar in the plot corresponds to an indicator pair, with the height of the bar representing the count of total error occurrence (error frequency) across all experts. This visual representation helps identify which indicator pairs are most frequently associated with inconsistent judgments, indicating areas where expert consensus is weakest and potentially affecting the reliability of the AHP results. For social indicators, the pairs SOC1_SOC2, namely Population Density vs. Vulnerable Groups, and SOC1_SOC4, Population Density vs. Land Use, exhibit the highest overall error frequencies. The comparison between Population Density vs. Vulnerable Groups (SOC1_SOC2) also has the highest proportion of top1 errors, indicating the highest proportion of inconsistency errors for all experts. For physical indicators, the pair PHY1_PHY2 (Shelter Density vs. Critical Infrastructure) has the highest top1 error frequency. Meanwhile, the pairs PHY3_PHY4 (Facilities Physical Vulnerability vs. Road) and again PHY1_PHY2 have the highest overall error frequencies. The comparison of the vulnerability dimensions is not further analysed on inconsistencies since after excluding the third dimension component, namely exposure, the comparison consisted only of one indicator pair (SOC vs. PHY vulnerability dimension). The results highlight that experts' judgments are most inconsistent for the indicator pairs SOC1_SOC2 and PHY1_PHY2 regarding top1 errors and highest overall error frequencies in SOC1_SOC2 and PHY3_PHY3, suggesting a need for further review or refinement in these indicators.

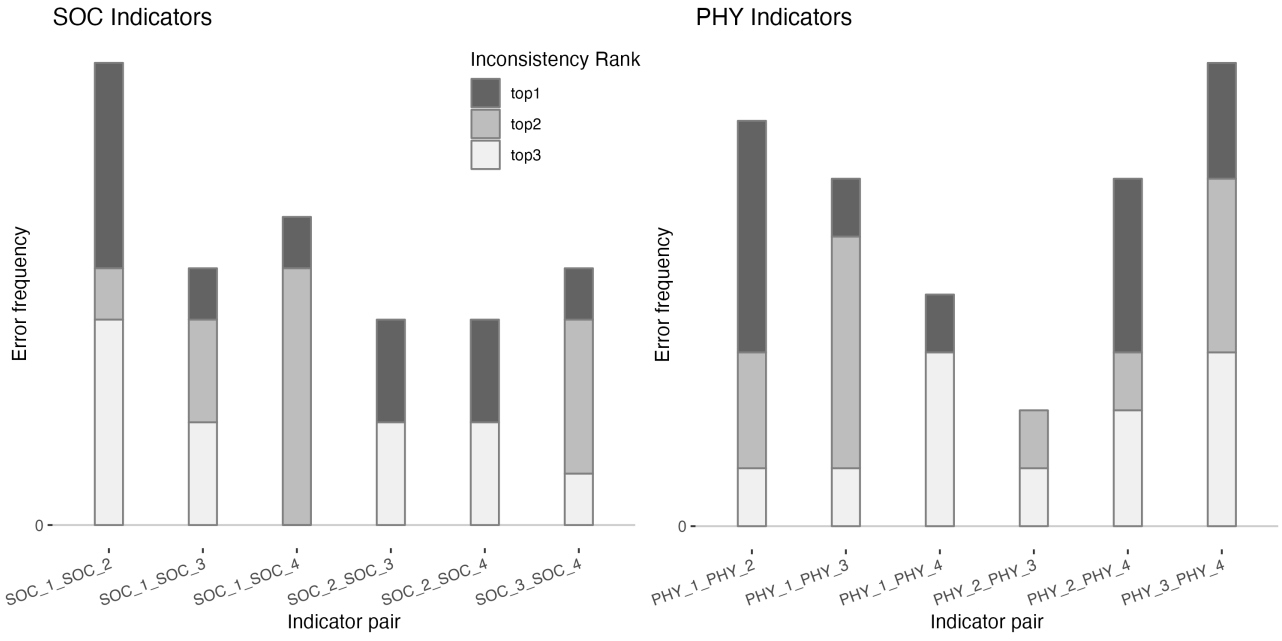

Figure 5.3: Indicator pairs and their frequency of inconsistent comparisons, classified into the frequency of top 3 maximum inconsistency errors per expert (top1 - top3).

5.1.2.2 Transforming inconsistent matrices

As described in Section 4.1.8.6, Harker's method is used to ultimately reduce the overall inconsistencies in the PCMs by iteratively replacing the values of the most inconsistent indicator pairs. The number of maximum iterations using the algorithm is set to 6 for both SOC and PHY indicator comparisons. Figure 5.4 displays the CR values for various iterations of the individual PCMs with $CR_T = 0.1$. For social vulnerability indicator weights, after 2 iterations ($i = 2$), inconsistencies are already minimal (compared to the CR_T exceedance at max. $i = 6$). This suggests that two iterations are sufficient to reduce inconsistencies significantly. In the case of physical indicator weights, inconsistencies are reduced to only one threshold exceedance after 4 iterations, indicating an effective transformation point at $i = 4$. Two iterations were considered for the vulnerability dimensions. Harker's algorithm is executed using the elaborated ideal number of iterations per indicator class, reducing the inconsistencies while minimizing the transformation in the indicator weights. The individual experts' weights can thereby be recalculated with improved consistency.

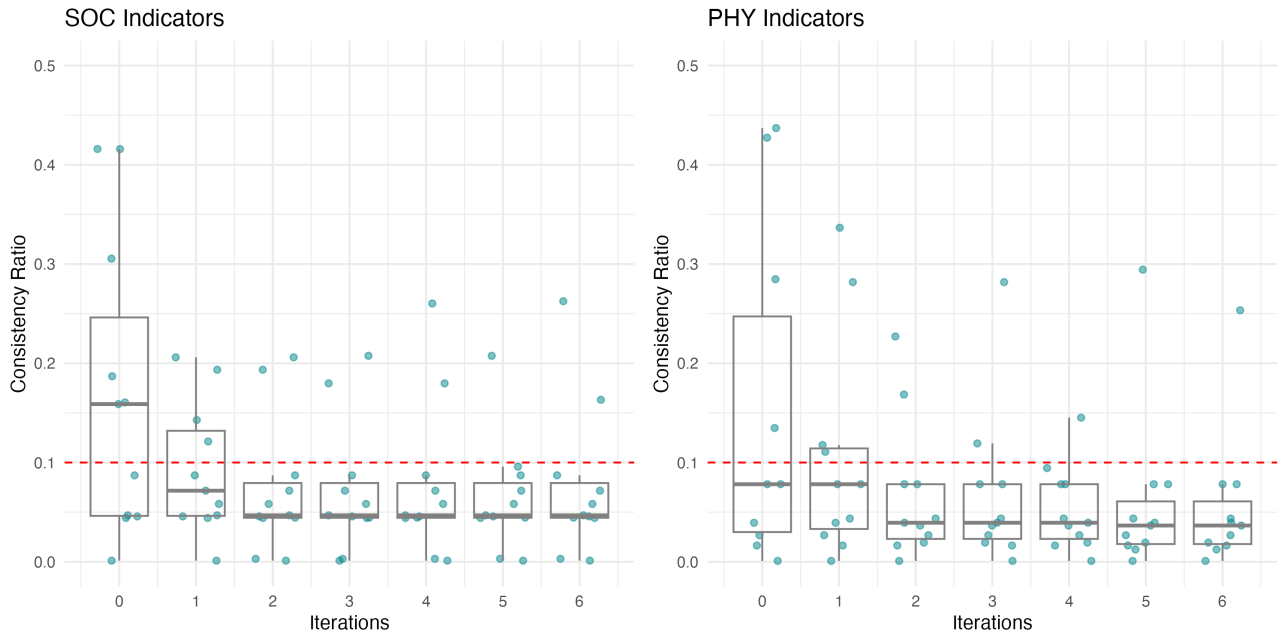

Figure 5.4: Number of iteration runs of Harker's method performed for the social and physical indicators consistency ratio exceedance.

The transformed individual preference weights for the social and physical vulnerability indicator and dimension weights are summarized in Table 5.2.

Table 5.4 summarizes the CR values from the transformed indicator weights after applying Harker's algorithm. The results show that Harker's transformation significantly reduces inconsistent indicator weights in the experts' PCMs. Only two inconsistent PCMs are left for the SOC and PHY indicators, respectively. The transformation of the vulnerability dimensions (DIM) results in only one PCM, which still shows inconsistency. Those still inconsistent PCMs (IDs 2 and 6 for the social indicators, IDs 6 and 11 for the physical indicators and ID 11 for the vulnerability dimensions) are filtered out in order not to influence the final weighting.

Table 5.2: Corrected individual preference weights and consistency results.

Social vulnerability indicators (SOC)					
ID	SOC1	SOC2	SOC3	SOC4	Consistency
1	0.403	0.431	0.108	0.057	TRUE
2	0.033	0.446	0.415	0.107	FALSE
3	0.066	0.427	0.444	0.063	TRUE
4	0.174	0.662	0.103	0.060	TRUE
5	0.411	0.218	0.284	0.087	TRUE
6	0.032	0.122	0.129	0.717	FALSE
7	0.410	0.232	0.060	0.298	TRUE
8	0.682	0.140	0.105	0.073	TRUE
9	0.200	0.565	0.169	0.066	TRUE
10	0.565	0.262	0.118	0.055	TRUE
11	0.472	0.056	0.416	0.056	TRUE

Physical vulnerability indicators (PHY)					
ID	PHY1	PHY2	PHY3	PHY4	Consistency
1	0.200	0.100	0.133	0.567	TRUE
2	0.315	0.315	0.326	0.044	TRUE
3	0.292	0.160	0.433	0.114	TRUE
4	0.053	0.243	0.551	0.152	TRUE
5	0.247	0.312	0.351	0.090	TRUE
6	0.055	0.051	0.433	0.461	FALSE
7	0.300	0.238	0.331	0.131	TRUE
8	0.064	0.467	0.396	0.073	TRUE
9	0.218	0.101	0.268	0.412	TRUE
10	0.522	0.200	0.200	0.078	TRUE
11	0.162	0.038	0.519	0.281	FALSE

Vulnerability Dimension (DIM)				
ID	EXP	SOC	PHY	Consistency
1	0.455	0.455	0.091	TRUE
2	0.333	0.333	0.333	TRUE
3	0.143	0.714	0.143	TRUE
4	0.648	0.122	0.230	TRUE
5	0.400	0.200	0.400	TRUE
6	0.121	0.083	0.796	FALSE
7	0.455	0.091	0.455	TRUE
8	0.600	0.200	0.200	TRUE
9	0.731	0.081	0.188	TRUE
10	0.600	0.200	0.200	TRUE
11	0.048	0.191	0.761	FALSE

ID	CR		
	SOC	PHY	DIM
1	0.045	0.429	0.242
2	0.408	0.001	0.278
3	0.001	0.077	0.164
4	0.086	0.039	0.002
5	0.046	0.026	0.000
6	0.408	0.865	0.182
7	0.184	0.077	0.000
8	0.158	0.280	0.000
9	0.156	0.132	0.036
10	0.043	0.016	0.000
11	0.300	0.420	0.242

Table 5.3: CR values of experts' PCMs.

ID	Transformed CR		
	SOC	PHY	DIM
1	0.046	0.044	0.000
2	0.193	0.001	0.000
3	0.001	0.078	0.000
4	0.087	0.078	0.004
5	0.047	0.027	0.000
6	0.206	0.247	0.095
7	0.058	0.078	0.000
8	0.044	0.019	0.000
9	0.072	0.037	0.062
10	0.044	0.016	0.000
11	0.003	0.145	0.312

Table 5.4: Transformed CRs of experts' PCMs.

5.1.3 Aggregated AHP weights

The transformed and corrected individual preference weights are aggregated using the arithmetic mean, resulting in the following rounded priority weights (Table 5.5). Vulnerability dimension weights are re-scaled to add up to account for the exclusion of the exposure component exclusion.

Table 5.5: Final AHP weights.

Indicator	Name	Aggregated weights	Dimension	Re-scaled weight
SOC1	Population Density	0.376	SOC	0.416
SOC2	Vulnerable Groups	0.329		
SOC3	Facilities of Social Importance	0.205		
SOC4	Land use	0.091		
PHY1	Shelter type	0.246	PHY	0.584
PHY2	Critical Infrastructure	0.238		
PHY3	Facilities Physical Vulnerability	0.332		
PHY4	Roads	0.185		

Population Density (SOC1) received the highest weight among the social vulnerability indicators, with a weight of 0.376 on the overall social flood vulnerability. In contrast, Land Use (SOC4) has a significantly lower priority weight, contributing to social flood vulnerability with a value of only 0.091. Among the physical vulnerability indicators, Facilities Physical Vulnerability (PHY3) is given the highest priority with 0.332, while the Roads indicator (PHY4) has the lowest priority weight with 0.185. When comparing the importance of social and physical vulnerability dimensions on the overall flood vulnerability in refugee camps, the weights are nearly equal, with the social dimension accounting for a slightly lower value of 0.416 than the physical vulnerability at 0.584.

5.1.4 Fuzzy AHP weights

The results of the subsequent Fuzzy AHP are used as the final weights for the HFVI calculation. Therefore, the consistency-corrected AHP weights are fuzzified, resulting in a list of Fuzzy PCMs. An example of such a transformed FPCM based on the AHP matrix of Expert 4 is illustrated below (Table 5.6).

Table 5.6: Matrix of Social Vulnerability Indicators with Intervals.

	SOC1	**SOC2**	**SOC3**	**SOC4**
SOC1	(1; 1; 1)	(0.167; 0.200; 0.250)	(2; 3; 4)	(1; 2; 3)
SOC2	(4; 5; 6)	(1; 1; 1)	(6; 7; 8)	(8; 9; 9)
SOC3	(0.250; 0.333; 0.500)	(0.125; 0.143; 0.167)	(1; 1; 1)	(2; 3; 4)
SOC4	(0.333; 0.500; 1)	(0.111; 0.111; 0.125)	(0.250; 0.333; 0.500)	(1; 1; 1)

As introduced in the Methods Chapter (Section 4.1.8.7, implementing the Triangular Fuzzy Number (TFN) membership function by looping through all FPCMs results in fuzzy AHP weights for each indicator and expert. Subsequently, using the arithmetic mean, aggregated Fuzzy AHP weights are calculated and then defuzzified and normalized into final aggregated FAHP indicator weights. The results are summarized in Table 5.7.

Table 5.7: Final FAHP weights.

Indicator	**wMin**	**wModal**	**wMax**	**wDefuzzified**	**Vulnerability Dimension**	**Re-scaled weight**
SOC1	0.274	0.403	0.603	0.397	SOC	0.483
SOC2	0.223	0.339	0.525	0.337		
SOC3	0.117	0.184	0.301	0.187		
SOC4	0.044	0.074	0.137	0.079		
PHY1	0.151	0.295	0.570	0.296	PHY	0.517
PHY2	0.150	0.258	0.478	0.258		
PHY3	0.167	0.307	0.576	0.306		
PHY4	0.082	0.141	0.255	0.139		

The defuzzifid FAHP and re-scaled vulnerability dimension weights serve as final input weights for the HFVI calculation. With that, the equation of the HFVI can be adjusted to the elaborated experts' weights, resulting in the adjusted HFVI equation 4.10.

$$HFVI = 0.483 \times \left[\sum_{i=1}^{n} (\text{soc}_i \ \times f\_\text{w\_soc}_i)\right] + 0.517 \times \left[\sum_{j=1}^{m} (\text{phy}_j \ \times f\_\text{w\_phy}_j)\right] \tag{5.1}$$

Here $f\_w\_soc_i$ and $f\_w\_phy_i$ are replaced by the defuzzified FAHP weights from Table 5.7. The range of the fuzzy social and physical vulnerability indicator weights and their modal and defuzzified values resulting from the FAHP procedure are visually presented in Figure 5.5. The plot illustrates the FAHP weights assigned to social (SOC) and physical (PHY) vulnerability indicators, where the two types of aggregated fuzzy weights are depicted: wModal (blue markers) and wDefuzzified (green markers). For each indicator, the plot shows the relative weight along with bars indicating the range of the fuzzy weights, limited by the upper and lower bounds wMin and wMax. This range reflects the uncertainty based on different experts' judgments. Population Density (SOC1) exhibits the highest relative weight in the SOC dimension, while the Vulnerable Groups indicator (SOC2) shows the largest range. On

the contrary, Land Use (SOC4) presents the lowest weight with a minimal range. Shelter Density (PHY1) and Facilities of Physical Vulnerability (PHY3) exhibit the highest weights with significant ranges, whereas the Roads indicator (PHY4) shows the lowest weights and the smallest range.

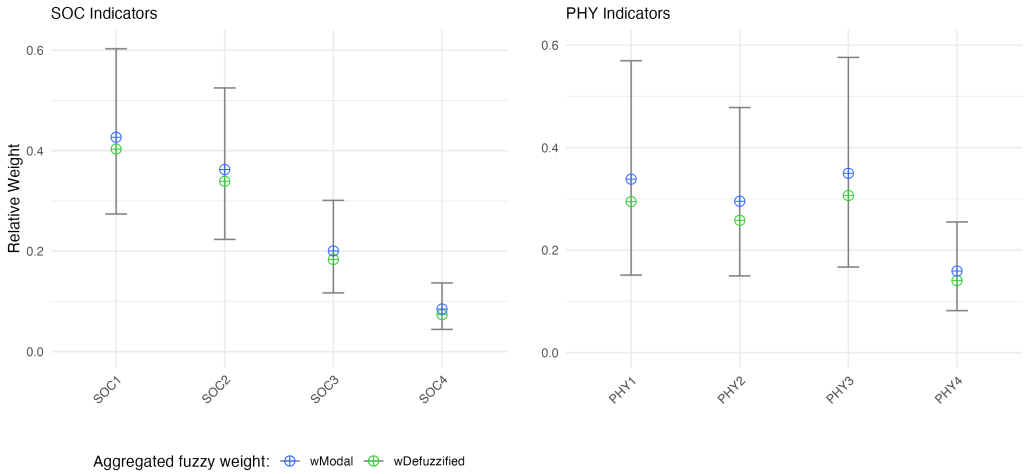

Figure 5.5: Fuzzy AHP weights and their range of the fuzzy number (wMin, wMax). Blue markers illustrate the fuzzy modal value (wModal) and green markers show the aggregated mean FAHP weight (defuzzified weight).

5.2 Mahama Case Study

5.2.1 Individual flood vulnerability indicator layers

The results of the Mahama case study are based on the described geospatial datasets (Section 4.1.7 and enable the application of the developed HFVI to a real test case. The quantification of the individual vulnerability indicators from the social and physical dimensions using the case study data and the proposed procedure, as described in Section 4.2, resulted in eight normalised raster layers. Figure 5.6 illustrates the individual raster layers. The resulting layers are tailored to the boundaries of the Mahama refugee camp and show raster values from 0 to 1, representing the flood vulnerability. The value for flood vulnerability is the result of quantifying the indicator subcategories on a grid basis, which represents a numerical value for the relative influence on flood vulnerability in the refugee camps.

When visually analysing the individual indicator layers, it becomes clear that SOC1 and PHY1, as well as SOC3 and PHY3, show a high degree of similarity in their spatial distribution within the Mahama refugee camp. The strong correlation between the Population Density (SOC1) and Shelter Type (PHY1) layer is primarily due to their derivation from the buildings dataset, which accurately depicts the built-up areas of the camp. The Shelter Type indicator (PHY1) is quantified by calculating the density of shelters, then ranked with vulnerability scores based on existing shelter type and its susceptibility to flooding. With that, areas with high population density naturally correlate with built-up regions and hence also show higher Shelter Density scores. However, there are small differences due to the different types of shelters and the associated vulnerability ranks or discrepancies resulting from the gridded quantification steps. The reason for considering both indicators despite their high spatial similarity is explained in the discussion section. The layers showing the Facilities of Social Importance (SOC3) and Facilities Physical Vulnerability (PHY3) correspond spatially, as they show

the locations of the facilities within the camp. However, small-scale differences in the vulnerability values arise due to the focus on different dimensions, namely social significance and physical robustness. The grid values differ slightly as facilities are assigned different vulnerability ranks depending on the vulnerability dimension. The results are compared to the Mahama Camp Layout to analyse these differences. For example, in the southwestern part of the camp in the upper left corner, SOC3 shows higher raster values where the hospital is located. This is because health centres are assigned a higher social vulnerability rank (3) than the physical vulnerability rank (2) (see categorical vulnerability ranks in Section 4.1.9.1, Table 4.7). Conversely, PHY3 shows slightly higher values than the SOC3 indicator in the southwestern part of the camp where a market is located. Markets categorized as "Cultural Facilities" have a higher physical vulnerability rank (3) than social (2).

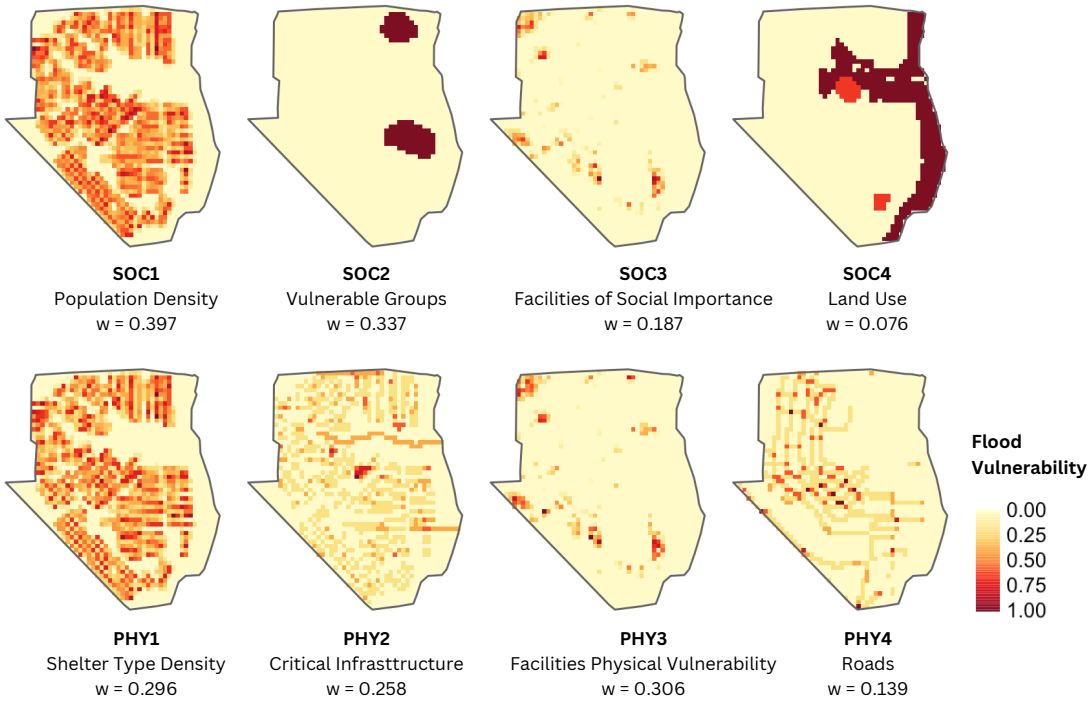

Figure 5.6: Normalized and categorized vulnerability indicator raster layers of the Mahama refugee camp as basis for calculating the HFVI. FAHP weights are given for each indicator but have not been applied to the raster yet.

The other indicators show distinct spatial patterns. The Vulnerable Groups indicator (SOC2) shows two very localized areas of high vulnerability in areas where especially vulnerable groups are present. On the other hand, Land Use (SOC4) shows the highest flood vulnerability along the eastern boundary of the camp, where agricultural land is present. Two small clusters of intermediate vulnerability are localized in areas classified as open spaces within the built-up area that show no vulnerability. Critical Infrastructure (PHY2) exhibits a more dispersed spatial pattern of low vulnerability across the camp due to sanitary units within the build-up areas. Moderate vulnerability values are the result of the spatial high density of Critical Infrastructure elements or the existence of drainage channels. High areas coincide with the critical building infrastructures in the camp's centre. Finally, the Roads indicator (PHY4) depicts the road infrastructure with higher vulnerability values in grid cells where either roads of high vulnerability rank are present (e.g., service roads) or at intersections between roads, serving as important connection nodes for accessibility in emergency situations.

5.2.2 Social and physical vulnerability maps

Applying the evaluated final FAHP indicator weights[2] to the raster layers, using the proposed weighted linear combination method (Equations 4.11 and 4.12) results in two maps (Figure 5.7) that illustrate the individual social and physical vulnerability dimensions in the Mahama Refugee Camp.

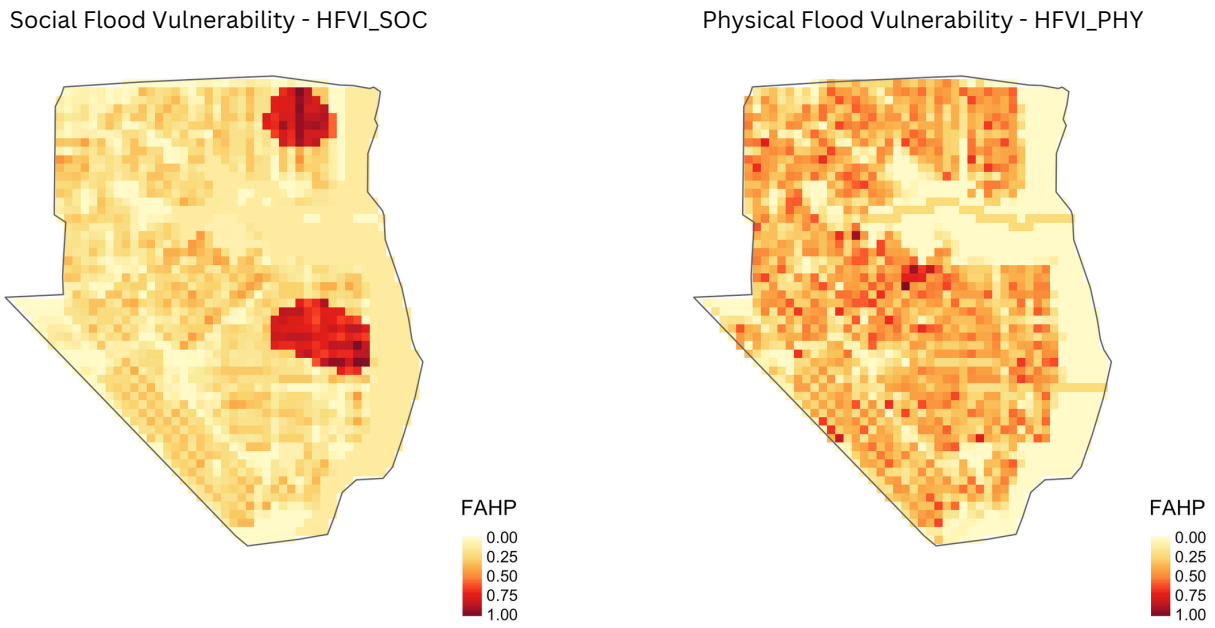

Figure 5.7: Social (right) and physical (left) flood vulnerability dimension of the HFVI mapped for the Mahama Refugee Camp.

The $HFVI_{SOC}$ map presents the social flood vulnerability across the camp. The areas with higher social vulnerability are marked with darker shades of red, indicating zones where the social conditions might amplify the impact of flooding. Lower vulnerability areas are shown in lighter shades of yellow. This visualization helps identify the parts of the camp where social factors contribute significantly to flood risk, emphasizing areas requiring targeted social interventions to mitigate vulnerability. The ($HFVI_{SOC}$) map shows pronounced clusters of high vulnerability in the northern and southern regions, driven primarily by high Population Density (SOC1) and the presence of Vulnerable Groups (SOC2), which have the highest weights. This pattern is further influenced by the presence of facilities with social importance (SOC3) and areas of specific Land Use (SOC4), however, with a reduced influence on the flood vulnerability due to lower weightings.

On the other hand, the $HFVI_{PHY}$ map illustrates the physical flood vulnerability within the camp. Similar to the social vulnerability map, the flood vulnerability values are displayed, where higher physical vulnerability areas, indicated by darker red shades, highlight regions where physical infrastructure and environmental conditions increase flood risk. Lighter yellow areas show lower physical vulnerability, suggesting better resilience against flooding impacts. This map serves to pinpoint the specific locations within the camp that may need infrastructural improvements or maintenance to reduce physical vulnerability.

[2]The weights represent general weights that were analysed on the basis of the expert questionnaires and are not specifically tailored to Mahama Camp. Rather, the weights were evaluated as global values and independent of the location.

The spatial pattern of physical vulnerability coincides with built-up areas, with little to no vulnerability in non-built-up regions. This is due to the nature of the physical indicators used, which are spatially bound to the camp's physical assets. The pattern particularly reflects the high weights assigned to shelter type density (PHY1) and the physical vulnerability of facilities (PHY3), resulting in broader areas of moderate to high vulnerability. Compared to the influence of facilities on social vulnerability, facilities (PHY3) have the highest weighting in physical vulnerability assessments. This slightly increases vulnerability values in areas with vulnerable facility types. Hotspots of physical flood vulnerability tend to align with the location of critical building infrastructure (PHY2) in the central part of the camp. Although the Roads vulnerability (PHY4) effect is not inherently visible, high roads vulnerability locations contribute to the overall physical flood vulnerability pattern. The more equally distributed weights for the physical indicators result in a broader dispersion of moderate vulnerability values. In contrast, the social flood vulnerability map displays greater spatial differences and distinct clustering due to the higher imbalance of indicator weights, highlighting areas with pronounced social vulnerabilities.

5.2.3 HFVI for the Mahama Refugee Camp

As the final result, the composite HFVI maps are displayed in Section in Figure 5.8. The HFVI is the output of the developed weighted overlay function (Equation 5.1) using the final FAHP weights of the vulnerability dimensions and individual indicators to construct a final flood vulnerability map, combining social and physical vulnerability factors, with weights of 0.483 and 0.517 assigned to the social and physical dimensions, respectively. For the representation of the HFVI, the visualization methods described in Section 4.2.2.3 are implemented, using Jenks Natural Breaks to classify the HFVI values into distinct vulnerability classes. Additionally, applying the focal filter method results in a second but smoother representation of the HFVI, converting clear edges into fuzzy transitions to account for spatial uncertainty.

The HFVI applied to the Mahama Refugee Camp shows a heterogeneous spatial pattern of varying flood vulnerability within the camp area, combining both social and physical vulnerability dimensions. The HFVI ranges from 0 to 1, where higher values indicate areas of increased relative flood vulnerability. The final map shows several clusters of high overall vulnerability with HFVI values close to 1. These hotspots are located in the northeastern and central parts of the camp's built-up area. Based on the results from the $HFVI_{SOC}$ and $HFVI_{PHY}$, the high vulnerability here can be explained through the combined effect of high population density (SOC1), the presence of Vulnerable Groups (SOC2) in the more eastern parts and Critical Infrastructure (PHY2) in the central areas. The remaining regions coinciding with the built-up areas of the camp display moderate vulnerability levels. These areas show a mix of social and physical factors that contribute to an overall moderate risk of flooding. However, these regions are presumably governed by the influences of Population Density (SOC1) and shelter type (PHY1) indicators. The eastern periphery of the camp shows lighter yellow shades, indicating lower flood vulnerability. These regions are agricultural areas with social importance for the camp population and are quantified by the Land Use indicator (SOC4). However, due to the comparably low weighting of the importance of Land Use, these areas result in low HFVI values. When comparing the HFVI results to the facility locations, it becomes apparent that the presence of facilities and their associated social (SOC3) and physical (PHY3) influences tend to lower the overall HFVI score in these areas compared to other regions. Additionally, the Roads (PHY4) do not seem to have a noticeable visual impact on the overall spatial pattern of the HFVI.

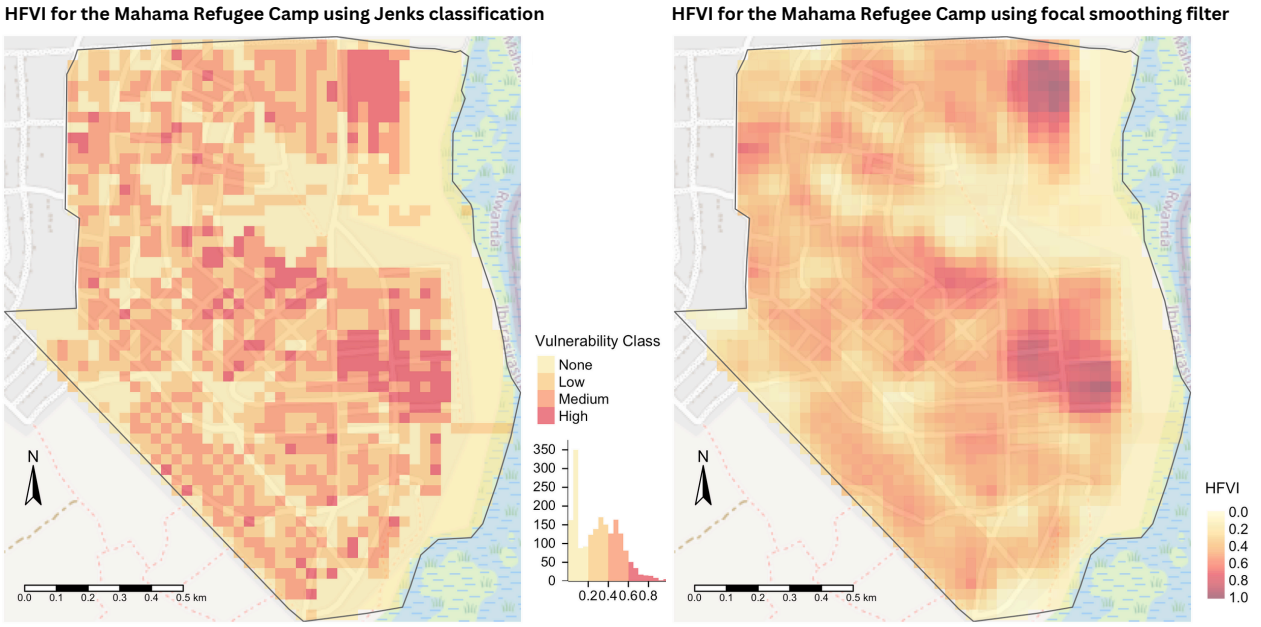

Figure 5.8: Final composite HFVI map for the Mahama Refugee Camp. Right: HFVI classification using Jenks Natural Breaks. Left: Smoothed HFVI result using low pass focal filter.

5.2.4 Spatial analysis

5.2.4.1 Spatial autocorrelation of the HFVI

In addition to visually analyzing the spatial pattern of the index results, spatial autocorrelation was tested using the Moran's I. The output is summarized in Table 5.8.

Table 5.8: Moran's I test for spatial autocorrelation of flood vulnerability values.

Statistic	**Output**
Moran I statistic standard deviate	27.796
p-value	$< 2.2e{-}16$
Moran I statistic	0.632

The results of Moran's I statistic depict the strength of the spatial relationships of the HFVI results for the Mahama Refugee Camp. The test yielded a positive value of 0.632, indicating a moderate positive spatial autocorrelation, implying a trend of similar values forming spatial clusters. This clustering pattern reflects that flood vulnerability within the Mahama Refugee camp is not randomly distributed but spatially dependent, which is in accordance to Tobler's first law of geography, which states that 'everything is related to everything else, but near things are more related than distant things' (Tobler, 1970). The standard deviation measures how many standard deviations the observed Moran's I statistic is different from the expected Moran's I under spatial randomness. The p-value indicates the significance of the Moran's I statistic. Here, the Moran I statistic standard deviation is 27.796, and the p-value is very small (p-value $<$ 2.2e-16), indicating strong evidence against the null hypothesis of spatial randomness. This rejection suggests that the HFVI provides meaningful spatial information rather than random noise, reinforcing the index's validity in assessing flood vulnerability. Overall, the high Moran's I value and low p-value suggest significant positive spatial autocorrelation

in the raster data, meaning similar values are clustered together in space.

5.2.4.2 Indicators correlation matrix

Having identified the spatial correlation of the HFVI spatial pattern, the spatial influence of the individual social and physical indicators on the final HFVI can be further assessed using a correlation matrix. The results of the indicators correlation analysis are plotted in Figure 5.9. The correlation matrix shows the spatial relationship between the individual HFVI indicators for the Mahama Refugee Camp case. Blue values indicate a positive spatial correlation, whereas red values indicate a negative spatial correlation. The values in the matrix cells are the p-values indicating the significance of the spatial relationship, where crossed-out values depict a non-significant correlation (significance level < 0.01) between two indicators.

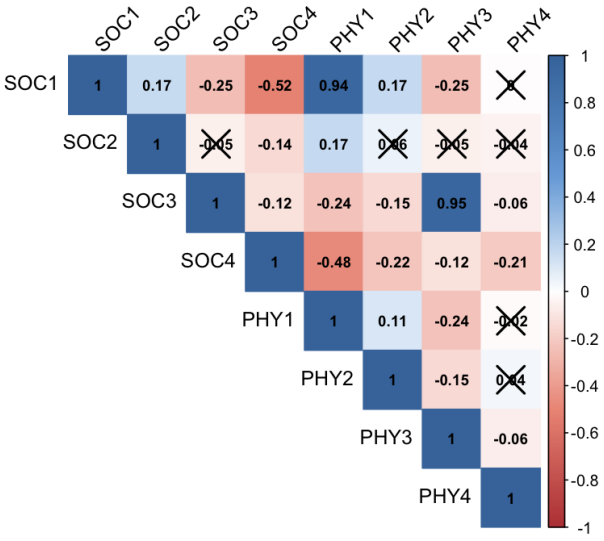

Figure 5.9: Spatial correlation matrix of the individual HFVI indicators.

The correlation matrix provides insights into how the individual vulnerability indicators relate to the overall flood vulnerability values. A strong positive correlation between Population Density (SOC1) and shelter type density (PHY1) suggests that areas with high population density, and thus high flood vulnerability, also have a high density of shelters, increasing their overall vulnerability. Similarly, the high correlation between Facilities of Social Importance (SOC3) and facilities' physical vulnerability (PHY3) indicates that areas with key social facilities are also where those facilities are physically vulnerable, which is expected given that these facilities are all assigned similarly high vulnerability ranks. Conversely, moderate negative correlations, such as between Population Density (SOC1) and Facilities of Social Importance (SOC3) and between Land Use (SOC4) and shelter type density (PHY1), indicate that areas with high social flood vulnerability might not always align with areas of high physical vulnerability. Weak or non-significant correlations between Vulnerable Groups (SOC2) and Road Density (PHY4) with other indicators suggest that these pairs do not have a significant linear relationship. Understanding these correlations helps in identifying specific areas where social and physical vulnerabilities either coincide or diverge, guiding towards a better interpretation of the spatial HFVI results.

5.2.5 Sensitivity analysis

As a final analysis step, sensitivity analysis using One-At-a-Time (OAT) method and the novel approach including fuzzy ranges from the FAHP method (as introduced in Section 4.1.10) was conducted to examine the impact of varying the input weights of different indicators on the resulting spatial pattern of the HFVI. Specifically, the sensitivity analysis focused on the individual assessment of the SOC and the PHY vulnerability indicators. Therefore, the elaborated FAHP weights wMin and wMax (see Table 5.7 and Figure 5.5) were applied to calculate each indicator's range of percentage change (RPC) weight range in relation to the original weight (i.e. the defuzzified FAHP indicator weight). The resulting fuzzy RPCs per indicator used as input for the OAT analysis are summarized in Table 5.9

and illustrate the range in which the original weight is allowed to change.

Table 5.9: Range of percentage changes from the fuzzy weights bounds to the original value.

SOC	- Change [%]	+ Change [%]	PHY	- Change [%]	+ Change [%]
SOC1	-12.31	20.58	**PHY1**	-14.49	27.35
SOC2	-11.39	18.76	**PHY2**	-10.87	22.00
SOC3	-6.96	11.45	**PHY3**	-13.92	27.00
SOC4	-3.47	5.78	**PHY4**	-5.74	11.57

The result of the OAT analysis using the SpatMCDA package in R is a collection of newly generated raster layers with adjusted weights. Each simulation run generates a single map depicting the spatial results of the weight change. This is done by changing each indicator's weight using a weight change step size of 1% within the defined RPCs while keeping the other indicator weights constant. To illustrate that, for the indicator SOC1, the simulation started at a RPC value of -12.31% from its initial fuzzy weight of w = 0.397 in the 1st simulation run and stops at a RPC value of +20.58 in its last (33rd) simulation run. Performing the OAT for all indicators results in a total of 227 simulation runs and associated weight maps. The visual comparison of the spatial pattern of the sensitivity map shows that the HFVI values for all indicators have not changed remarkably, which indicates a generally high stability of the HFVI results.

The SpatMCDA function additionally outputs difference maps, which quantify the differences between the initial HFVI map and the raster with adjusted weights. Mean Absolute Change Rates (MACRs) were calculated to measure the sensitivity of the individual indicators to weight changes. The resulting plot (Figure 5.10) displays the MACRs for the social and physical as a function of the Change Rate of Weights (CWR). Each line in the plot represents an indicator, showing how the MACR changes when its weight is varied. For both social and physical indicators, the MACR values generally increase symmetrically with increasing CWR, indicating the sensitivity of the overall social and physical vulnerability to weight changes. Steeper lines thereby indicate higher sensitivity to weight changes. For the social indicators, Population Density (SOC1) shows the highest sensitivity to weight changes, whereas Facilities of Social Importance (SOC3) and Land use (SOC4) show the lowest sensitivity. The

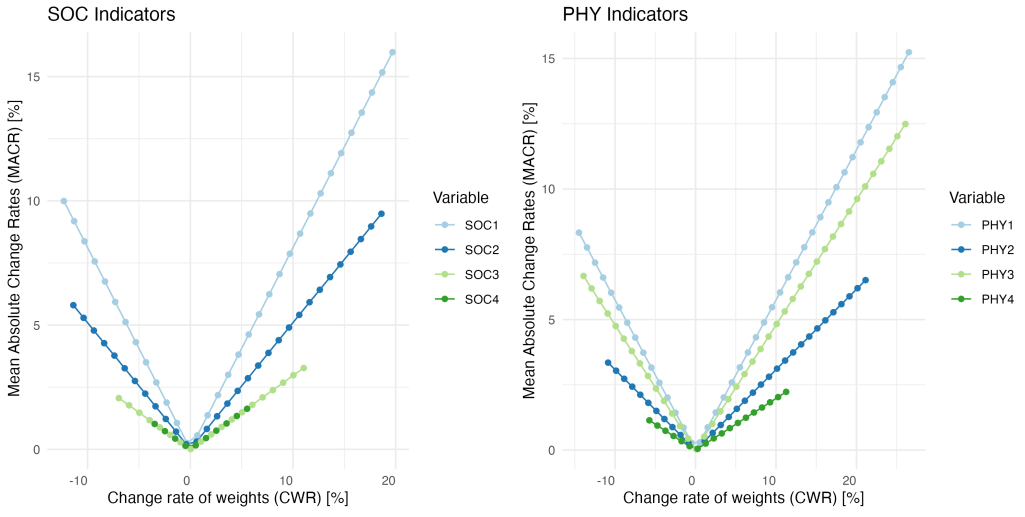

Figure 5.10: Mean absolute change rates per weight change for social and physical vulnerability indicators.

physical indicators show a similar pattern, with the highest sensitivity for the Shelter type indicator (PHY1), followed by the Facilities Physical Vulnerability (PHY3) and the lowest sensitivity for the Roads indicator (PHY4).

5.2.5.1 Weight uncertainty

Finally, uncertainty maps were generated to visualize the spatial distribution of uncertainty in the vulnerability assessments. The resulting plots in Figure 5.7 show the social and physical uncertainty maps, indicating the variability in the vulnerability assessment due to changes in indicator weights. The uncertainty maps in Figure 5.11 highlight areas with higher uncertainty values, indicating regions where changes in the social and physical indicator weights significantly impact the overall HFVI. Both maps show rather uniform distribution of weight uncertainty with higher values in the built-up areas and low to no uncertainty in the bordering agricultural land or bare land. Comparing the resulting maps, it can be observed that in areas where facilities are located, the physical vulnerability shows higher sensitivity to weight changes compared to the social vulnerability those facilities exhibit. Further high areas of uncertainty seem to coincide with grid cells, where shelter density and, hence, population density are high.

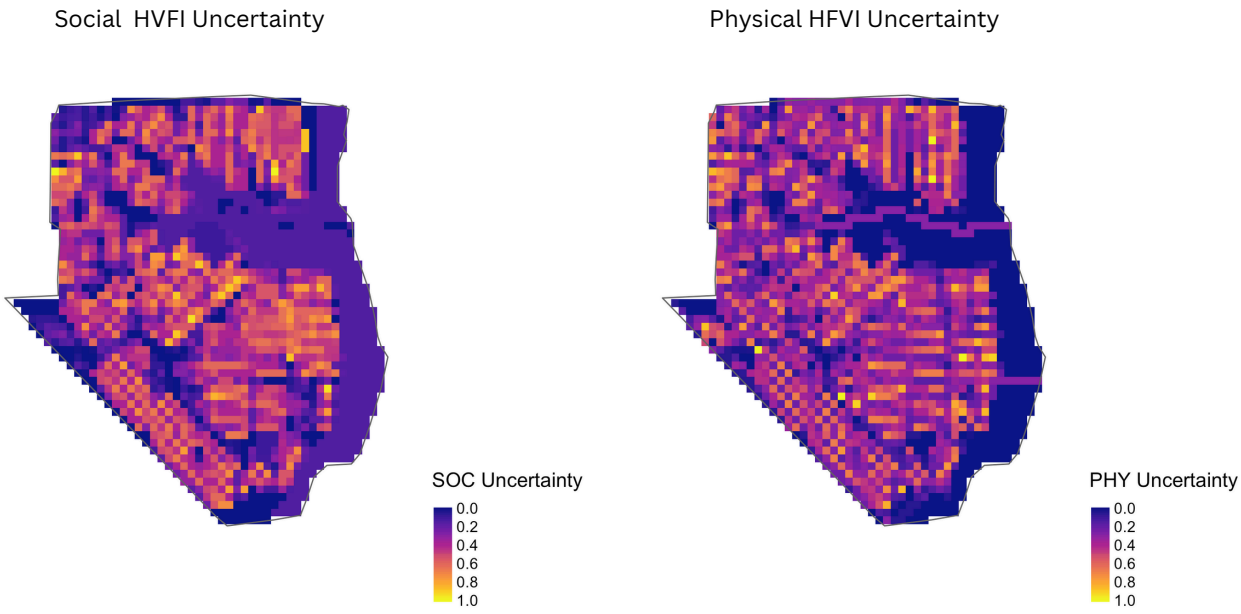

Figure 5.11: Spatial weight uncertainty maps for the social and physical HFVI.

The combined uncertainty map aggregates the uncertainties from both social and physical indicators, providing a comprehensive view of the spatial distribution of weight uncertainty. The results are illustrated in Figure 5.12, showing the rasterized output of the weight uncertainty in the Mahama Refugee Camp (right) and its smoothed result using low-pass filtering (left). The highest weight uncertainty values are found in the region of the upper right corner of the camp near the camp boundary and are illustrated in yellow shades. Regions of high uncertainty values indicate larger changes in the overall vulnerability output for small changes in weight and hence can be considered to be more influential in driving the overall instability or uncertainty. Here, minor changes in indicator weights have the most significant impact on the HFVI results. Notable hotspots of uncertainty in the

resulting maps can further be seen in the central part of the camp, likely influenced by the presence of weight-sensitive critical building infrastructure and Shelter Density. The high concentration of buildings and critical facilities in these regions contributes to the overall uncertainty. The northeastern part of the camp shows moderate uncertainty, reflecting variability in the vulnerability assessment due to the presence of facilities of high physical vulnerability (community centre) and vulnerable groups. The uncertainty here suggests that weight adjustments in these indicators significantly impact the HFVI values. The lowest uncertainty is observed in the eastern parts of the camps, where agricultural land is present and in uncultivated regions. Here, the low uncertainty values suggest more robustness to changes in criteria weights.

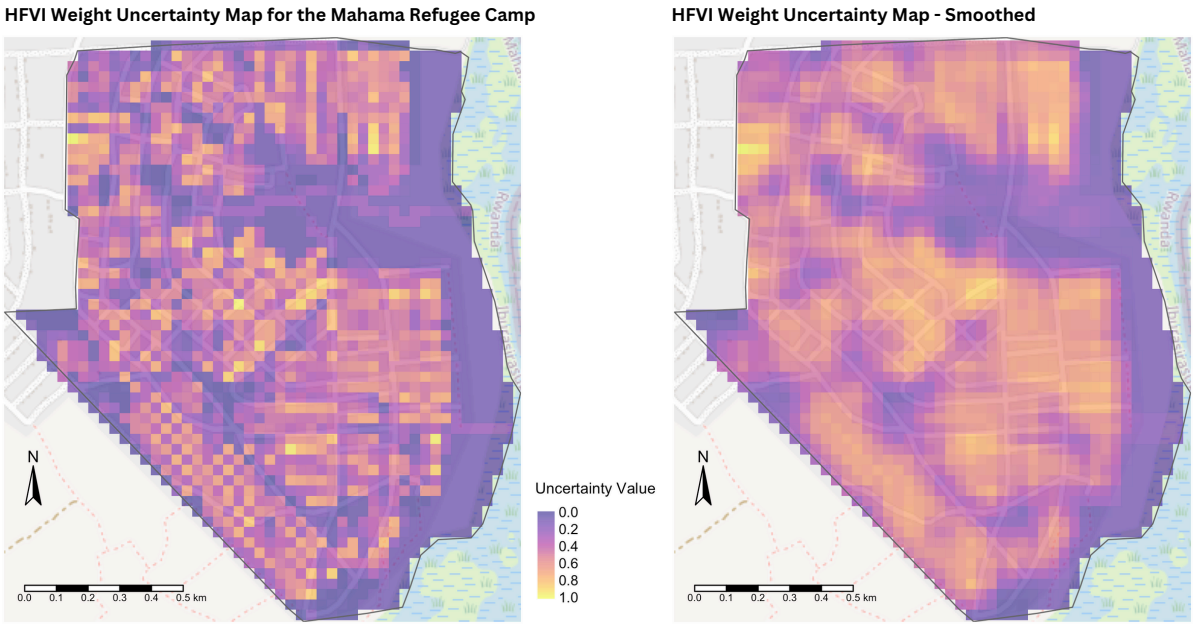

Figure 5.12: Final weight uncertainty maps resulting from the OAT sensitivity analysis in the Mahama Refugee Camp.

5.2.6 Final map layout: Combining HFVI and uncertainty

The final result of this case study is a detailed map layout for the Mahama Camp, illustrated in Figure 5.13, which overlays the HFVI with the spatial weight uncertainty map. This approach visualises the vulnerability values and the associated uncertainty in a single map, thus enabling the simultaneous identification of hazard hotspots and locations with high uncertainty.

For better interpretability and understanding, the uncertainty values are classified into four distinct classes: no, low, medium, and high uncertainty, again using Jenks Natural Breaks. The classes are subsequently represented by different hatching patterns and superimposed on the HFVI map. This final illustration helps to identify areas where flood vulnerability values are more confident or where caution is necessary in interpreting the HFVI results. The map layout additionally presents the unweighted and normalized vulnerability indicator layers utilized to calculate the final HFVI results.

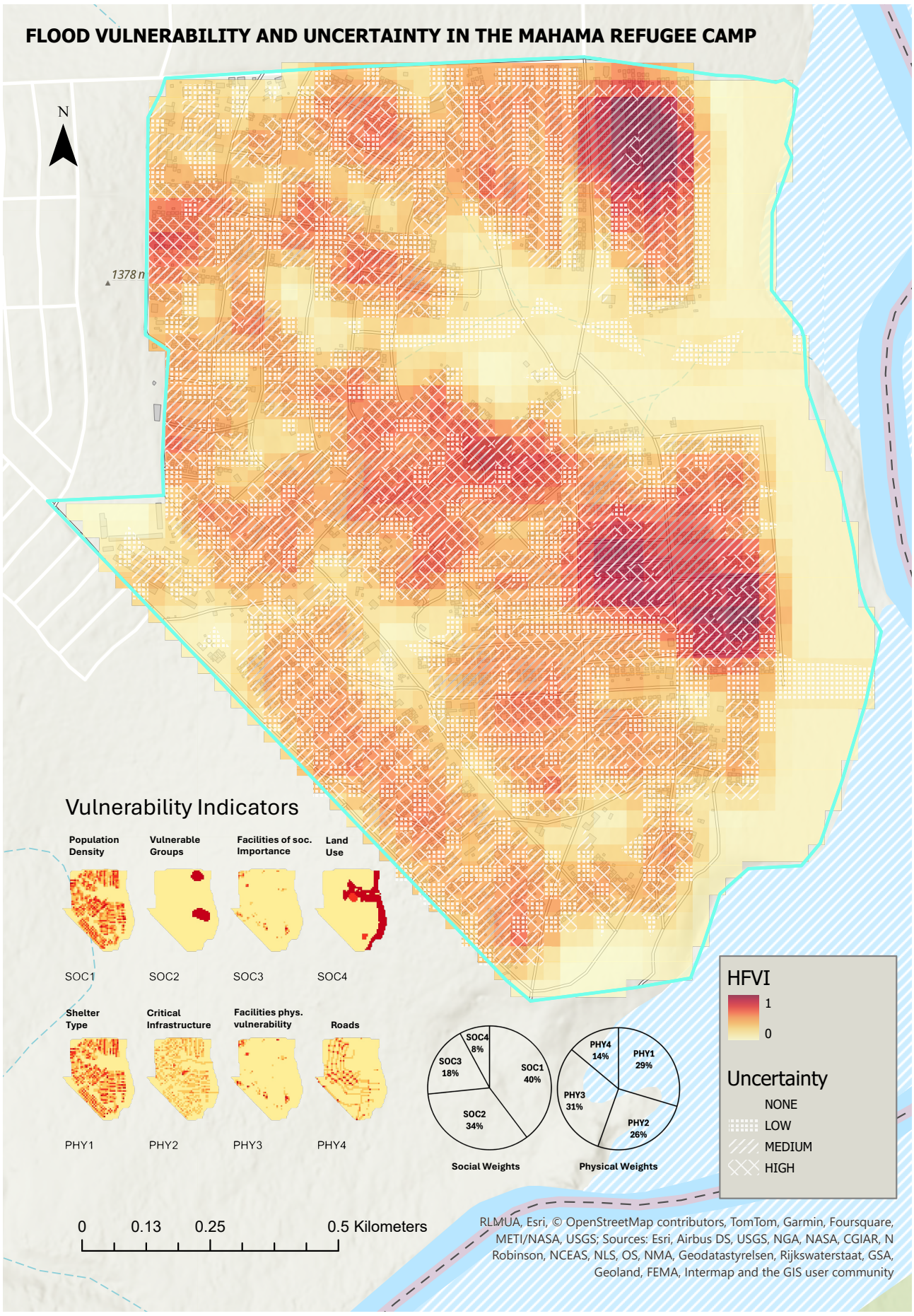

Figure 5.13: Final map layout illustrating the HFVI overlayed with weight uncertainty classes and individual indicator layers for the Mahama Refugee Camp.

6 Discussion

This discussion chapter addresses the principles of the conceptual development process and discusses the findings by providing a comprehensive analysis of the case study results in relation to the application of the developed Humanitarian Flood Vulnerability Index (HFVI) in Mahama Refugee Camp. Particular emphasis will be laid on answering the research question, which focuses on how flood vulnerability as a multidimensional concept can be modelled to fit the context of refugee camps (RQ1) and what indicators most importantly influence this vulnerability (RQ1.1). It further identifies the main challenges and limitations of the study in terms of the conceptual model, data, and methodology and assesses how these limitations might affect the results and validity of the index developed (RQ1.2). Lastly, this chapter also reflects on possible future work that could address these limitations and expand the scope of the study (RQ1.2). The discussion is divided into two main sections, where Section 6.1 addresses the HFVI conceptual choices and limitations, while Section 6.2 discusses the case study application and performance of the HFVI.

6.1 HFVI conceptual choices and limitations

The Humanitarian Flood Vulnerability Index (HFVI) is developed with the aim of being integrated into the Flood Risk Mapping GIS tool as part of the flood risk assessment for refugee camps, combining hazard and vulnerability into a single metric. However, this thesis examines flood vulnerability from an isolated viewpoint without analyzing the results of integrating the vulnerability model into the broader risk assessment. By isolating vulnerability from the hazard component, decision-makers can focus on addressing the underlying factors contributing to vulnerability (Nasiri et al., 2016). This section justifies conceptual steps, including the choice of indicators and vulnerability dimensions, spatial modelling choices and the influence of expert input on weighting, providing answers to the overreaching research question. Further, it discusses the limitations of the HFVI associated with data availability, standardization, and weighting methods, focusing on issues like data resolution, handling inconsistencies, and dealing with missing data.

6.1.1 HFVI conceptual model for refugee camps

Flood vulnerability is a multifaceted concept that demands a detailed and nuanced approach to accurately capture the diverse dimensions of vulnerability, particularly within the unique environment of refugee camps, which is significantly different to standard urban settings. As refugee camps are often located in remote and flood-prone areas, unique challenges for flood risk assessments are present, primarily due to data scarcity, lack of up-to-date maps, and their structural differences compared to urban areas (Akola et al., 2019; Anwana & Owojori, 2023; Hassan et al., 2018; Owen et al., 2023). Additionally, the differing flood vulnerability issues experienced by the camp population compared

to those of settled populations in standard urban areas, combined with the lack of approaches to quantify this context-specific vulnerability, make it difficult to assess the flood vulnerability within those camps (ARSET, 2024). The developed Humanitarian Flood Vulnerability Index (HVFI) is able to consider those challenges, aiming to provide a standardized quantitative and spatial measure to assess flood vulnerability within refugee camps worldwide. However, given the difficulties of flood vulnerability modelling within the given context, the conceptual model of the HFVI brings multiple steps of generalizations as well as limitations, which are discussed below.

The conceptual framework for modelling flood vulnerability accounts for various indicators to effectively capture the multidimensional nature of vulnerability in refugee camps. This includes incorporating vulnerability's social and physical dimensions, which are both described through four influential vulnerability indicators, ensuring a holistic assessment. The developed HFVI attempts to combine the social and physical factors tailored to the given conditions into a single measure, but it inevitably oversimplifies the complex and nuanced nature of vulnerability. This generalization might overlook critical local variations and specific contextual details, leading to potential inaccuracies or misrepresentations in assessing flood vulnerability.

Considering social vulnerability for flood vulnerability assessment in refugee camps is particularly important for risk analysis and disaster response reduction (Tascón-González et al., 2020; Tate et al., 2021). As Malgwi et al. (2020) highlighted, there is a strong connection between physical vulnerability and other vulnerability dimensions, emphasizing that the disruption of physical elements can directly impact social and economic activities within a society. Incorporating both types of indicators provides a holistic understanding of vulnerability, enabling more effective planning and response strategies. For instance, areas with high social resilience but lower physical robustness may require infrastructure improvements, while regions with robust physical infrastructure but fewer social services might benefit from increased resilience of social facilities. However, as observed in other vulnerability assessments, including the social vulnerability dimension (Eriksen et al., 2021; Nyborg & Nawab, 2017), the HFVI is prone to suffer from an insufficient understanding of the underlying social processes. The assessment relies on predetermined indicators, failing to adequately capture the complex socio-economic relations and processes through which specific groups are marginalized based on gender, race, age, disability and class. Other dimensions of vulnerability, such as economic, environmental, and institutional aspects, are neglected due to diverse reasons, including data unavailability, quantification difficulties, non-spatiality or reduced relevance for the specific context of refugee camps. Future models could, however, benefit from incorporating additional dimensions to provide a more comprehensive assessment (Birkmann, 2013; Chan et al., 2022; Kienberger et al., 2009).

The social vulnerability dimension in the HFVI includes Population Density (SOC1), Vulnerable Groups (SOC2), Facilities of Social Importance (SOC3) and Land Use (SOC4). The physical dimension is composed of Shelter Type (Density) (PHY1), Critical Infrastructure (PHY2), Facilities Physical Vulnerability (PHY3) and Roads (PHY4). The selection process of these indicators is based on the existing literature (see Indicator Table in the Appendix A) and adds on the vulnerability components used in the Risk Mitigation for Humanitarian Settlements project. The selection was guided by the in Section 4.1.6 defined criteria for selecting suitable indicators. The main constraining criterion for including indicators into the HFVI is primarily the availability of data. Thus, other indicators that could also contribute to flood vulnerability in refugee camps (such as the population's coping capacity or historical experience) are not considered. When critically evaluating the selected indicators against the defined criteria retrospectively, it is essential to consider that all indicators at least partially rely

on local data inputs. Consequently, reproducibility, data accuracy, and comparability issues must be stressed. The accuracy and topicality of the local data (i.e. camp layout map and camp population statistics) are crucial to the reliability of the local data, especially since refugee camp settings possess a dynamic nature with fast-changing conditions. (Bernhofen et al., 2023) suggests, for example, that further research could incorporate and evaluate additional global datasets, such as night-time light data. This data, with its high temporal resolution, could be particularly useful for capturing changes in camp boundaries and populations - an aspect that the used building footprint datasets cannot address effectively. Additionally, camp-specific local data often depends on the availability of information from participatory workshops or interviews, which provide details about the locations of vulnerable groups or fragile infrastructure within the camp. While the information obtained through these participatory approaches is highly valuable, especially when other data is unavailable, it must be acknowledged that this data carries significant uncertainties due to subjectivity and potential inaccuracies. Therefore, the heavy reliance on local data inputs restricts the indicators' reproducibility, comparability, and validity.

6.1.2 Spatial modelling of refugee camp vulnerability

Incorporating a composite raster-based index approach to quantify flood vulnerability within refugee camps, as proposed by Birkmann (2013), allows for a detailed representation of spatial variations in vulnerability, making it particularly effective for assessing the impacts of flood hazards. This raster-based approach differs from the procedure used in the Risk Mitigation for Humanitarian Settlements project, which utilizes vector data to assess vulnerable assets (Kaufmann et al., 2022). Regardless, the raster-based approach offers several advantages, particularly in quantifying vulnerability indicators such as population density or counts of facility types per grid cell, enabling a more nuanced representation of spatial relations.

As found in Kocsis et al. (2022) the use of raster data is particularly effective for flood risk modelling where hazard data is already rasterized. Here, it enables seamless integration of the HFVI within the Flood Risk Mapping GIS tool, which uses rasterized flood hazard data, ensuring compatibility and allowing for a more accurate overlay and analysis of spatial data. Raster data can represent continuous variation in vulnerability levels across different areas, which is essential for detailed flood risk assessments. While vector data is precise for specific assets, it may not capture spatial variability as effectively when integrated with rasterized hazard data (Fernandez et al., 2016). Although raster data is suitable for visualising continuous spatial variations, it also has its limitations. The resolution of raster data can affect the accuracy of vulnerability assessments. For the HFVI, a resolution of 30 meters is used in order for the HFVI to depict the spatial differences within refugee camp boundaries. The choice of grid cell size significantly impacts the analysis's level of detail and precision. Smaller grid cells capture more detail but can also introduce noise and variability that may lead to overestimating certain features or attributes. Conversely, larger grid cells might oversimplify the data, missing critical spatial variations (Zabota et al., 2021).

Further, using a composite index approach, as recommended by the JRC and OECD (2008) to spatially quantify flood vulnerability, the HFVI generalizes the multidimensional concept of vulnerability. Using a composite index is especially effective for modelling in data-scare regions because it provides a comprehensive overview of flood vulnerability by combining multiple indicators from various sources into a single metric, providing a more robust basis for decision-making and planning in regions where data is scarce (Malgwi et al., 2020). As a single and standardized metric, the HFVI approach further

enables inter-comparability between different camps. The HFVI can theoretically be applied to any refugee camp globally, offering a scalable method for first-order vulnerability analysis. However, it is essential to note that the reproducibility and performance of the HFVI applied to diverse camp settings have not yet been validated, as it has only been applied to a single case study so far. Future work will be necessary to test, compare and confirm its effectiveness in various refugee camp contexts. This is crucial because it would allow the HFVI to measure and compare flood vulnerabilities across various camps, which could facilitate better resource allocation and policy-making. By applying the same set of indicators and weighting methods, stakeholders could effectively compare the vulnerability levels of different camps, identify the most at-risk areas, and prioritize regional interventions accordingly (Bernhofen et al., 2023). While using composite indices in flood vulnerability assessments offers several benefits, it also comes with limitations. Birkmann (2007) argues that while indicators are important tools, they must be handled carefully to avoid oversimplifying complex interactions. This simplification can potentially lead to the loss of important contextual information, which is crucial for understanding the nuanced dynamics of vulnerability in different settings. Morse (2004) highlights the limitations of reducing multifaceted development challenges to numerical values, emphasizing the need for a more holistic and nuanced approach that considers qualitative factors, local contexts, and stakeholder perspectives.

In conclusion, it is worth mentioning that modelling flood vulnerability proves to be a complex task because vulnerability is an abstract concept that is not directly measurable in reality. It highly depends on specific spatial and contextual factors, making it challenging to create accurate and universally applicable models, especially in data-scare regions and fast-changing conditions. As a result, the index developed to represent flood vulnerability can only serve as a simplified generalization, which needs to be interpreted critically. An extensive validation of the HFVI is essential for the future use of the index, guaranteeing its accuracy, reliability, and applicability in real-world scenarios. This could involve UNHCR camp officers' knowledge inclusion to counteract the highlighted data scarcity and uncertainties.

6.1.3 HFVI indicator weights

Having identified the indicators contributing to flood vulnerability in refugee camps, expert knowledge is utilized to assign appropriate weights to these indicators, which are finally used as factors in the HFVI calculation. Here, the evaluation of these indicator weights is discussed critically, focusing on constraints in the questionnaire design, inconsistencies in experts' responses, and the resulting indicator priorities, ultimately providing the answers to the research question RQ1.2.

Using questionnaires, the aim was to determine the relative influence of each specific indicator on overall vulnerability. Given the abstract and multidimensional character of vulnerability, gathering experts' opinions on the relative importance of these indicators helps derive the most suitable weights that match the context of refugee camp settings. Such methods incorporating experts' knowledge are invaluable for assessments in the given context and employ the "the wisdom of the crowd" principle introduced by Galton (1907), which highlights the value of collective judgment to generate quantitative weights as inputs for the composite index. Studies such as those by Cutter et al. (2003) and Birkmann (2007) have similarly highlighted the importance of expert-based weighting methods in vulnerability assessments, demonstrating the effectiveness of this approach in various contexts.

To incorporate expert knowledge into the HFVI approach, the Analytic Hierarchy Process (AHP) is used to evaluate and prioritize various flood vulnerability indicators for refugee camps. The AHP method is chosen because it can manage complex decision-making processes by breaking down problems into more straightforward pairwise comparisons. This approach is particularly suited to this study because addressing the issue of vulnerability being an ill-structured problem with multiple solution paths and inherent uncertainties regarding the importance of different criteria (Brito et al., 2018).

6.1.3.1 Survey design limitation

The AHP survey (see Appendix A) is designed to gather expert opinions on the relative importance of the eight selected HFVI indicators. However, several challenges were encountered during the design and implementation of the questionnaire. Some indicators may have been insufficiently defined, leading to varied interpretations among respondents. All indicators are defined in the introduction of the questionnaire. However, in critical revision of the questionnaire design, it becomes apparent that while most of the indicators are sufficiently defined by providing some examples of subcategories, the Critical Infrastructure indicator (PHY2) suffers from a vague definition. The description did not mention the elements falling into this category, namely the presence of fragile building infrastructure, sanitation network, drainage system, water tanks, communication infrastructure, and power stations. Another limitation of the questionnaire is that the response rate is limited to 20%, yielding only 11 participants' answers. A larger sample would have provided a more robust dataset, improving the reliability of the AHP results. Notably, no responses were received from UNHCR officers, who are intimately familiar with the refugee camp settings. Their insights would have significantly enriched the understanding of the on-ground realities of flood vulnerability in camps, hence providing invaluable knowledge to the indicators' influence on the overall vulnerability. The subjective nature of responses posed another challenge. Experts' answers are influenced by their broad ranges in background, experiences, and the conditions they are accustomed to. While inherent in AHP, this subjectivity can introduce biases into the results, which in turn justifies the use of the Fuzzy AHP approach, as introduced in the Methods Section 4.1.8.7.

6.1.3.2 AHP results and inconsistencies

The AHP methodology applied results in individual priority weights for each of the eleven experts, highlighting the relative importance of social and physical vulnerability indicators (see Table 5.1. Population Density (SOC1) is considered the most critical social indicator, with a median priority weight of 40.33%, followed by Vulnerable Groups (SOC2) at 26.22%. Facilities Physical Vulnerability (PHY3) and Shelter Type (PHY1) are the highest-rated physical indicators, with median weights of 33.12% and 29.20%, respectively. Notably, there is substantial disagreement among experts regarding Population Density (SOC1) and Vulnerable Groups (SOC2), reflected by a wide range of weights. Conversely, Land Use (SOC4) shows the most minor variability, indicating greater consensus. The overall comparison of social versus physical vulnerability dimensions shows equal importance of both dimensions, with a slightly higher aggregated weight and range in individual weights assigned to the physical dimension.

The survey shows that the answers of many experts lead to inconsistent results. The inconsistency analysis aims mainly to observe whether the respondents would have made inconsistent choices due to poorly defined attributes or because a pairwise comparison between those attributes inherently does

not make sense. As the preference weights of an AHP survey highly depend on subjective decision-making, the AHP methodology often includes inconsistencies, especially in complex cases, including many sets of comparisons (Pascoe, 2022). Inconsistencies are, hence, a notable aspect of the AHP results.

Of all 11 experts, only three experts do not reveal a single inconsistency in all their answers, as indicated by a low consistency ratio of $CR < 0.1$ (Table 5.3). Specifically, half of all 33 pairwise comparison matrices (PCMs) based on the experts' answers show inconsistent results. For the pairwise comparison of social vulnerability indicators, 6 out of 11 responses are inconsistent. Similarly, for the physical indicators and the comparison between social and physical dimensions, 5 out of 11 responses show inconsistency. The most frequent judgment errors are identified for each PCM, revealing that the pairs Population Density vs. Vulnerable Groups (SOC1 vs. SOC2) and Shelter Density vs. Critical Infrastructure (PHY1 vs. PHY2) exhibit the highest top1 error frequencies. High error frequencies are also observed in the comparison of Critical Infrastructure vs. Roads (PHY2 vs. PHY4). The high frequency of errors when comparing indicators with critical infrastructure (PHY2) could be due to the aforementioned vague definition of this indicator in the introduction to the questionnaire.

The high error rates, as illustrated in Figure 5.3 in comparisons SOC1 vs. SOC2 and PHY1 vs. PHY2 might be attributed to the structure of the AHP survey design. These combinations are the first to be compared, and respondents may answer them without considering the subsequent comparisons. As they progress through the questionnaire, they better understand the relative importance of the other indicators. However, if they do not go back to revise their initial comparisons, these early answers could remain inconsistent. This pattern suggests that respondents might benefit from revisiting and adjusting their initial comparisons after completing the entire questionnaire to ensure consistency across all judgments. This observation is supported by Ishizaka and Labib (2011), who highlight the benefits of revising initial comparisons to enhance overall consistency. They emphasize that respondents should consider the entirety of their judgments and make revisions where necessary to align their initial responses with their final understanding of the indicators' relative importance. Pascoe (2022) also argues that respondents often don't double-check their answers, and even if they do, achieving a perfectly consistent set of responses when comparing numerous attributes can be challenging. The selection of a specific value may also be influenced by factors like the respondent's focus, mood, emotions, and cognitive abilities. Inconsistencies can emerge due to random errors stemming from fluctuations in their mental states. Additionally, the discrete nature of the 1-9 scale used in AHP might contribute to inconsistency since achieving perfect consistency might necessitate fractional preference scores (Pascoe, 2022).

To address these inconsistencies, Harker's method is employed, reducing the inconsistencies by iteratively replacing the most inconsistent values. Applying this approach effectively minimizes inconsistencies in the PCMs, with most CR values falling below the threshold after the transformation. Only 5 out of 33 PCMs remain inconsistent (Table 5.4), highlighting the challenge of achieving perfect consistency in complex AHP evaluations. The high variability and inconsistencies associated with the initial results suggest a need for more precise definitions and additional questionnaire revision to improve consensus. Future work should focus on refining indicator definitions, increasing participant numbers, or incorporating automated consistency checks to improve the reliability of AHP results in this context, as also highlighted by several studies Brito et al. (2018), Ishizaka and Labib (2011), and Saaty (2008).

6.1.4 Addressing uncertainty in vulnerability assessment

As stressed in the Literature Review in Section 3.2.2, incorporating uncertainty and sensitivity analysis into the assessment of local flood vulnerability addresses a current research gap and is essential for enhancing the reliability of flood vulnerability modelling (An et al., 2022). One way to manage the uncertainty in AHP weights is using the Fuzzy Analytical Hierarchy Process (FAHP). The FAHP extends the traditional AHP by incorporating fuzzy logic, which allows for the representation of uncertain or imprecise expert judgments. This is particularly relevant given the inherently vague definition of flood vulnerability and the difficulty of evaluating it using crisp numbers. Fuzzy logic, with its multi-valued approach, provides a more nuanced framework for decision-making, enabling statements to be partially true or false rather than strictly binary (Metzger et al., 2018; Pinheiro et al., 2018).

While this study focuses on epistemic uncertainty within the AHP methodology, it is crucial to recognize that other types of uncertainties also affect vulnerability assessments. For instance, this study does not address aleatory uncertainty arising from inherent randomness and variability in natural processes. Further, spatial and attribute-related uncertainty in the used data and model uncertainty stemming from assumptions and simplifications in the modelling process is ignored. Accounting for these additional uncertainties is essential for a comprehensive assessment and would further enhance the reliability and applicability of the vulnerability model (Walker et al., 2003).

6.1.5 Incorporating fuzzy logic into the HFVI

Incorporating fuzzy logic into the HFVI model is crucial in addressing the inherent uncertainty and variability in expert opinions (Roy et al., 2023). Traditional AHP methods assume that experts can provide precise, unambiguous judgments. However, as the consistency analysis of the AHP results and the large spread in the expert's answers have shown, the judgments are accompanied by subjectivity and uncertainty. FAHP offers a way to model these uncertainties more accurately, enhancing the robustness and reliability of the final vulnerability assessment (Ganji et al., 2022). However, the fuzzification process also brings limitations which need to be highlighted to better understand results in the final HFVI and uncertainty maps.

By using triangular fuzzy numbers (TFNs) to represent the pairwise comparisons, FAHP captures the range of possible values reflecting the uncertainty in the experts' judgments (Metzger et al., 2018; Pinheiro et al., 2018). In this study, the initial PCMs are transformed into fuzzy pairwise comparison matrices (FPCMs), subsequently aggregating into the final fuzzy weights (wMin, wModal and wMax and a defuzzified weight) using the Buckley's method (Buckley, 1985) as described in the Methods Chapter 4.1.8.7.

Comparing the resulting weight of the fuzzy AHP to the traditional AHP weights, it can be observed that the final weighting of both methods results in the same ranking of relative importance between the indicators, with Population Density (SOC1) and Facilities Physical Vulnerability (PHY3) being the most influential indicators. However, it can be observed that the FAHP enhances the differences between high and low weights compared to the standard AHP weights. This could be explained by the fact that by considering the range of expert opinions, FAHP can amplify differences where there is strong agreement among experts. For example, if the majority of experts strongly prioritize one indicator over another, the fuzzification process will capture this strong preference and the subsequent defuzzification will reflect it as a higher weight and vice versa for lower weights.

Further, it is discovered that the fuzzification process introduces asymmetrical behaviour in the weights by transforming the PCM answers into the TFNs. This means that the range of possible values, given through the upper and lower fuzzy numbers, is not evenly distributed around the modal value, often skewing towards higher values. When representing fuzzy numbers for reciprocals, the difference between the lower and modal values is typically smaller than between the upper and modal values. For example, a fuzzy number represented as (1/7, 1/6, 1/5 or 0.14, 1.66, 0.2) illustrates the asymmetry. This asymmetrical representation means that when experts judge an indicator as much less important (hence, a small reciprocal value), the fuzzification process captures a wider range of uncertainty on the higher end. Consequently, the TFN membership function's modal value is closer to the lower bound of the fuzzy number, leading to a general reduction of low-importance indicators. For indicators judged to be highly important (integer elements), the fuzzy numbers are symmetrically spread around the modal value. However, the integer fuzzy numbers exhibit a higher spread in absolute terms, always equal to $\pm$ 1. Contrarily, the reciprocal TFNs exhibit a smaller absolute spread, leading to more distinct weights for less important indicators due to reduced overlap when aggregating TFNs. In conclusion, the observed asymmetry can impact the final results, as indicators with higher upper bounds in their fuzzy numbers may significantly influence the overall vulnerability assessment. Consequently, using FAHP weights results in more precise differentiation between high and low weights than traditional AHP values, accurately reflecting expert consensus and uncertainty.

Enhanced differentiation in the FAHP weights benefits decision-making processes by allowing for clearer prioritization of the most critical indicators. This approach is supported by Qian Zheng and Shen (2021), who demonstrated that the FAHP method is more efficient in identifying high-risk areas than the original AHP. However, there is a lack of studies dealing with the asymmetric effect of the TFN approach and its possible impact on the application results. Further research and analysis are therefore needed to fully understand the influence of this asymmetrical behaviour of FAHP on the final HFVI results.

Generally, the results of including Fuzzy AHP show that the approach provides a more nuanced representation of relative importance and ensures that variability in judgments is accounted for, thus yielding more stable and reliable outcomes (Metzger et al., 2018; Pinheiro et al., 2018). Regardless of accounting for subjectivity by including fuzziness, the results remain subjective and inevitably uncertain, as argued by Qian Zheng and Shen (2021). The fuzzification of AHP weights, using triangular fuzzy numbers, addresses some uncertainty in the evaluation process, but some studies highlight challenges with this approach. For instance, Saaty (2008) suggested that the fuzzification of the AHP method might not always yield optimal outcomes and recommended using intermediate values to address uncertainty as done in Fozaie and Wahid (2022). Despite these challenges, the benefits of incorporating fuzzy logic into AHP, such as better handling of uncertainty and improved model robustness, often outweigh the drawbacks as shown in multiple studies such as Fozaie and Wahid (2022), S. Lee (2014), Roy et al. (2023), and Torfi et al. (2010).

6.1.6 Sensitivity analysis: The novel FAHP-OAT approach

Although often neglected, sensitivity analysis is a critical component of flood vulnerability assessment (Y. Chen et al., 2010), helping to identify the most influential indicators in determining the final vulnerability index and reveal uncertainties indicator weights. In this study, a novel approach is employed that extends the traditional One-At-a-Time (OAT) method, as described in the Methods Section 4.1.10, by incorporating calculated ranges from the fuzzy weights for each indicator adjustment to account for inherent weight uncertainty.

The novel FAHP-OAT approach adopted in this study provides a robust framework for evaluating the uncertainty and sensitivity of the HFVI. The traditional OAT methods, which involve varying one indicator's weight within a fixed range while keeping others constant (Y. Chen et al., 2010), is extended in this study by incorporating the calculated ranges from the fuzzy weights. This integration allows for a more comprehensive sensitivity analysis, capturing the variability in expert judgments and the potential impact on the HFVI. Using fuzzy weights in sensitivity analysis ensures that the assessment considers the full range of possible values, providing a more realistic picture of the uncertainty involved. The resulting uncertainty maps could also be interpreted as different scenarios depending on minor weight changes in the given fuzzy weight range. The OAT method, extended with fuzzy weight ranges, helps identify which indicators are most influential in determining the final HFVI. This analysis is crucial for verifying the resilience of the HFVI results when input data undergoes minor alterations. Thereby, sensitivity analysis examines uncertainties in evaluating indicator criteria and the spatial implementation of the HFVI, ensuring that the model remains robust under various scenarios of expert judgment variability. The practical application of this novel FAHP-OAT approach is discussed in more detail in section 6.2.1.4 using the case study data.

6.2 HFVI case study application and performance

The following section discusses the application of the HFVI to the Mahama refugee camp case study (RQ1, RQ1.1) and discusses the results and challenges associated with its usability (RQ1.2). Further, it highlights the importance of validating the index to ensure its effectiveness and reliability in different refugee camps (RQ1.2).

6.2.1 Flood vulnerability in the Mahama Refugee Camp

6.2.1.1 Spatial HFVI pattern

Applying the HFVI in the Mahama Refugee Camp provides insights into the spatial behaviour of flood vulnerability within the camp. Analyzing the spatial pattern in the final HFVI map in Figure 5.13 reveals significant vulnerability hotspots. Moderate to high HFVI values are primarily found in areas of dense residential shelters. These regions suggest high flood vulnerability due to factors such as high population and shelter densities and inadequate building infrastructure. This result is not surprising given the high positive spatial correlation between those indicators, as illustrated in the correlation matrix 5.9 in the Results Section 5.2.4. Hotspots of the highest HFVI values are noted at specific locations, particularly in the camp's northeastern and central parts, where the especially vulnerable population is present. These areas include zones with high densities of shelters housing predominantly elderly people, often exhibiting higher vulnerability due to health concerns, emphasizing the need for targeted flood risk reduction measures in these critical areas. As expected, low HFVI values are

located in non-built-up areas, such as open spaces or agricultural land, primarily in the eastern parts of the camp, indicating lower flood vulnerability. Here, the reason for HFVI values is twofold. First, the spatial vulnerability of the non-built-up areas is only influenced by one indicator, namely Land Use (SOC4). Consequently, no other indicator is present to enhance the multilayered effect of the HFVI. Also, the Land Use Indicator (SOC4) was assigned the lowest weight in the experts' judgment, leading to low flood vulnerability in such areas. Conversely, multiple indicators overlay each other in many regions of the built-up areas, hence increasing the HFVI values. Most notably, indicators that are weighted highest (Population Density (SOC1), Vulnerable Groups (SOC2), and Shelter Type Density (PHY1)), therefore, determine the spatial pattern of vulnerability hotspots within the Mahama Refugee camp.

Interestingly, Facilities Physical Vulnerability (PHY3), despite being assigned the highest weight among physical indicators, does not significantly contribute to increased vulnerability values. Instead, the presence of Critical Infrastructure (PHY2) appears to elevate the HFVI value in some areas more substantially. Also, when analyzing the $HFVI_{PHY}$ map in Figure 5.7 individually, the effect of the facilities seems rather low. Consequently, in the final HFVI map, despite the doubled effect of the facilities' location through SOC3 and PHY3, facility areas do not exhibit high vulnerability values. This behaviour could be attributed to the linear aggregation procedure offering a higher compensability with other indicators of low importance, as discussed by Moreira et al. (2021), reducing the overall HFVI value. Another influencing cause could lie in the quantification method of the indicators. For facilities vulnerability quantification, relative building area per grid cell was considered, whereas counts were used for shelter density quantification. Additional validation and testing are required to study coupling effects in more detail as the relationships become complex post-normalization. While normalization is necessary to construct the HFVI and ensures uniformity between individual indicators for spatial overlay, this process introduces a layer of abstraction that complicates the interpretation of final results. Thus, while the HFVI provides a robust framework for identifying flood vulnerability, the nuanced understanding of specific indicators' contributions necessitates careful consideration of their quantification and normalization processes.

The $HFVI_{SOC}$ and $HFVI_{PHY}$ maps in Figure 5.7, along with the individual layers of vulnerability indicators in Figure 5.6, which depict normalized indicators, provide crucial supporting information alongside the final HFVI map. These maps are essential for identifying the driving factors behind the spatial behaviour of vulnerability and explaining the origins of hotspots. By analyzing these individual maps, decision-makers can gain valuable additional insights. However, only when these maps are combined into the final HFVI can a holistic view of vulnerability as a multidimensional construct be obtained. The analysis of the combined HFVI spatial patterns from the case study indicates that the HFVI effectively reveals hotspots and is able to map the relative behaviour of flood vulnerability within the Mahama camp.

Reflecting on the questions posed by Kienberger (2013) to understand the spatial behaviour of vulnerability (as introduced in the Literature Review Chapter 3.2), the resulting HFVI can effectively answer the "where" (spatial variations of vulnerability are depicted and hotspots are identified), "what" (vulnerability encompasses different dimensions, namely social and physical vulnerability), and "how" (vulnerability is indirectly assessed and characterized by these indicators that also enable the representation of individual vulnerability dimensions) questions. In conclusion, by providing a single quantitative metric that includes social and physical dimensions and their quantitative indicators, the HFVI effectively illustrates spatial differences within the camp. Thus, the HFVI provides essential an-

swers to these questions, which are crucial for addressing challenges in cooperative planning contexts, particularly in disaster risk reduction (Kienberger, 2013).

Despite the ability of the HFVI to depict spatial vulnerability patterns, interpreting the results from a single metric can be challenging at first glance. Therefore, it is recommended to use the individual indicator layer maps of the $HFVI_{SOC}$ and $HFVI_{PHY}$ as supplementary information sources, particularly for identifying the driving forces behind high-vulnerability regions. Future work should aim to enhance the interpretability of the HFVI's spatial patterns. One potential approach is to develop an interactive tool that visually represents the influence of individual indicators on the overall HFVI value for any given location, possibly through the use of pie charts or other advanced visualisation methods. This would allow for more precise tailoring of mitigation and response actions to address the key driving forces behind vulnerability hotspots.

6.2.1.2 Spatial correlation

The results of the spatial correlation analysis in Section 5.2.4 confirm the effectiveness of the HFVI in visualising flood vulnerability hotspots. The results reveal a positive spatial autocorrelation, indicating a clustering of similar HFVI values. This clustering is critical as it demonstrates the HFVI's efficacy in identifying areas with varying levels of flood vulnerability. The ability of the HFVI to detect these spatial clusters of vulnerability is vital for strategic planning and intervention, particularly in resource-constrained environments like refugee camps.

Further, the results of spatial correlation analysis (see Figure 5.9 between the individual vulnerability indicators show that some indicators, such as Vulnerable Groups (SOC2) and Roads (PHY4), exhibit weak correlations. Others show a negative correlation, such as Population Density (SOC1) and Facilities of Social Importance (SOC3) and Land Use (SOC4) and shelter type density (PHY1). However, the weak or negative correlations could serve as an argument in favour of the importance of including these indicators as they measure different aspects of vulnerability and thus provide a holistic view of vulnerability. This independence is valuable, as it ensures each indicator contributes unique information to the index, enriching the overall assessment. Conversely, strong correlations, such as those between Population Density (SOC1) and Shelter Density (PHY1), as well as between the social and physical facilities vulnerability indicators (SOC3 and SOC4), may suggest redundancies. If two indicators are highly positively correlated, they might be measuring similar phenomena. In such cases, simplifying the index by removing or adjusting one of the redundant indicators could enhance its efficiency without losing essential information. As (Fernandez et al., 2016) have argued, Principal Component Analysis (PCA) provides an alternative to subjective variable selection by objectively reducing a large number of variables into a few uncorrelated factors that capture the variability in the underlying data. However, in cases of strong correlation involving indicators from different dimensions, preserving both indicators is here justified due to their distinct contextual consequences. In a densely populated part of the camp, a flood event affects not only many people and their livelihoods but also more shelters that can be destroyed by flooding, which significantly increases the overall flood vulnerability. Therefore, it is important to include both indicators in the assessment despite their high spatial similarity.

6.2.1.3 Missing local data and associated uncertainties

One significant limitation in the HFVI assessment for the Mahama Refugee Camp is the issue of missing local data. For example, the facility buildings in the western corner of the camp are not depicted in the Camp Layout map (see Appendix A), which is used to categorize buildings. Despite being covered in the building dataset, these newly constructed buildings are neglected in the HFVI overlay as the facility type information was missing. This omission results in artificially low vulnerability values in that particular area of the HFVI map (Figure 4.7, contributing to attribute and positional uncertainties. However, as the approach only addresses the epistemic uncertainty in indicator weight, such uncertainties are ignored. Addressing the limitation of missing information requires either obtaining more up-to-date local data or introducing additional uncertainty measures to account for such gaps.

Another way to reduce such uncertainties is the enhancement of participatory knowledge inclusion. However, participatory information often comes with its own set of uncertainties. For instance, data from the participatory mapping workshop with Mahama camp officers, conducted by researchers from the project on Risk Mitigation for Humanitarian Settlements during the summer of 2023, was used to map locations of critical infrastructure and the presence of vulnerable groups. The researchers noted that the virtual participatory workshop had significant limitations and did not yield data as detailed as that obtained from an in-person workshop (Kaufmann et al., 2022). Despite these challenges, the integration of local knowledge remains crucial to the assessment. Leveraging the use of participatory knowledge, future work should account for the positional vagueness of such mapping exercises to enhance the accuracy and reliability of the assessments. Therefore, the approach used in this work is not fully capable of addressing the highlighted research gap of including uncertainties in flood vulnerability assessment, as it ignores other types of uncertainties. However, the developed approach presents a way to partially cover this research gap by considering epistemic uncertainty analysis as a starting point. This inclusion provides an initial framework for uncertainty consideration, although further development is needed to integrate the remaining types of uncertainties due to vagueness and lack of spatial information into flood vulnerability assessments.

6.2.1.4 Interpreting uncertainty results

The sensitivity analysis results from the Mahama case study (see Section 5.2.5 show that certain indicators substantially impact the HFVI more than others. For instance, Population Density (SOC1) and Shelter Density (PHY1) exhibit the highest sensitivity to weight changes, indicating their critical role in the flood vulnerability assessment (see Figure 5.10. These indicators also show significant ranges, reflecting the high degree of uncertainty associated with their weights. Conversely, indicators like Facilities of Social Importance (SOC3), Land Use (SOC4) and Roads (PHY4) have lower sensitivity and narrower ranges, suggesting a more consistent expert consensus on their importance. Not surprisingly, the results indicate that higher-weight indicators generally exhibit higher sensitivity. This correlation could be explained by the proportional impact that each indicator's weight has on the overall HFVI calculation. Indicators assigned higher weights have a more substantial influence on the final vulnerability index, making changes in their weights more impactful on the overall HFVI results. For instance, Population Density (SOC1) and Shelter Density (PHY1), which have the highest weights among the social and physical indicators, respectively, also exhibit the highest sensitivity to weight changes. The high sensitivity underscores their critical role in determining flood vulnerability within the Mahama Refugee Camp. This behaviour of sensitivity values following the order of the

criteria weights is also observed by Y. Chen et al. (2010), who performed a spatial sensitivity analysis of multi-criteria weights in GIS-based land suitability evaluation. Furthermore, integrating the fuzzy ranges of the FAHP weights allows these weights to change within a broader range, especially for indicators with higher expert disagreement. Consequently, the uncertainty of these influential indicators is also the highest. This broader range of allowed scenarios for high-weight indicators results from the experts' varying opinions, which is captured through the FAHP methodology. Thus, indicators with higher weights, such as SOC1 and PHY1, not only exhibit higher sensitivity due to their substantial influence but also because their weight ranges are more extensive due to higher expert disagreement. Interestingly, Facilities of Social Importance (SOC3) and Land Use (SOC4) exhibit similar sensitivity values despite having different weights. This anomaly suggests that these indicators might share similar characteristics in their contribution to vulnerability, or it may reflect a limitation in the current modelling approach that doesn't fully differentiate their impacts.

Putting the quantified uncertainties into a spatial context, the resulting uncertainty maps reveal that both social and physical vulnerability uncertainty maps (see Figure 5.11 exhibit a relatively uniform distribution of weight uncertainty. Higher uncertainty values are predominantly observed in built-up areas, while bordering agricultural or bare land areas show low to no uncertainty. This suggests that densely populated regions or areas with significant infrastructure are more susceptible to variations in vulnerability values due to changes in weight criteria. The combined uncertainty map 5.12 reveals that weight uncertainty hotspots are located in the upper right corner of the Mahama Refugee Camp near the camp boundary and in the central part of the camp, influenced by weight-sensitive critical infrastructure and high shelter density. Moderate uncertainty is observed in the northeastern region due to facilities with high physical vulnerability and vulnerable groups.

Overall, the sensitivity analysis confirms the proportional relationship between indicator weights and sensitivity, with higher-weight indicators showing greater sensitivity. This relationship is further accentuated by the integration of fuzzy logic, which captures the variability and uncertainty in expert opinions, ultimately affecting the robustness and reliability of the HFVI results. Future work should focus on refining these weights and possibly integrating more sophisticated methods to handle expert disagreements and uncertainties more effectively. However, visualising these uncertainties spatially in conjunction with HFVI maps as done here, could provide a valuable tool for decision-makers. By overlaying uncertainties onto the final HFVI map, the associated uncertainties become visible, helping to identify and prioritize areas for action and ensuring that these uncertainties are acknowledged rather than ignored. This approach could lead to a more informed and effective response to flood vulnerability in refugee camps.

However, this observed relationship between indicator weights and their sensitivity disappears when overlaying the uncertainties to a combined metric. In the overlaid final map in Figure 5.13, which depicts the HFVI pattern alongside with uncertainty classes, it is evident that the hotspots of the HFVI and the uncertainty do not necessarily coincide spatially. This indicates that areas with high HFVI scores, indicating greater vulnerability, are not always the same areas with high uncertainty in weight assessments. The driving causes of the discrepancy between sensitivity hotspots and final HFVI hotspots are primarily due to the interactions between different indicators and the methods used to aggregate them. The final HFVI map, including the uncertainty map overlay in Figure 5.13, offers the potential for improved decision-making by highlighting areas where high HFVI values do not correspond to the highest uncertainty classes. For the Mahama Refugee Camp, this approach would suggest prioritising locations where vulnerable groups are present, as these areas exhibit the

highest relative HFVI values compared to other camp locations while showing only medium levels of uncertainty.

6.2.2 Future applicability and validation

The HFVI is designed to provide insights into the spatial distribution of vulnerability within a camp, and shows practical values for the Mahama Camp application. However, it is crucial to critically consider whether the index is reliable when applied to other spatial scales or camps. Unlike hazard, which is influenced by topographic settings, vulnerability, as defined in this study, is determined by the camp's characteristics and does not inherently vary with the terrain (Birkmann, 2007; Malgwi et al., 2020). Integrating the HFVI with spatial flood hazard data to provide a comprehensive flood risk assessment would provide more meaningful insights into actually exposed vulnerable areas.

As highlighted by Malgwi et al. (2020) and Papathoma-Köhle et al. (2019), vulnerability indicators are often specific to regional contexts, meaning a set of indicators may not be directly transferable to all camps. The spatial variability of vulnerability is thus dependent on the camp's layout, infrastructure and social setting (Eriksen et al., 2021). The HFVI alone may not be as meaningful in camps where the setting does not differ significantly in space. For instance, the shelter type is homogeneous in the Mahama case study. All residential shelters in the Mahama camp are uniform and have the same structural design as described by UNHCR (2023a). This uniformity leads to less variability in the HFVI results. However, in camps with more significant spatial variability, the HFVI could reveal more meaningful insights (An et al., 2022; Kaufmann et al., 2022).

The conceptual framework of the HFVI offers scope for considering these context-related variations. The sub-categories of the indicators and their associated vulnerability ranks allow camp-specific differences to be taken into account. How well the indicator works in other camps, however, is the subject of future research. Prospective work should therefore focus on assessing the HFVI performance in multiple camps, including detailed validation. Further, the potential spatial dependency of the judgment of relative indicators importance raises additional concerns about the reproducibility of the index. Although experts assigned weights to the indicators independently of location, suggesting these weights are globally applicable, it could be argued that the individual indicators weights might vary depending on the specific settings of each camp. This might necessitate different prioritization based on local conditions (Malgwi et al., 2020; Papathoma-Köhle et al., 2019).

Additionally, the absence of validation for the HFVI results and performance presents a significant limitation to the HFVI's credibility and practical utility. This section critically examines the challenges associated with the lack of validation and discusses potential approaches to address this gap. Validation is crucial to ensure the HFVI accurately reflects flood vulnerability in refugee camps and provides reliable information for decision-making (Fernandez et al., 2016). However, this study has not included a formal validation process, raising concerns about the accuracy and applicability of the results. In fact, most studies which deal with the development of vulnerability indices lack detailed validation, as stated by An et al. (2022) and Moreira et al. (2021), who undertook a comprehensive review of approaches to flood vulnerability indicators.

While the Mahama case study serves to apply the developed index in a real-world context using geospatial data, it does not fully assess the index's validity and performance. Incorporating uncertainty and sensitivity analysis can also serve as a form of validation by highlighting the robustness of the HFVI results for the case study implementation. The FAHP-OAT approach identified which indicators

have the most significant impact on the overall index and revealed areas where the model may be particularly sensitive to changes in input data or weights (Metzger et al., 2018; Pinheiro et al., 2018). However, the sensitivity analysis used here is bound to the spatial context of the Mahama Refugee Camp and is therefore not regarded as general validation of the HFVI performance. Including detailed validation is particularly crucial for assessing the reproducibility of the HFVI. Therefore, to thoroughly evaluate the HFVI, future research must include detailed validation through its application in multiple refugee camps. This broader application would help confirm the index's reliability and applicability across diverse settings, ensuring the approach is robust and adaptable.

One primary reason for the lack of detailed validation of the HFVI is the scarcity of comprehensive flood impact data in refugee camps. Many studies have highlighted the difficulty in validating flood vulnerability maps due to the lack of standardized workflows and reliable data sources. This issue is particularly pronounced in the context of refugee camps, where data collection is often hindered by logistical and resource constraints (An et al., 2022; Hussain et al., 2021). Despite these challenges, several qualitative approaches could be considered for future validation of the HFVI. Expert-based validation, through the engagement with UNHCR officers and other field experts through interviews and participatory mapping workshops, could provide valuable qualitative insights into the accuracy and relevance of the HFVI. Participatory approaches can provide localized knowledge and insights, ensuring that the index considers the camp population's unique vulnerabilities and coping mechanisms. In addition, experts' practical knowledge and experience can help identify discrepancies in the model and suggest improvements, ensuring that the HFVI reflects the on-ground realities of flood vulnerability refugee camps (Hussain et al., 2021; Kaufmann et al., 2022). Another alternative validation method involves conducting field visits to refugee camps to collect data on flood impacts and gather feedback from camp residents and officials. This approach provides qualitative validation of the HFVI by incorporating firsthand observations and insights from those directly affected, ensuring that the index accurately reflects on-the-ground realities and needs. Personal discussions and observations can provide context-specific information that may not be captured through remote data sources, enhancing the reliability of the index (Hussain et al., 2021). If available, historical flood data and records of flood impacts in refugee camps can be used to validate the HFVI as it was done by Ramkar and Yadav (2021). By comparing the index's predictions with past flood events and their consequences, researchers can assess the accuracy of the HFVI in identifying vulnerable areas (An et al., 2022). However, no such data was available for the particular case of the Mahama Refugee Camp.

The Flood Risk Mapping GIS tool developed as part of the Risk Mitigation for Humanitarian Settlements project by ETH and the UNHCR will be tested in the field in autumn 2024. The testing examines the tool's performance in one UNHCR pilot camp (location to be defined) using participatory methods to collect and incorporate the local knowledge of UNHCR field officers in the respective camp. As this thesis is part of the project, the developed index will also be validated during this testing phase in the field

In conclusion, the lack of validation for the HFVI results and performance is a critical limitation that must be addressed to enhance the index's credibility and practical utility. Future work should prioritize validation efforts and comparison of the HFVI performance across different camps. While the HFVI is a valuable tool for quantifying relative vulnerability to flooding in refugee camps and localising potential hotspots, its applicability and effectiveness may vary depending on the spatial and structural characteristics of the camp. Future research should focus on validating the HFVI across multiple camps with diverse settings to enhance its robustness and utility in supporting flood risk management and

resource allocation in humanitarian contexts (Chan et al., 2022). These approaches will help ensure that the HFVI provides an accurate, reliable and reproducible assessment of flood vulnerability in refugee camps, ultimately supporting more effective flood risk management and mitigation strategies in these vulnerable settings.

7 Conclusion

In this thesis, the Humanitarian Flood Vulnerability Index (HFVI) is developed to assess flood vulnerability in refugee camps, with a specific application to the Mahama Refugee Camp as a case study. The HFVI aims to provide insights into the spatial distribution of within-camp flood vulnerability, providing a standardized, quantitative, and spatial measure to assess flood vulnerability within refugee camps, addressing the challenges unique to these environments. The thesis answers the research questions addressed by elaborating a comprehensive approach to model flood vulnerability in the context of refugee camps and testing its usability in a case study. The presented results and discussion have identified the most critical factors influencing refugee camp vulnerability. In addition, strengths and weaknesses, as well as recommendations for future work, are discussed. The key findings in answering these research questions can be concluded as follows.

Flood vulnerability in refugee camps is modelled by incorporating both social and physical dimensions, each characterized by four influential vulnerability indicators. This comprehensive approach ensures a thorough assessment of flood vulnerability in refugee camps. A composite raster-based index method with a spatial resolution of 30 meters is employed, allowing for a detailed representation of spatial variations in vulnerability. This method is particularly suitable for assessing flood vulnerability in data-scarce regions, as it enables the quantification and spatial overlay of various vulnerability dimensions. By integrating multiple vulnerability indicators relevant to the refugee camp context and weighting them based on expert knowledge, the index provides an overall view of the spatial distribution of flood vulnerability. Breaking down the composite metric to its indicators further allows for a detailed understanding of the individual contributions to overall vulnerability, facilitating the planning of targeted interventions and mitigation measures.

Key findings indicate that Population Density and Facilities Physical Vulnerability are the most influential indicators highlighted by the expert weighting process. The use of the Analytic Hierarchy Process (AHP) and its extension through the Fuzzy AHP (FAHP) method enables a nuanced representation of relative importance, accommodating variability in expert judgments and yielding more stable and reliable outcomes. By integrating expert knowledge, the study provides a standardized overall statement on the degree of vulnerability. The application of the HFVI in the case study shows spatially explicit patterns of vulnerability and emphasises its efficiency in identifying hotspots. The index identifies areas where vulnerability is intensified due to the convergence of multiple contributing factors. The Mahama case study shows that there are significant hotspots of vulnerability in areas with high shelter and population density where vulnerable populations reside. Given their high positive spatial correlation, these factors significantly increase the combined HFVI score and shape the overall spatial pattern of flood vulnerability within the Mahama camp.

A vital aspect of this research is the incorporation of uncertainties into the assessment. By incorporating the FAHP, the developed Humanitarian Flood Vulnerability Index (HFVI) addresses subjectivity and disagreements in expert judgments. Combining the fuzzy weight ranges with the One-At-a-Time (OAT) sensitivity method proposes a novel approach that spatially maps the indicators' weight uncertainties on flood vulnerability, considering the full range of possible values in expert judgments. Communicating such uncertainties, instead of ignoring them, addresses a current research gap and could additionally assist decision-makers in taking more targeted measures. This combination of HFVI and uncertainty maps could help prioritize areas of high vulnerability and low associated uncertainty, thereby enhancing the prioritization of response actions.

The primary challenge remains the refugee camps' dynamic and data-scarce nature. Future efforts could be placed on enhancing local data collection, extensively including spatial or attribute-related uncertainties, and improving the visual communication of the results. Further, the results cannot be conclusively validated within the scope of this study. Model reproducibility is critical as the HFVI has only been applied to a single case study, and its performance in diverse settings remains invalidated. The integration and testing of the HFVI in combination with hazard data within the Flood Risk GIS tool of the project Risk Mitigation for Humanitarian Settlements is the subject of future work. Future research should hence focus on comparing the HFVI performance across multiple camps to ensure the HFVI's reproducibility, incorporating detailed validation processes using historical flood data or conducting validation workshops with camp officers and field visits for more qualitative insights.

In conclusion, the HFVI contributes to the field of science by advancing methodologies for assessing flood vulnerability in complex, data-scarce environments, particularly tailored refugee camps. As such approaches are currently lacking, this research addresses a critical gap by providing a standardized index for vulnerability assessment in refugee camps. This research lays a foundation for flood vulnerability assessment in refugee camps but requires future refinement to address the outlined limitations. Enhancing the HFVI's accuracy and applicability across diverse settings will ultimately aid in better resource allocation, disaster preparedness, and targeted interventions, thereby improving the resilience of vulnerable populations in refugee camps against the increasing risk of floods.

Bibliography

Aahlaad, M., Mozumder, C., Tripathi, N., & Pal, I. (2021). An object-based image analysis of WorldView-3 image for urban flood vulnerability assessment and dissemination through ESRI story maps. *Journal of the Indian Society of Remote Sensing*, *49*, 2639–2654. https://doi.org/10.1007/s12524-021-01416-4

Aguarón, J., Escobar, M., & Moreno-Jiménez, J. M. (2003). Consistency stability intervals for a judgment in AHP-decision support systems. *European Journal of Operational Research*, *145*, 382–393. https://doi.org/10.1016/S0377-2217(02)00544-1

Akola, J., Binala, J., & Ochwo, J. (2019). Guiding developments in flood-prone areas: Challenges and opportunities in Dire Dawa city, Ethiopia. *Jàmbá Journal of Disaster Risk Studies*, *11*. https://doi.org/10.4102/jamba.v11i3.704

Alduraidi, H., Abdulla Aqel, A., Saleh, Z., Almansour, I., & Darawad, M. (2021). Unrwa's role in promoting health outcomes of palestinian refugees in jordan: A systematic literature review. *Public Health Nursing*, *38*(4), 692–700. https://doi.org/https://doi.org/10.1111/phn.12889

An, T. T., Izuru, S., Narumasa, T., Raghavan, V., Hanh, L. N., An, N. V., Long, N. V., Thuy, N. T., & Minh, T. P. (2022). Flood vulnerability assessment at the local scale using remote sensing and GIS techniques: A case study in Da Nang City, Vietnam. *Journal of Water and Climate Change*, *13*, 3217–3238. https://doi.org/10.2166/wcc.2022.029

Anselin, L., Syabri, I., & Kho, Y. (2005). GeoDa: An introduction to spatial data analysis. *Geographical Analysis*, *38*, 5–22. https://doi.org/10.1111/j.0016-7363.2005.00671.x

Anwana, E. O., & Owojori, O. M. (2023). Analysis of Flooding Vulnerability in Informal Settlements Literature: Mapping and Research Agenda. *Social Sciences*, *12*(1). https://doi.org/10.3390/socsci12010040

Apel, H., Merz, B., & Thieken, A. H. (2008). Quantification of uncertainties in flood risk assessments. *International Journal of River Basin Management*, *6*, 149–162. https://doi.org/10.1080/15715124.2008.9635344

Archer, G., Saltelli, A., & Sobol, I. (1997). Sensitivity measures, ANOVA-like techniques and the use of bootstrap. *Journal of Statistical Computation and Simulation - J STAT COMPUT SIM*, *58*, 99–120. https://doi.org/10.1080/00949659708811825

ARSET. (2024). Earth Observations for Humanitarian Applications. NASA Applied Remote Sensing Training Program (ARSET) [Acessed: 18.06.2024]. http://appliedsciences.nasa.gov/get-involved/training/english/arset-earth-observations-humanitarian-applications

Baky, A. A., Islam, M., & Paul, S. (2019). Flood hazard, vulnerability and risk assessment for different land use classes using a flow model. *Earth Systems and Environment*, *4*, 225–244. https://doi.org/10.1007/s41748-019-00141-w

Balijepalli, C., & Oppong, O. (2014). Measuring vulnerability of road network considering the extent of serviceability of critical road links in urban areas. *Journal of Transport Geography*, *39*, 145–155. https://doi.org/10.1016/j.jtrangeo.2014.06.025

Barclay, J., Robertson, R., Scarlett, J. P., Pyle, D. M., & Armijos, M. T. (2022). Disaster aid? Mapping historical responses to volcanic eruptions from 1800–2000 in the English-speaking Eastern Caribbean: Their role in creating vulnerabilities. *Disasters*, *46*, S10–S50. https://doi.org/10.1111/disa.12537

Bernhofen, M. V., Blenkin, F., & Trigg, M. A. (2023). Unknown risk: Assessing refugee camp flood risk in Ethiopia. *Environmental Research Letters*, *18*. https://doi.org/10.1088/1748-9326/acd8d0

Bernhofen, M. V., Cooper, S., Trigg, M., Mdee, A., Carr, A., Bhave, A., Solano-Correa, Y. T., Pencue-Fierro, E. L., Teferi, E., Haile, A. T., Yusop, Z., Alias, N. E., Sa'adi, Z., Ramzan, M. A. B., Dhanya, C. T., & Shukla, P. (2022). The role of global data sets for riverine flood risk management at national scales. *Water Resources Research*, *58*. https://doi.org/10.1029/2021WR031555

Birkmann, J. (2013). *Measuring vulnerability to natural hazards: Towards disaster resilient societies* (2nd edition). United Nations University Press.

Birkmann, J., Cardona, O. D., Carreño, M. L., Barbat, A. H., Pelling, M., Schneiderbauer, S., Kienberger, S., Keiler, M., Alexander, D., Zeil, P., & Welle, T. (2013). Framing vulnerability, risk and societal responses: The MOVE framework. *Natural Hazards*, *67*, 193–211. https://doi.org/10.1007/s11069-013-0558-5

Birkmann, J. (2007). Risk and vulnerability indicators at different scales: Applicability, usefulness and policy implications. *Environmental Hazards*, *7*, 20–31. https://doi.org/10.1016/j.envhaz.2007.04.002

Bogardi, J., & Birkmann, J. (2004). Vulnerability assessment: the first step towards sustainable risk reduction. *Disaster and Society - From Hazard Assessment to Risk Reduction*, 75–82.

Brito, M. M. D., Evers, M., & Almoradie, A. D. S. (2018). Participatory flood vulnerability assessment: A multi-criteria approach. *Hydrology and Earth System Sciences*, *22*, 373–390. https://doi.org/10.5194/hess-22-373-2018

Bruijn, K. d., Lips, N., Gersonius, B., & Middelkoop, H. (2015). The storyline approach: A new way to analyse and improve flood event management. *Natural Hazards*, *81*, 99–121. https://doi.org/10.1007/s11069-015-2074-2

Buckley, J. J. (1985). Fuzzy hierarchical analysis. *Fuzzy Sets and Systems*, *17*, 233–247. https://doi.org/https://doi.org/10.1016/0165-0114(85)90090-9

Cardona, O. (2004). The need for rethinking the concepts of vulnerability and risk from a holistic perspective: A necessary review and criticism for effective risk management. *Mapping vulnerability. Disasters, development and people*.

Chan, S. W., Abid, S. K., Sulaiman, N., Nazir, U., & Azam, K. (2022). A systematic review of the flood vulnerability using geographic information system. *Heliyon*, *8*. https://doi.org/10.1016/j.heliyon.2022.e09075

Chang, D.-Y. (1996). Applications of the extent analysis method on fuzzy AHP. *European Journal of Operational Research*, *95*, 649–655.

Chen, H., Wood, M. D., Linstead, C., & Maltby, E. (2011). Uncertainty analysis in a GIS-based multi-criteria analysis tool for river catchment management. *Environmental Modelling and Software*, *26*, 395–405. https://doi.org/10.1016/j.envsoft.2010.09.005

Chen, J., Yang, S., Li, H., Zhang, B., & Lv, J. (2013). Research on geographical environment unit division based on the method of natural breaks (jenks). *The International Archives of the Photogrammetry, Remote Sensing and Spatial Information Sciences*, *XL-4/W3*, 47–50. https://doi.org/10.5194/isprsarchives-xl-4-w3-47-2013

Chen, Y., Yu, J., & Khan, S. (2010). Spatial sensitivity analysis of multi-criteria weights in GIS-based land suitability evaluation. *Environmental Modelling and Software*, *25*, 1582–1591. https://doi.org/10.1016/j.envsoft.2010.06.001

Chen, Y., Yu, J., & Khan, S. (2013). The spatial framework for weight sensitivity analysis in AHP-based multi-criteria decision making. *Environmental Modelling and Software*, *48*, 129–140. https://doi.org/10.1016/j.envsoft.2013.06.010

Cho, F. (2019). *ahpsurvey: Analytic Hierarchy Process for Survey Data* [R package version 0.4.1]. https://CRAN.R-project.org/package=ahpsurvey

Coppock, J. T. (1995). GIS and Natural Hazards: An overview from a GIS Perspective. In A. Carrara & F. Guzzetti (Eds.), *Geographical information systems in assessing natural hazards* (pp. 21–34). Springer Netherlands. https://doi.org/10.1007/978-94-015-8404-3_2

Crosetto, M., & Tarantola, S. (2001). Uncertainty and sensitivity analysis: Tools for GIS-based model implementation. *International Journal of Geographical Information Science*, *15*, 415–437. https://doi.org/10.1080/13658810110053125

Cutter, S. L., Boruff, B. J., & Shirley, W. L. (2003). Social vulnerability to environmental hazards. *Social Science Quarterly*, *84*, 242–261. https://doi.org/10.1111/1540-6237.8402002

Dall'osso, F., Gonella, M., Gabbianelli, G., Withycombe, G., & Dominey-Howes, D. (2009). Natural Hazards and Earth System Sciences A revised (PTVA) model for assessing the vulnerability of buildings to tsunami damage. *Hazards Earth Syst. Sci*, *9*, 1557–1565. www.nat-hazards-earth-syst-sci.net/9/1557/2009/

Daniel, C. J. M. (1973). One-at-a-Time Plans. *Journal of the American Statistical Association*, *68*, 353–360. https://api.semanticscholar.org/CorpusID:121049354

Delavar, M. R., & Sadrykia, M. (2020). Assessment of enhanced Dempster-Shafer theory for uncertainty modeling in a GIS-based seismic vulnerability assessment model, case study - Tabriz city. *ISPRS International Journal of Geo-Information*, *9*. https://doi.org/10.3390/ijgi9040195

Dottori, F., Alfieri, L., Salamon, P., Bianchi, A., Feyen, L., & Hirpa, F. (2016). Flood hazard map of the World - 10-year return period [Dataset]. http://data.europa.eu/89h/jrc-floods-floodmapgl_rp10y-tif

Dutta, P. (2015). Uncertainty modeling in risk assessment based on Dempster–Shafer Theory of Evidence with generalized fuzzy focal elements. *Fuzzy Information and Engineering*, *7*, 15–30. https://doi.org/10.1016/j.fiae.2015.03.002

Eriksen, S., Schipper, E. L. F., Scoville-Simonds, M., Vincent, K., Adam, H. N., Brooks, N., Harding, B., Khatri, D., Lenaerts, L., Liverman, D., Mills-Novoa, M., Mosberg, M., Movik, S., Muok, B., Nightingale, A., Ojha, H., Sygna, L., Taylor, M., Vogel, C., & West, J. J. (2021). Adaptation interventions and their effect on vulnerability in developing countries: Help, hindrance or irrelevance? *World Development*, *141*. https://doi.org/10.1016/j.worlddev.2020.105383

FAO. (2023). Emergency support to the rehabilitation of the agricultural production for farmers affected by floods in Kirehe district. Food and Agricultural Organisation of the United States.

Fernandez, P., Mourato, S., Moreira, M., & Pereira, L. (2016). A new approach for computing a flood vulnerability index using cluster analysis. *Physics and Chemistry of the Earth*, *94*, 47–55. https://doi.org/10.1016/j.pce.2016.04.003

Finan, J. S., & Hurley, W. J. (1997). The analytic hierarchy process: Does adjusting a pairwise comparison matrix to improve the consistency ratio help? *Computers and Operations Research*, *24*, 749–755. https://doi.org/https://doi.org/10.1016/S0305-0548(96)00090-1

Ford, J. D., Champalle, C., Tudge, P., Riedlsperger, R., Bell, T., & Sparling, E. (2015). Evaluating climate change vulnerability assessments: a case study of research focusing on the built environment in northern Canada. *Mitigation and Adaptation Strategies for Global Change*, *20*, 1267–1288. https://doi.org/10.1007/s11027-014-9543-x

Fozaie, M. T. A., & Wahid, H. (2022). A guide to integrating expert opinion and Fuzzy AHP when generating weights for composite indices (B. Sahin, Ed.). *Advances in Fuzzy Systems*, *2022*, 3396862. https://doi.org/10.1155/2022/3396862

Gairing, M., Schalbetter, L., Antenen, N., Kostenwein, D., Rohling, B., Schmid, E., Nimri, R., Kaufmann, D., & Grêt-Regamey, A. (2024). User Manual for the Risk Mitigation Strategy Tool in QGIS. General Manual.

Galton, F. (1907). *One vote, one value* (Vol. 75). Nature.

Ganji, K., Gharechelou, S., Ahmadi, A., & Johnson, B. A. (2022). Riverine flood vulnerability assessment and zoning using geospatial data and MCDA method in Aq'Qala. *International Journal of Disaster Risk Reduction*, *82*, 103345. https://doi.org/10.1016/J.IJDRR.2022.103345

Gao, J., Nickum, J., & Pan, Y. (2007). An assessment of flood hazard vulnerability in the Dongting Lake region of China. *Lakes and Reservoirs: Research and Management*, *12*, 27–34. https://doi.org/10.1111/j.1440-1770.2007.00318.x

GFDRR. (n.d.). River flood hazard report for Kirehe, Rwanda. Think Hazard. Global Facility for Disaster Reduction and Recovery (GFDRR) [Accessed: 29.05.2024]. https://thinkhazard.org/en/report/21986-rwanda-east-iburasirazuba-kirehe/FL

Greene, R., Devillers, R., Luther, J., & Eddy, B. (2011). GIS-based Multiple-Criteria Decision Analysis. *Geography Compass*, *5*, 412–432. https://doi.org/10.1111/j.1749-8198.2011.00431.x

Guillard-Gonçalves, C., & Zêzere, J. L. (2018). Combining social vulnerability and physical vulnerability to analyse landslide risk at the municipal scale. *Geosciences (Switzerland)*, *8*. https://doi.org/10.3390/geosciences8080294

Gupta, L., & Dixit, J. (2022). A GIS-based flood risk mapping of Assam, India, using the MCDA-AHP approach at the regional and administrative level. *Geocarto International*, *37*, 11867–11899. https://doi.org/10.1080/10106049.2022.2060329

Harker, P. T. (1987). Derivatives of the Perron root of a positive reciprocal matrix: With application to the analytic hierarchy process. *Applied Mathematics and Computation*, *22*, 217–232. https://doi.org/https://doi.org/10.1016/0096-3003(87)90043-9

Hassan, M. M., Smith, A. C., Walker, K., Rahman, M., & Southworth, J. (2018). Rohingya refugee crisis and forest cover change in Teknaf, Bangladesh. *Remote Sensing*, *10*, 689. https://doi.org/10.3390/rs10050689

Houston, D., Werritty, A., Ball, T., & Black, A. (2020). Environmental vulnerability and resilience: Social differentiation in short- and long-term flood impacts. *Transactions of the Institute of British Geographers*, *46*, 102–119. https://doi.org/10.1111/tran.12408

Hussain, M., Tayyab, M., Zhang, J., Shah, A. A., Ullah, K., Mehmood, U., & Al-Shaibah, B. (2021). GIS-Based multi-criteria approach for flood vulnerability assessment and mapping in district Shangla: Khyber Pakhtunkhwa, Pakistan. *Sustainability*, *13*, 3126. https://doi.org/10.3390/su13063126

IPCC. (2012). *Managing the Risks of Extreme Events and Disasters to Advance Climate Change Adaptation. Special report of the Intergovernmental Panel on Climate Change (IPCC)* (C. Field, V. Barros, T. Stocker, D. Qin, D. Dokken, K. Ebi, M. Mastrandrea, K. Mach, G.-K. Plattner, S. Allen, & M. T. Midgley, Eds.). Cambridge University Press.

Ishizaka, A., & Labib, A. (2011). Review of the main developments in the analytic hierarchy process. *Expert Systems with Applications*, *38*(11), 14336–14345. https://doi.org/https://doi.org/10.1016/j.eswa.2011.04.143

Jackson, M., Huang, L., Xie, Q., & Tiwari, R. C. (2010). A modified version of Moran's I. *International Journal of Health Geographics*, *9*, 33. https://doi.org/10.1186/1476-072x-9-33

JRC and OECD. (2008, August). *Handbook on constructing composite indicators: Methodology and user guide*. European Union; Joint Research Centre. https://doi.org/10.1787/9789264043466-en

Kaoje, I. U., Rahman, M. Z. A., Tam, T. H., Salleh, M. R. M., Idris, N. H., & Omar, A. H. (2021). An indicator-based approach for micro-scale assessment of physical flood vulnerability of individual buildings. *International Journal of Built Environment and Sustainability*, *8*, 23–33. https://doi.org/10.11113/ijbes.v8.n2.700

Kaufmann, D., Rohling, B., & Kostenwein, D. (2022). *Risk Mitigation Strategy Mahama Refugee Camp Case Study*, ETH Zurich - Institute for Spatial and Landscape Development.

Kienberger, S., Lang, S., & Zeil, P. (2009). Spatial vulnerability units-expert-based spatial modelling of socio-economic vulnerability in the Salzach catchment, Austria. *Hazards Earth Syst. Sci*, *9*, 767–778. www.nat-hazards-earth-syst-sci.net/9/767/2009/

Kienberger, S. (2012). Spatial modelling of social and economic vulnerability to floods at the district level in Búzi, Mozambique. *Natural Hazards*, *64*, 2001–2019. https://doi.org/10.1007/s11069-012-0174-9

Kienberger, S. (2013). Mapping vulnerability – Integration of GIScience and participatory approaches at the local and district levels. In J. Birkmann (Ed.), *Measuring vulnerability to natural hazards: Towards disaster resilient societies* (2nd edition). United Nations University Press.

Kocsis, I., Bilașco, Ș., Irimuș, I.-A., Dohotar, V., Rusu, R., & Roșca, S. (2022). Flash flood vulnerability mapping based on FFPI using GIS spatial analysis case study: Valea Rea Catchment area, Romania. *Sensors*, *22*(9). https://doi.org/10.3390/s22093573

Lee, J.-Y., & Kim, J.-S. (2021). Detecting areas vulnerable to flooding using hydrological-topographic factors and logistic regression. *Applied Sciences*, *11*, 5652. https://doi.org/10.3390/app11125652

Lee, J. S., & Choi, H. I. (2018). Comparison of flood vulnerability assessments to climate change by construction frameworks for a composite indicator. *Sustainability*, *10*, 768. https://doi.org/10.3390/su10030768

Lee, S. (2014). Determination of Priority Weights under Multiattribute Decision-Making Situations: AHP versus Fuzzy AHP. https://doi.org/10.1061/(ASCE)CO.1943-7862

Len, N. L. S., Bolong, N., Roslee, R., Tongkul, F., Mirasa, A. K., & Ayog, J. L. (2018). Flood vulnerability of critical infrastructures - Review. *Malaysian Journal Geosciences*, *2*, 31–34. https://doi.org/10.26480/mjg.01.2018.31.34

Lyu, H. M., Sun, W. J., Shen, S. L., & Arulrajah, A. (2018). Flood risk assessment in metro systems of mega-cities using a GIS-based modeling approach. *Science of the Total Environment*, *626*, 1012–1025. https://doi.org/10.1016/j.scitotenv.2018.01.138

Malgwi, M. B., Fuchs, S., & Keiler, M. (2020). A generic physical vulnerability model for floods: Review and concept for data-scarce regions. *Natural Hazards and Earth System Sciences*, *20*, 2067–2090. https://doi.org/10.5194/nhess-20-2067-2020

Malgwi, M. B., Schlögl, M., & Keiler, M. (2021). Expert-based versus data-driven flood damage models: A comparative evaluation for data-scarce regions. *International Journal of Disaster Risk Reduction*, *57*. https://doi.org/10.1016/j.ijdrr.2021.102148

Maskrey, A. (1989). *Disaster Mitigation: A community based approach*. Oxfam GB. http://hdl.handle.net/10546/121119

Mekonnen, T. M., Mitiku, A. B., & Woldemichael, A. T. (2023). Flood hazard zoning of upper Awash river basin, Ethiopia, using the Analytical Hierarchy Process (AHP) as compared to sensitivity analysis. *The Scientific World Journal*, *2023*, 1–15. https://doi.org/10.1155/2023/1675634

Metzger, O., Spengler, T., & Volkmer, T. (2018). Valuation of crisp and intuitionistic fuzzy information. *A Quarterly Journal of Operations Research*, 113–119. https://doi.org/10.1007/978-3-319-89920-6_16

Moreira, L. L., de Brito, M. M., & Kobiyama, M. (2021). Effects of different normalization, aggregation, and classification methods on the construction of flood vulnerability indexes. *Water*, *13*(1). https://doi.org/10.3390/w13010098

Morse, S. (2004, January). *Indices and indicators in development: An unhealthy obsession with numbers*. Earthscan. https://doi.org/10.4324/9781849771719

Mosadeghi, R., Warnken, J., Tomlinson, R., & Mirfenderesk, H. (2015). Comparison of Fuzzy-AHP and AHP in a spatial multi-criteria decision making model for urban land-use planning. *Computers, Environment and Urban Systems*, *49*, 54–65. https://doi.org/10.1016/j.compenvurbsys.2014.10.001

Muhangi, J., Ainamani, H. E., & Opio, F. (2022). Contribution of agriculture in the enhancement of refugees livelihoods in Nakivale settlement. *Open Journal of Applied Sciences*, *12(09)*, 1505–1526. https://doi.org/https://doi.org/10.4236/ojapps.2022.129103

Mwalwimba, I. K., Manda, M., & Ngongondo, C. (2024). Flood vulnerability assessment in rural and urban informal settlements: Case study of Karonga district and Lilongwe city in Malawi. *Natural Hazards*. https://doi.org/10.1007/s11069-024-06601-5

Nachappa, T. G., Piralilou, S. T., Gholamnia, K., Ghorbanzadeh, O., Rahmati, O., & Blaschke, T. (2020). Flood susceptibility mapping with machine learning, multi-criteria decision analysis and ensemble using Dempster Shafer Theory. *Journal of Hydrology*, *590*. https://doi.org/10.1016/j.jhydrol.2020.125275

Nasiri, H., Yusof, M. J. M., & Ali, T. A. M. (2016). An overview to flood vulnerability assessment methods. *Sustainable Water Resources Management*, *2*, 331–336. https://doi.org/10.1007/s40899-016-0051-x

Ndabula, C., & Oyatayo, K. T. (2021). Spatial multi-criteria evaluation of proportional accountability of flood causal factors and vulnerable areas in Makurdi, Benue State, Nigeria. *Journal of Resources Development and Management*. https://doi.org/10.7176/jrdm/77-03

Niang, I., Ruppel, O., Abdrabo, M., Essel, A., Lennard, C., Padgham, J., & Urquhart, P. (2014, January). Africa. In *Climate Change 2014: Impacts, Adaptation, and Vulnerability. Part B: Regional Aspects. Contribution of Working Group II to the Fifth Assessment Report of the Intergovernmental Panel on Climate Change* (pp. 1199–1265). Cambridge University Press.

Nkwunonwo, U. C. (2021). Flood risk analysis for critical infrastructure protection: issues and opportunities in less developed societies. *Issues on Risk Analysis for Critical Infrastructure Protection*. https://doi.org/10.5772/intechopen.95364

Nsengiyumva, J. B. (2012, March). Disaster high risk zones on floods and landslides.

Nyborg, I., & Nawab, B. (2017). Social vulnerability and local adaptation in humanitarian response: The case of Pakistan. *Courting Catastrophe? Humanitarian Policy and Practice in a Changing Climate*, *48*. https://doi.org/10.19088/1968-2017.153

OpenStreetMap contributors. (2017). Planet dump retrieved from https://planet.osm.org.

Osman, S. A., & Das, J. (2023). GIS-based flood risk assessment using multi-criteria decision analysis of Shebelle River basin in southern Somalia. *SN Applied Sciences*, *5*. https://doi.org/10.1007/s42452-023-05360-5

Ouma, Y. O., & Tateishi, R. (2014). Urban flood vulnerability and risk mapping using integrated multi-parametric AHP and GIS: Methodological overview and case study assessment. *Water (Switzerland)*, *6*, 1515–1545. https://doi.org/10.3390/w6061515

Owen, M., Kruczkiewicz, A., & Hoek, J. V. D. (2023). Indexing climatic and environmental exposure of refugee camps with a case study in East Africa. *Scientific Reports*, *13*. https://doi.org/10.1038/s41598-023-31140-7

Pant, R., Thacker, S., Hall, J. W., Alderson, D., & Barr, S. (2017). Critical infrastructure impact assessment due to flood exposure. *Journal of Flood Risk Management*, *11*, 22–33. https://doi.org/10.1111/jfr3.12288

Papathoma-Köhle, M., Cristofari, G., Wenk, M., & Fuchs, S. (2019). The importance of indicator weights for vulnerability indices and implications for decision making in disaster management. *International Journal of Disaster Risk Reduction*, *36*. https://doi.org/10.1016/j.ijdrr.2019.101103

Pascoe, S. (2022). A simplified algorithm for dealing with inconsistencies using the Analytic Hierarchy Process. *Algorithms*, *15*. https://doi.org/10.3390/a15120442

Pebesma, E., & Bivand, R. (2023). *Spatial data science: With applications in R*. Chapman; Hall/CRC. https://doi.org/10.1201/9780429459016

Pinheiro, J., Bedregal, B., Santiago, R., & Santos, H. (2018). Crisp Fuzzy Implications. In G. A. Barreto & R. Coelho (Eds.), *Fuzzy information processing* (pp. 348–360). Springer International Publishing. https://doi.org/10.1007/978-3-319-95312-0_30

Potapov, P., Hansen, M. C., Pickens, A., Hernandez-Serna, A., Tyukavina, A., Turubanova, S., Zalles, V., Li, X., Khan, A., Stolle, F., & Harris, N. (2022). The global 2000-2020 land cover and land use change dataset derived from the Landsat archive: first results. https://doi.org/10.3389/frsen.2022.856903

Qian Zheng, A. Z., Hai-Min Lyu, & Shen, S.-L. (2021). Risk assessment of geohazards along Cheng-Kun railway using fuzzy AHP incorporated into GIS. *Geomatics, Natural Hazards and Risk*, *12*(1), 1508–1531. https://doi.org/10.1080/19475705.2021.1933614

Radmehr, A., & Araghinejad, S. (2015). Flood vulnerability analysis by fuzzy spatial multi-criteria decision making. *Water Resources Management*, *29*, 4427–4445. https://doi.org/10.1007/s11269-015-1068-x

Ramkar, P., & Yadav, S. M. (2021). Flood risk index in data-scarce river basins using the AHP and GIS approach. *Natural Hazards*, *109*, 1119–1140. https://doi.org/10.1007/s11069-021-04871-x

Refsgaard, J. C., van der Sluijs, J. P., Højberg, A. L., & Vanrolleghem, P. A. (2007). Uncertainty in the environmental modelling process - A framework and guidance. *Environmental Modelling and Software*, *22*, 1543–1556. https://doi.org/10.1016/j.envsoft.2007.02.004

Rohling, B., Kostenwein, D., Gairing, M., Kaufmann, D., Al-Mahdawi, A., Schmid, E., & Bardou, E. (2023). *Flood Risk in Humanitarian Settlements: Compendium of Mitigation Measures*. ETH Zurich, UNHCR. https://doi.org/10.3929/ethz-b-000645680

Roy, D., Dhar, A., & Desai, V. R. (2023). A grey fuzzy analytic hierarchy process-based flash flood vulnerability assessment in an ungauged Himalayan watershed. *Environment, Development and Sustainability*. https://doi.org/10.1007/s10668-023-03385-9

Ruiter, M. C. D., Ward, P. J., Daniell, J. E., & Aerts, J. C. (2017). Review Article: A comparison of flood and earthquake vulnerability assessment indicators. *Natural Hazards and Earth System Sciences*, *17*, 1231–1251. https://doi.org/10.5194/nhess-17-1231-2017

Saaty, T. (1977). A scaling method for priorities in hierarchical structures. *Journal of Mathematical Psychology*, *15*(3), 234–281. https://doi.org/https://doi.org/10.1016/0022-2496(77)90033-5

Saaty, T. (1980). *The Analytic Hierarchy Process*. McGraw-Hill.

Saaty, T. (1987). The Analytic Hierarchy Process – What it is and how it is used. *Mathematical Modelling*, *9*, 161–176. https://doi.org/10.1016/0270-0255(87)90473-8

Saaty, T. (2003). Decision-making with the AHP: Why is the principal eigenvector necessary. *European Journal of Operational Research*, *145*, 85–91. https://doi.org/https://doi.org/10.1016/S0377-2217(02)00227-8

Saaty, T. (2008). Decision making with the analytic hierarchy process.

Sadr, S. M. K., Saroj, D., Mierzwa, J. C., McGrane, S. J., Skouteris, G., Farmani, R., Kazos, X., Aumeier, B. M., Kouchaki, S., & Ouki, S. K. (2018). A multi-expert decision support tool for the evaluation of advanced wastewater treatment trains: A novel approach to improve urban sustainability. *Environmental Science and Amp; Policy*, *90*, 1–10. https://doi.org/10.1016/j.envsci.2018.09.006

Saeedullah, A., Khan, M. S., Andrews, S. C., Iqbal, K., Ul-Haq, Z., Qadir, S. A., Khan, H., Iddrisu, I., & Shahzad, M. (2021). Nutritional Status of Adolescent Afghan Refugees Living in Peshawar, Pakistan. *Nutrients*, *13*(9). https://doi.org/10.3390/nu13093072

Seneviratne, S., Zhang, X., Adnan, M., Badi, W., Dereczynski, C., Di Luca, A., Ghosh, S., Iskandar, I., Kossin, J., Lewis, S., Otto, F., Pinto, I., Satoh, M., Vicente-Serrano, S., Wehner, M., & Zhou, B. (2021). Weather and climate extreme events in a changing climate. In V. Masson-Delmotte, P. Zhai, A. Pirani, S. Connors, C. Péan, S. Berger, N. Caud, Y. Chen, L. Goldfarb, M. Gomis, M. Huang, K. Leitzell, E. Lonnoy, J. Matthews, T. Maycock, T. Waterfield, O. Yelekçi, R. Yu, & B. Zhou (Eds.), *Climate Change 2021: The Physical Science Basis. Contribution of Working Group I to the Sixth Assessment Report of the Intergovernmental Panel on Climate Change (IPCC)* (pp. 1513–1766). Cambridge University Press. https://doi.org/10.1017/9781009157896.013

Sirko, W., Kashubin, S., Ritter, M., Annkah, A., Bouchareb, Y. S. E., Dauphin, Y., Keysers, D., Neumann, M., Cisse, M., & Quinn, J. (2021). Continental-Scale Building Detection from High Resolution Satellite Imagery. http://arxiv.org/abs/2107.12283

Sphere Association. (2018). *The Sphere Handbook: humanitarian charter and minimum standards in humanitarian response* (Fourth edition). https://www.spherestandards.org/handbook/

Tascón-González, L., Ferrer-Juliá, M., Ruiz, M., & García-Meléndez, E. (2020). Social vulnerability assessment for flood risk analysis. *Water*, *12*, 558. https://doi.org/10.3390/w12020558

Tate, E., Rahman, A., Emrich, C. T., & Sampson, C. (2021). Flood exposure and social vulnerability in the United States. *Natural Hazards*, *106*, 435–457. https://doi.org/10.1007/s11069-020-04470-2

Tobler, W. R. (1970). A computer movie simulating urban growth in the Detroit region. *Economic Geography*, *46*, 234–240. Retrieved June 20, 2024, from http://www.jstor.org/stable/143141

Torfi, F., Farahani, R. Z., & Rezapour, S. (2010). Fuzzy AHP to determine the relative weights of evaluation criteria and Fuzzy TOPSIS to rank the alternatives. *Applied Soft Computing Journal*, *10*, 520–528. https://doi.org/10.1016/j.asoc.2009.08.021

Totschnig, R., & Fuchs, S. (2013). Mountain torrents: Quantifying vulnerability and assessing uncertainties. *Engineering Geology*, *155*, 31–44. https://doi.org/https://doi.org/10.1016/j.enggeo.2012.12.019

Tschirpig, V. (2022). Risk assessments of natural hazards in refugee camp planning in Greece. Challenges and recommended actions. http://www.risk.lth.se

Ullah, W. (2016). Climate Change Vulnerability of Pakistan Towards Natural Disasters: A Review. *International Journal of Environmental Protection and Policy*, *4*, 126. https://doi.org/10.11648/j.ijepp.20160405.13

UNHCR. (2020). Mahama Camp Site Layout.

UNHCR. (2021). Refugee camps explained [Accessed: 15.06.2024]. https://www.unrefugees.org/news/refugee-camps-explained/#Howmanyrefugeesliveinrefugeecamps?

UNHCR. (2023a). *Profile of Mahama Refugee Camp*. United Nations High Commissioner for Refugees.

UNHCR. (2023b). Refugee Camps [Accessed: 15.06.2024]. https://www.unrefugees.org/refugee-facts/camps

UNHCR. (2024). *Global trends forced displacement in 2023*. Copenhagen: Statistics and Demographics Section, United Nations High Commissioner for Refugees Global Data Service. https://www.unhcr.org/sites/default/files/2024-06/global-trends-report-2023.pdf

UNHCR & MINEMA. (2023). Mahama Refugee Camp Factsheet September 2023 [Accessed: 2024-05-28]. https://data.unhcr.org/en/documents/details/96735

UNISDR. (2015). Sendai Framework for Disaster Risk Reduction 2015–2030 [Accessed: 2024-06-1]. https://www.undrr.org/publication/sendai-framework-disaster-risk-reduction-2015-2030

United Nations. (2024, May). *East Africa: UN support continues amid heavy rains, severe floods and cyclone threat* [Accessed: 2024-06-18]. https://news.un.org/en/story/2024/05/1149311

Walker, W., Harremoës, P., Rotmans, J., van der Sluijs, J., van Asselt, M., Janssen, P., & von Krauss, M. K. (2003). Defining uncertainty: A conceptual basis for uncertainty management in model-based decision support. *Integrated Assessment*, *4*, 5–17. https://doi.org/10.1076/iaij.4.1.5.16466

Wang, H., Zeng, J., Liu, T., Gao, X., Hongbin, W., & Jianhua, X. (2024, April). *SpatMCDA: An R package for assessing areas at risk of infectious diseases based on spatial multi-criteria decision analysis*. Zenodo. https://doi.org/10.5281/zenodo.11044224

Wang, P., Zhu, Y., & Yu, P. (2022). Assessment of Urban Flood Vulnerability Using the Integrated Framework and Process Analysis: A Case from Nanjing, China. *International Journal of Environmental Research and Public Health*, *19*(24). https://doi.org/10.3390/ijerph192416595

Xie, Y., Yi, S., Cao, Y., & Lu, Y. (2011). Uncertainty information fusion for flood risk assessment based on DS-AHP method. *19th International Conference on Geoinformatics*, 1–6. https://doi.org/10.1109/GeoInformatics.2011.5980761

Xu, J., & Xie, G. (2019). A novel hybrid method of spatially filtered FDTD and subgridding technique. *IEEE Access*, *7*, 85622–85626. https://doi.org/10.1109/access.2019.2925835

Yang, X.-l., Ding, J.-h., & Hou, H. (2013). Application of a triangular fuzzy AHP approach for flood risk evaluation and response measures analysis. *Natural Hazards*, *68*, 657–674. https://doi.org/10.1007/s11069-013-0642-x

Yi, S., & Xie, Y. (2010). Vulnerability Analysis of Disaster Risk Based on Geographic Information and Dempster-Shafer Theory. *18th International Conference on Geoinformatics*, 1–6.

Zabota, B., Mikoš, M., & Kobal, M. (2021). Rockfall modelling in forested areas: The role of digital terrain model grid cell size. *Applied Sciences*, *11*(4). https://doi.org/10.3390/app11041461

Zadeh, L. A. (1965). Fuzzy Sets. *Information Control*, *8*, 338–353. https://doi.org/http://dx.doi.org/10.1016/S0019-9958(65)90241-X

Zahedi, F. (1986). The Analytic Hierarchy Process: A survey of the method and its Applications. *16*, 96–108. https://about.jstor.org/terms

Zhang, H., Fang, W., Zhang, H., & Li, Y. (2021). Assessment of direct economic losses of flood disasters based on spatial valuation of land use and quantification of vulnerabilities: a case study on the 2014 flood in Lishui City of China. *Natural Hazards and Earth System Sciences*, *21*, 3161–3174. https://doi.org/10.5194/nhess-21-3161-2021

A Appendix

Appendix A: List of vulnerability indicators

Table A.1: Potential Indicators found in the existing literature.

Vulnerability Dimension	**Indicator**	**Literature**
Social	Population density	An et al. (2022); Birkmann et al. (2013); Djamaluddin et al. (2020); Moreira et al. (2021); Roy et al. (2021)
	Dependency rate	Moreira et al. (2021)
	Households with more than 5 people	Moreira et al. (2021)
	Illiterate people	Moreira et al. (2021)
	Vulnerable groups (gender, age distribution)	An et al. (2022); Cutter et al. (2003); Djamaluddin et al. (2020); Kienberger et al. (2009); Moreira et al. (2021); Rohling et al.
Social / Physical	Schools	Kienberger (2013)
	Health facilities	Kienberger (2013); Roy et al. (2021)
Physical	Buildings (type, material, location, number of floors)	Birkmann et al. (2013); De Ruiter et al. (2017); Kienberger et al. (2009); Malgwi et al. (2021)
	Infrastructure	Djamaluddin et al. (2020); Kienberger (2013)
	Roads	An et al. (2022); De Ruiter et al. (2017); Kienberger (2012); Kienberger (2013); Roy et al. (2021)
Exposure	Distance to water body	An et al. (2022); Ballais et al. (2005); Kazakis et al. (2015); Manfreda et al. (2011); Tran et al. (2021)
	Elevation	An et al. (2022); Ballais et al. (2005); Kazakis et al. (2015); Manfreda et al. (2011); Tran et al. (2021)
	Flow accumulation	An et al. (2022)
	Slope	
	TWI and MNDWI	
Economic	People living in rented houses	Moreira et al. (2021)
	Per capita income	
	Unemployed people	
Adaptive Capacity	Access to information	Cutter et al. (2003); Lindersson and Brandimarte (2016)
	Historical experience	Birkmann (2007); Cutter et al. (2003)
	Risk perception	Grothmann and Reusswig (2006); Wachinger et al. (2013)
	Social networks and cohesion	Aldrich and Meyer (2015); Norris et al. (2008)
	Adaptive capacity	Brooks et al. (2005); Smit and Wandel (2006)
Institutional	Emergency services	Cutter et al. (2003); Wisner et al. (2004)
	Institutional capacity	Adger et al. (2005); Birkmann (2007)

Appendix B: List of experts

- **Dr. Mark Bernhofen:** Postdoctoral researcher at the University of Oxford in physical climate risk with special expertise in flood risk in refugee camps
  Disciplines: Physical Climate Risk, Flood Risk Assessment in Refugee Camps
- **Dr. Viviroli:** Research Group Leader in Hydrology and Climate at the Department of Geography, University of Zurich
  Disciplines: Hydrology, Geoinformatics (GIS), Geography, Environmental Engineering
- **Dr. Veruska Muccione:** Senior scientist in Environment and Climate at the Department of Geography, University of Zurich
  Disciplines: Meteorology, Climatology, Oceanography
- **Dr. Kamran Abid:** Doctor of Philosophy in Technology Management, Graduate Research Assistant at Universiti Tun Hussein Onn Malaysia in Risk Management and Insurance
  Disciplines: Risk Management and Insurance, Business Administration, Remote Sensing, Geoinformatics (GIS), Environmental Engineering
- **Nadine Antenen:** Researcher from the Sustainable Humanitarian Settlements project at the Institute for Spatial and Landscape Development, ETH Zurich
  Disciplines: Environmental Engineering, Ecological Engineering, Hydrology, Limnology, Ecology
- **Muhammad Ibrahim:** Researcher at the Centre for Disaster Preparedness and Management, University of Peshawar
  Disciplines: Geoinformatics (GIS), Climatology, Cartography, Agricultural Plant Science
- **Neel Chaminda Withanage:** PhD Researcher in Cartography and Geographical Information Sciences and Lecturer at University of Ruhuna
  Disciplines: Geography, Geoinformatics (GIS)
- **Chukwunonso Emmanue Ozim:** Research on GIS-Based Analysis of Niger-Benue River Flood Risk and Vulnerability of Communities in Kogi State, Nigeria
  Disciplines: Geography, Geoinformatics (GIS), Cartography
- **Jonathan Parkinson:** Expert in wastewater in humanitarian settings and emergency response, flood risk mitigation, WASH interventions
  Disciplines: Wastewater Management, Humanitarian Response, Flood Risk Mitigation, WASH
- **Tanja Matijevic:** ESG Specialist, Risk Assessment and Management, Solid Waste Management Specialist. Humanitarian work as Environment and Health Officer at Moria / Mavrovouni Refugee Camp
  Disciplines: Environmental Research, Environmental Protection, Solid Waste Management
- **Kamrul Hasan:** Emergency Response and Readiness Officer at American Red Cross
  Disciplines: Emergency Response, Refugee Protection, Humanitarian Assistance, Camp Settlement, Contingency Planning

Appendix C: AHP expert questionnaire design

Vulnerability Indicators Questionnaire

Introduction
Assessing flood risk in refugee camps is challenging, especially when mapping vulnerability at refugee camp level. Vulnerability, which describes the likelihood of harm and potential damage or loss when exposed to floods, is influenced by various physical and socioeconomic factors, called vulnerability indicators. To enhance flood risk assessment and identify areas with high vulnerability in refugee camps, we want to examine the relative importance of each indicator.

Below you will find a list of indicators that are thought to have a significant impact on the vulnerability of refugee camps to flooding. Please review these indicators and the scale of relative importance carefully before answering the following questions. *Additional information can be found on the last page of this survey.

Description of vulnerability indicators:

Abbr.	Indicator	Description
Social Susceptibility		
SOC_1	**Population density**	Camp population density exposed to a flood.
SOC_2	**Vulnerable Groups**	Existence of vulnerable groups of camp inhabitants (elderly people, women, children).
SOC_3	**Facilities of social importance**	Facilities (health centers, schools, distribution centers, …) which are of social importance for the camp population and functioning.
SOC_4	**Land use**	Existence of land use or agricultural land with social importance for the camp population.
Physical Susceptibility		
PHY_1	**Shelter type**	Type of residential shelter (emergency, transitional, durable, abandoned). *
PHY_2	**Critical Infrastructure**	Existence of critical/fragile infrastructure.
PHY_3	**Facilities physical vulnerability**	Facilities (health centers, schools, distribution centers, …) especially prone to flooding damage.
PHY_4	**Roads / Transport**	Road density (guarantees accessibility).

Scale of relative importance:

1 = Equally important	**3** = Moderately more important	**5** = Strongly more important	**7** = Very strongly more important	**9** = Extremely more important

2, 4, 6 and 8 are halfway positions between the values above

To determine the significance of these indicators in relation to flood vulnerability, we ask you to compare each indicator's importance relative to the others. You will assign a scale of importance for each comparison pair. Before completing the questionnaire, please review the example provided below for clarity.

Example
Which indicator (A or B) has a greater importance/influence on the flood vulnerability in a particular area in a given refugee camp? Based on the given "scale of relative importance", how much more important is the chosen indicator relative to the other one?

1. *What factor has a greater importance/influence on the flood vulnerability in a particular area in a given refugee camp?*
   - ☐ Indicator A
   - ☑ Indicator B
   - ☐ Equally important

Based on your selection, how much more important is the chosen factor? Please tick the according number.
Please use the above-defined scale of relative importance and circle the according score.

1 ☐	2 ☐	3 ☐	4 ☐	5 ☑	6 ☐	7 ☐	8 ☐	9 ☐
Equally important		Moderately more important		Strongly more important		Very strongly more important		Extremely more important

2. *What factor has a greater importance/influence on the flood vulnerability in a particular area in a given Refugee camp?*

- ☐ Indicator A
- ☑ Indicator C
- ☐ Equally important

Based on your selection, how much more important is the chosen factor?

1 ☐	2 ☑	3 ☐	4 ☐	5 ☐	6 ☐	7 ☐	8 ☐	9 ☐
Equally important		Moderately more important		Strongly more important		Very strongly more important		Extremely more important

Explanation

1. We compare Indicator A with Indicator B. In the example, **Indicator B** is judged to have a stronger influence/importance on the flood vulnerability than Indicator A. The selected value of **5 indicates that Indicator B is "strongly more important"** for the flood vulnerability than Indicator A.

2. Now we compare Indicator A to Indicator C. Also, here **Indicator C** has a stronger influence on vulnerability than Indicator A. But compared to example 1, Indicator C only lies between "equally important" and "moderately more important" than Indicator A and therefore was assigned the importance value 2.

AHP-Questionnaire

Task: *Please compare the indicator pairs with respect to their relative influence on the flood vulnerability by answering the questions below. Please only tick* **ONE** *option per question.*

Part A: Social Susceptibility

1. *What factor has a greater importance/influence on the flood vulnerability in a particular area in a given refugee camp?*

- ☐ Population density (SOC_1)
- ☐ Vulnerable groups (SOC_2)
- ☐ Equally important

Based on your selection, how much more important is the chosen factor?
Please use the above-defined scale of relative importance and circle the according score.

1 ☐	2 ☐	3 ☐	4 ☐	5 ☐	6 ☐	7 ☐	8 ☐	9 ☐
Equally important		Moderately more important		Strongly more important		Very strongly more important		Extremely more important

2. *What factor has a greater importance/influence on the flood vulnerability in a particular area in a given refugee camp?*

- ☐ Population density (SOC_1)
- ☐ Facilities of social importance (SOC_3)
- ☐ Equally important

Based on your selection, how much more important is the chosen factor?

1 ☐	2 ☐	3 ☐	4 ☐	5 ☐	6 ☐	7 ☐	8 ☐	9 ☐
Equally important		Moderately more important		Strongly more important		Very strongly more important		Extremely more important

3. *What factor has a greater importance/influence on the flood vulnerability in a particular area in a given regfugee camp?*
   - ☐ Population density (SOC_1)
   - ☐ Land use (SOC_4)
   - ☐ Equally important

Based on your selection, how much more important is the chosen factor?

1 ☐	2 ☐	3 ☐	4 ☐	5 ☐	6 ☐	7 ☐	8 ☐	9 ☐
Equally important		Moderately more important		Strongly more important		Very strongly more important		Extremely more important

4. *What factor has a greater importance/influence on the flood vulnerability in a particular area in a given refugee camp?*
   - ☐ Vulnerable groups (SOC_2)
   - ☐ Facilities of social importance (SOC_3)
   - ☐ Equally important

Based on your selection, how much more important is the chosen factor?

1 ☐	2 ☐	3 ☐	4 ☐	5 ☐	6 ☐	7 ☐	8 ☐	9 ☐
Equally important		Moderately more important		Strongly more important		Very strongly more important		Extremely more important

5. *What factor has a greater importance/influence on the flood vulnerability in a particular area in a given refugee camp?*
   - ☐ Vulnerable groups (SOC_2)
   - ☐ Land use (SOC_4)
   - ☐ Equally important

Based on your selection, how much more important is the chosen factor?

1 ☐	2 ☐	3 ☐	4 ☐	5 ☐	6 ☐	7 ☐	8 ☐	9 ☐
Equally important		Moderately more important		Strongly more important		Very strongly more important		Extremely more important

6. *What factor has a greater importance/influence on the flood vulnerability in a particular area in a given regufee camp?*
   - ☐ Facilities of social importance (SOC_3)
   - ☐ Land use (SOC_4)
   - ☐ Equally important

Based on your selection, how much more important is the chosen factor?

1 ☐	2 ☐	3 ☐	4 ☐	5 ☐	6 ☐	7 ☐	8 ☐	9 ☐
Equally important		Moderately more important		Strongly more important		Very strongly more important		Extremely more important

Part B: Physical Susceptibility

1. *What factor has a greater importance/influence on the flood vulnerability in a particular area in a given refugee camp?*
   - ☐ Shelter type (PHY_1)
   - ☐ Critical Infrastructure (PHY_2)
   - ☐ Equally important

Based on your selection, how much more important is the chosen factor?

1 ☐	2 ☐	3 ☐	4 ☐	5 ☐	6 ☐	7 ☐	8 ☐	9 ☐
Equally important		Moderately more important		Strongly more important		Very strongly more important		Extremely more important

2. *What factor has a greater importance/influence on the flood vulnerability in a particular area in a given refugee camp?*

- ☐ Shelter type (PHY_1)
- ☐ Facilities physical vulnerability (PHY_3)
- ☐ Equally important

Based on your selection, how much more important is the chosen factor?

1 ☐	2 ☐	3 ☐	4 ☐	5 ☐	6 ☐	7 ☐	8 ☐	9 ☐
Equally important		Moderately more important		Strongly more important		Very strongly more important		Extremely more important

3. *What factor has a greater importance/influence on the flood vulnerability in a particular area in a given refugee camp?*

- ☐ Shelter type (PHY_1)
- ☐ Roads / Accessibility (PHY_4)
- ☐ Equally important

Based on your selection, how much more important is the chosen factor?

1 ☐	2 ☐	3 ☐	4 ☐	5 ☐	6 ☐	7 ☐	8 ☐	9 ☐
Equally important		Moderately more important		Strongly more important		Very strongly more important		Extremely more important

4. *What factor has a greater importance/influence on the flood vulnerability in a particular area in a given refugee camp?*

- ☐ Critical Infrastructure (PHY_2)
- ☐ Facilities physical vulnerability (PHY_3)
- ☐ Equally important

Based on your selection, how much more important is the chosen factor?

1 ☐	2 ☐	3 ☐	4 ☐	5 ☐	6 ☐	7 ☐	8 ☐	9 ☐
Equally important		Moderately more important		Strongly more important		Very strongly more important		Extremely more important

5. *What factor has a greater importance/influence on the flood vulnerability in a particular area in a given refugee camp?*

- ☐ *Critical Infrastructure (PHY_2)*
- ☐ Roads / Accessibility (PHY_4)
- ☐ Equally important

Based on your selection, how much more important is the chosen factor?

1 ☐	2 ☐	3 ☐	4 ☐	5 ☐	6 ☐	7 ☐	8 ☐	9 ☐
Equally important		Moderately more important		Strongly more important		Very strongly more important		Extremely more important

6. *What factor has a greater importance/influence on the flood vulnerability in a particular area in a given refugee camp?*

- ☐ Facilities physical vulnerability (PHY_3)
- ☐ Roads / Accessibility (PHY_4)
- ☐ Equally important

Based on your selection, how much more important is the chosen factor?

1 ☐	2 ☐	3 ☐	4 ☐	5 ☐	6 ☐	7 ☐	8 ☐	9 ☐
Equally important		Moderately more important		Strongly more important		Very strongly more important		Extremely more important

Part C: Vulnerability Classes

Vulnerability can be further classified into different classes, including susceptibility (social and physical) and exposure towards floods.

Abbr.	Indicator	Description
F_EXP	Flood Exposure	Flood exposure refers to how much physical and social systems are at risk due to their location, including indicators such as the *Distance of a location to a waterbody*, *Elevation*, *and Slope*, …
S_SOC	Social Susceptibility	Social susceptibility deals with how likely people are to be negatively affected by disruptions to their social systems, including the indicators of *Population density*, *Vulnerable Groups*, *Facilities of social importance and Land use* (SOC_1 – 4)
S_PHY	Physical Susceptibility	Physical susceptibility focuses on the likelihood of damage to physical assets or infrastructure, including the indicators *Shelter type*, *Critical Infrastructure*, *Facilities physical vulnerability*, *Roads/Accessibility* (PHY_1 – 4)

Task: *Again, please compare the indicator pairs with respect to their relative influence on the flood vulnerability by answering the questions below. Use the same scale of importance as in Parts A and B.*

1. *What factor has a greater importance/influence on the flood vulnerability in a particular area in a given camp?*
   - ☐ Flood Exposure (F_EXP)
   - ☐ Social Susceptibility (S_SOC)
   - ☐ Equally important

Based on your selection, how much more important is the chosen factor? Please tick the according number.
Please use the above-defined scale of relative importance and circle the according score.

1 ☐	2 ☐	3 ☐	4 ☐	5 ☐	6 ☐	7 ☐	8 ☐	9 ☐
Equally important		Moderately more important		Strongly more important		Very strongly more important		Extremely more important

2. *What factor has a greater importance/influence on the flood vulnerability in a particular area in a given camp?*
   - ☐ Flood Exposure (F_EXP)
   - ☐ Physical Susceptibility (S_PHY)
   - ☐ Equally important

Based on your selection, how much more important is the chosen factor?

1 ☐	2 ☐	3 ☐	4 ☐	5 ☐	6 ☐	7 ☐	8 ☐	9 ☐
Equally important		Moderately more important		Strongly more important		Very strongly more important		Extremely more important

3. *What factor has a greater importance/influence on the flood vulnerability in a particular area in a given camp?*
   - ☐ Social Susceptibility (S_SOC)
   - ☐ Physical Susceptibility (S_PHY)
   - ☐ Equally important

Based on your selection, how much more important is the chosen factor?

1 ☐	2 ☐	3 ☐	4 ☐	5 ☐	6 ☐	7 ☐	8 ☐	9 ☐
Equally important		Moderately more important		Strongly more important		Very strongly more important		Extremely more important

PART D: (Optional)

Can you think of any other indicators/factors that significantly influence the vulnerability to flooding in refugee camps that are not included in the questions from above?

*** Additional Information**

Shelter Type:

Emergency: Habitable covered living space providing a secure and healthy environment with privacy and dignity. The shelters typically simple, one room structures implemented to provide critical life saving emergency assistance

Transitional: A range of shelter options that help populations affected by a humanitarian crises progress from an initial emergency arrangement to a more suitable shelter solution, better adapted to their needs in terms of habitability.

Durable: Beyond the emergency and transitional phase, shelters that are adapted and contextualized according to the following elements: climate, cultural practice and habits, local availability of skills, access to adequate construction materials and geographical context.

Abandoned: Not inhabited, fragile structure

Appendix D: Mahama camp layout

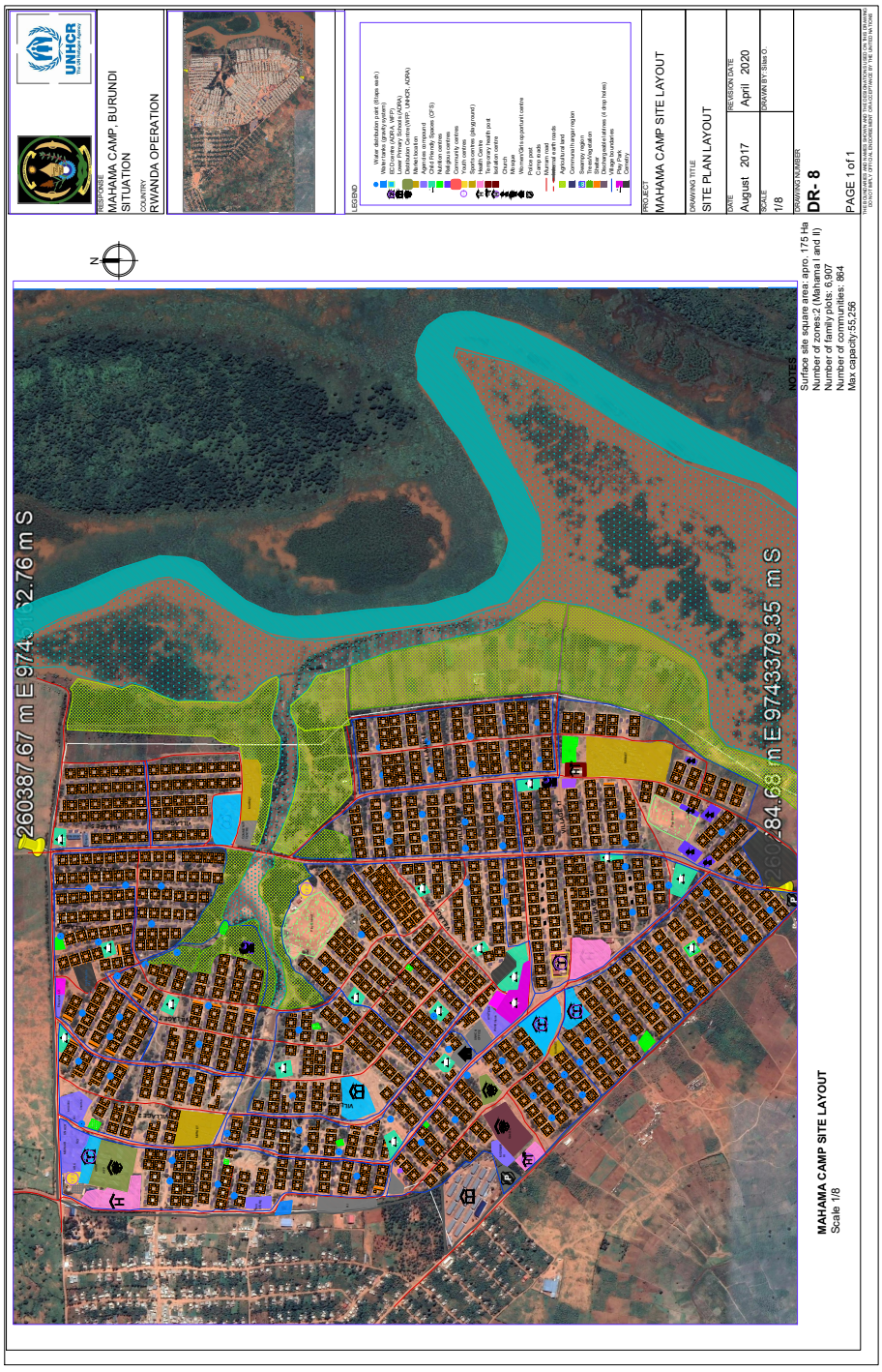

Figure A.1: Mahama Camp Layout Map. Source: UNHCR (2020).

Personal declaration: I hereby declare that the submitted thesis results from my own independent work. All external sources are explicitly acknowledged in the thesis.

Disclaimer: The tools Deepl Translator and ChatGPT were used for translation and rewording in some circumstances. ChatGPT was occasionally used as support in certain coding problems.

Zurich, June 30, 2024

Annika Kunz